MECHANICAL PROPERTIES AND MICROSTRUCTURE OF EXPLOSIVE-WELDED Al/Cu/Al SHEET AFTER EQUAL CHANNEL ANGULAR ROLLING PROCESS IN ROUTE A AND C

By

SINA GHAFFARI

Thesis Submitted to the School of Graduate Studies, Universiti Putra Malaysia, in Fulfilment of the Requirements for the degree of Doctor of Philosophy

October 2023

FK 2023 42

Abstract of thesis presented to the Senate of Universiti Putra Malaysia in fulfilment of the requirement for the degree of Doctor of Philosophy

MECHANICAL PROPERTIES AND MICROSTRUCTURE OF EXPLOSIVE-WELDED Al/Cu/Al SHEET AFTER EQUAL CHANNEL ANGULAR ROLLING PROCESS IN ROUTE A AND C

By

SINA GHAFFARI

October 2023

Chairman : Associate Professor Suraya Mohd Tahir, PhD
Faculty : Engineering

In contemporary times, the utilization of multilayer sheets and novel materials across diverse industries such as aerospace, nuclear, medical devices, and industrial machinery has garnered attention. The explosive welding technique has been widely adopted by researchers and artisans as a suitable method for joining similar and dissimilar metals, thereby enabling the production of a broad spectrum of materials with high circulation. Enhancing the mechanical properties and grain size of explosive weld samples can be achieved through the deformation process of the sheet using the Equal Channel Angular Rolling (ECAR) process. This study investigates the mechanical and metallurgical properties of a three-layer Al/Cu/Al sheet following the ECAR process in two distinct routes, A and C. To this end, Al/Cu/Al explosive welding sheet samples were prepared by subjecting them to varying numbers of passes (ranging from one to five passes) through the ECAR machine. The mechanical properties of the samples were assessed post-ECAR process through micro-hardness tests, uniaxial tensile tests, and residual stress tests. Furthermore, the grain size of the explosive welding samples was examined using a scanning electron microscope (SEM) after the ECAR process. The findings from the mechanical properties tests indicate a significant increase in tensile strength, hardness, and residual stress, alongside a decrease in elongation, following the ECAR process in different passes and routes (A and C). Specifically, the tensile strength and yield strength of the specimen reached their peak levels after the third pass, with values of 152.07 MPa and 126.25 MPa in route A, and 139.85 MPa and 126.76 MPa after one and two passes, respectively, in route C. Moreover, the micro-hardness increased to a maximum of 136 HV after the third pass in route C and 141.7 HV after the second pass in route A. The residual stress test revealed the highest levels at 213.83 MPa and 171.76 MPa in routes A and C, respectively, after the third pass. SEM results also demonstrated that an increase in the number of passes led to a reduction in grain size, reaching nanostructure dimensions. Specifically, the grain size decreased from 6000 nm to 29.02 nm and 30.49 nm in routes A and C, respectively, resulting in enhanced sample strength. The study concludes that the ECAR process yielded a material with specific properties,

and that route A was more effective than route C for the three-layer Al/Cu/Al sheet, as was evident by the mechanical properties and microstructure.

Keywords: explosive welding, ECAR process, mechanical properties, nanostructure

SDG: GOAL 9: Industry, innovation and infrastructure

Abstrak tesis yang dikemukakan kepada Senat Universiti Putra Malaysis sebagai memenuhi keperluan untuk ijazah Doktor Falsafah

SIFAT MEKANIKAL DAN STRUKTUR MIKRO KIMPALAN LETUPAN Al/Cu/Al 3 LAPISAN SELEPAS PROSES GULUNGAN SALURAN BERSUDUT SAMA PADA LALUAN A AND C

Oleh

SINA GHAFFARI

Oktober 2023

Pengerusi : Profesor Madya Suraya Mohd Tahir, PhD
Fakulti : Kejuruteraan

Pada masa kini, penggunaan kepingan berbilang lapisan dan bahan baharu dalam pelbagai industri seperti aeroangkasa, nuklear, peranti perubatan dan industri mesin telah dipertimbangkan. Hal ini adalah disebabkan oleh penggunaan bahan yang berbeza sifatnya secara bersama. Kaedah kimpalan letupan telah digunakan oleh ramai penyelidik serta dalam bidang pertukangan sebagai salah satu kaedah yang sesuai untuk menyambung kepingan yang serupa dan tidak serupa, yang boleh menghasilkan pelbagai bahan dalam peredaran yang tinggi. Bagi menambah baik sifat mekanikal dan saiz butiran sampel kimpalan letupan, proses ubah bentuk kepingan menggunakan proses gulungan saluran bersudut sama (ECAR: Equal Channel Angular Rolling) boleh dipertimbangkan. Dalam penyelidikan ini, sifat mekanikal bagi kepingan tiga lapisan Al/Cu/AL selepas proses ECAR bagi dua jenis laluan berbeza (A dan C) telah disiasat. Dalam hal ini, sampel kepingan kimpalan letupan Al/Cu/ AL telah dihasilkan dengan menggunakan bilangan hantaran yang berbeza (1 hingga 5 kali hantaran) melalui mesin ECAR. Sifat mekanikal sampel dikaji selepas kimpalan letupan dan proses ECAR dalam saluran bersudut melalui ujian kekerasan mikro, ujian tegangan ekapaksi dan tegasan baki. Saiz butiran sampel kimpalan bahan letupan telah disiasat menggunakan mikroskop elektron pengimbasan (SEM) selepas proses ECAR pada kepingan. Keputusan ujian sifat mekanikal menunjukkan bahawa dengan melakukan proses ECAR ke atas sampel dalam bilangan hantaran dan dan laluan yang berbeza (A dan C), kekuatan tegangan dan kekerasan serta tegasan baki telah meningkat dengan ketara dan pemanjangan berkurangan. Keputusan ujian tegangan menunjukkan selepas hantaran ketiga, kekuatan tegangan dan kekuatan alah hasil spesimen mencapai tahap tertinggi iaitu 152.07 MPa dan 126.25 MPa bagi laluan A, manakala kekuatan tegangan tertinggi ialah 139.85 MPa selepas satu hantaran dan kekuatan alah selepas hantaran kedua menghasilkan hasil tertinggi iaitu 126.76 MPa bagi laluan C. Selain itu, peningkatan kekerasan mikro mencapai maksimum 136 Hv selepas hantaran ketiga bagi laluan C dan 141.7 Hv selepas hantaran kedua bagi laluan A. Keputusan ujian baki menunjukkan tahap tegasan baki yang tertinggi ialah 213.83 MPa bagi laluan A dan 171.76 MPa bagi laluan C selepas hantaran ketiga. Keputusan SEM juga menunjukkan bahawa dengan menggunakan lebih banyak hantaran, saiz butiran sampel telah menjadi lebih kecil dan telah mencapai saiz struktur nano. Dengan menggunakan lebih banyak hantaran, saiz butiran berkurangan daripada 6 mikrometer kepada 29.02 nanometer dan 30.49 nanometer bagi laluan A dan C yang menghasilkan peningkatan kekuatan sampel. Keputusan menunjukkan bahawa dengan proses ECAR yang dilakukan pada sampel menghasilkan bahan baharu dengan sifat khusus dan proses ECAR pada laluan A adalah lebih berkesan daripada laluan C untuk kepingan Al/Cu/Al tiga lapisan, seperti yang diperolehi pada sifat mekanikal dan struktur mikro.

Kata Kunci: kimpalan letupan, proses ECAR, sifat mekanikal, struktur nano kimpalan letupan, proses ECAR, sifat mekanikal, struktur nano

SDG: MATLAMAT 9: Industri, inovasi dan infrastruktur

ACKNOWLEDGEMENTS

I would like to express my sincere gratitude to God Almighty and all the people who contributed in one way or the other to the successful completion of this research particularly, to my supervisor, Assoc. Prof. Dr. Suraya Mohd Tahir for her timely and continuous guidance, counsel, encouragement, moral and financial support throughout my study. I was always inspired each time I conversed with Dr Suraya about this research. I would also like to thank my co-supervisors, Assoc. Prof. Dr. Azmah Hanim Binti Mohamed Ariff and Assoc. Prof. Dr Mohd Idris Shah Ismail for their creative ideas and support.

My appreciation also goes to the Technicians of the Department of Mechanical Engineering, University Putra Malaysia (UPM).

May I also appreciate my group mates under the same supervision for their creative and wonderful support during my study. I would like to acknowledge all my friends in UPM.

Finally, I would like to express my acknowledgement for the love and support of my parents, Daryoosh Ghaffari and Mahdokht Farazmand and my brother, Saeed Ghaffari.

This thesis was submitted to the Senate of Universiti Putra Malaysia and has been accepted as fulfilment of the requirement for the degree of Doctor of Philosophy. The members of the Supervisory Committee were as follows:

Suraya binti Mohd Tahir, PhD
Associate Professor
Faculty of Engineering
Universiti PutraMalaysia
(Chairman)

Azmah Hanim binti Mohamed Ariff, PhD
Associate Professor
Faculty of Engineering
Universiti PutraMalaysia
(Member)

Mohd Idris Shah bin Ismail, PhD
Associate Professor
Faculty of Engineering
Universiti PutraMalaysia
(Member)

ZALILAH MOHD SHARIFF, PhD
Professor and Dean
School of Graduate Studies
Universiti Putra Malaysia

Date: 13 June 2024

TABLE OF CONTENTS

LIST OF TABLES

LIST OF FIGURES

LIST OF ABBREVIATIONS

SPD	Severe Plastic Deformation
ECAP	Equal Channel Angular Pressing
CEC	Cyclic Extrusion Compression
HPT	High Pressure Torsion
ARB	Accumulative Roll Bonding
ECAR	Equal Channel Angular Rolling

CHAPTER 1

INTRODUCTION

1.1 Overview

This chapter provides an overview of the research context, explosive welding, and the equal channel angular rolling process (ECAR). It also includes statement of the problem, research objectives, scope of the study, significance of the study, and an outline of the thesis.

1.2 Background of ECAR Process and Explosive Welding

In contemporary times, there is a growing demand for materials possessing distinct characteristics, driven by the rapid progress in various industries and the evolution of advanced manufacturing technologies, machinery, and equipment, including those utilized in the aerospace, military, industrial, and furnace sectors. This necessitates the utilization of novel materials with specific properties that are not inherent in conventional substances, such as nanometre (nm) grain size, high strength, and corrosion resistance.

A new approach has been implemented to integrate technology with the welding of dissimilar materials, including the utilization of explosive welding technique. The primary advantage of this method lies in its ability to join dissimilar metals that cannot be effectively joined through conventional welding techniques due to the formation of brittle intermetallic compounds and significant disparity in melting temperatures (Davim, 2021; Zhang & Liu; 2019).

Numerous scholars and industry experts consider explosive welding to be a viable technology for bonding dissimilar sheets, with the capability to produce a diverse array of materials in large quantities.

Severe plastic deformation encompasses various techniques for subjecting metal to significant mechanical work without inducing fracture or fissures. It is noteworthy that this approach not only improves the strength of the metal but also reduces its elongation, distinguishing it from other plastic deformation methods (Mahmoodi et al., 2012; Volokitina et al., 2022). The distinctive characteristic of this process is likely attributed to the creation of a metal nanostructure via severe plastic deformation.

Deformation in equal channel angular pressing (ECAP) is a significant mechanism in metal processing. This process involves extruding a metal sample into a mould with channels that are angular to each other. Another relevant method is cyclic extrusion compression (CEC), which has been associated with ECAP. In CEC, the metal sample, typically cylindrical, undergoes extrusion to reduce its diameter, followed by compression within the mould to increase its diameter back to its original size.

Additionally, high pressure torsion (HTP) is another procedure that entails the torsional deformation of a thin disc under high pressure (Wojtas et al., 2020; Yan et al., 2020, and Kaviyani et al., 2022). First, the metal disc is inserted into the mould, followed by the insertion of a ramrod to apply a specific pressure to the disc. Another method, accumulative roll bonding (ARB), is employed to subject the material to severe plastic deformation, resulting in a structure with grains of nanometre size. The final technique discussed is plate deformation in the mould using equal channel angular rolling (ECAR), which enhances the mechanical properties and structure of the plate throughout multiple passes within angular channels.

The ECAR procedure is classified as a severe plastic deformation (SPD) process. It is considered a viable technology for the direct production of metal materials with significant dimensions and nanometre grain size, resulting in a substantial increase in the strength of metal samples due to the reduced grain size. The ECAR method involves applying strain to a metal material while preserving its overall dimensions.

The employment of strain enables the creation of microstructures, reduction of grain size to the nanometre scale, and improvement of mechanical characteristics. The consistent size and shape of ECAR throughout the process render it unique. Therefore, the utilization of strain is not constrained, and significant strains can be readily achieved, leading to enhanced strength and modification of grain structure without the inclusion of alloy or ceramic components (Rahimi et al., 2018; Honarpisheh et al., 2019).

1.3 Statement of the Problem

In contemporary industrial settings, the demand for novel materials possessing specific properties and nanostructures has become imperative in order to achieve cost and weight reduction. SPD methods and explosive welding have emerged as viable approaches for the development of materials on a large scale. It is essential for severe plastic deformation methods to fulfill certain criteria in order to be effective. These criteria encompass the following (Balasubramanian et al., 2021):

1) It is crucial to achieve an ultrafine grain structure with a grain boundary featuring a significant angle, as this is the only way to bring about a qualitative transformation in the material's properties.
2) It is essential to achieve a consistent nanostructure throughout the entire volume of the sample in order to establish enduring properties.
3) Although the specimens may undergo significant plastic deformation, they should not exhibit any mechanical impairment or fractures.

Conventional severe plastic deformation techniques such as ECAP, CEC, HPT and ARB are inadequate for meeting these requirements. However, ECAR method, a type of severe plastic deformation, is capable of addressing these challenges by changing the shape of the grains, which increases the hardness and decreases the grain size after several passes of the ECAR process. Additionally, the scarcity of materials possessing unique properties and nanostructures in large dimensions and low thickness presents a further obstacle. The ECAR process enables the continuous production of thin and elongated sheets, leading to enhanced strength and reduced grain size through higher speeds and routes. While the ECAR process can enhance properties and reduce grain size in a single sheet, its impact on cost and weight reduction is limited. To achieve this, explosive welding of sheets with specialized properties that are not present in a single material is necessary. Materials with nanometre-sized grains, high strength, corrosion resistance, residual stress, elongation, and other properties are essential for reducing costs and weight in industrial applications.

1.4 Objectives of the Study

The objectives of this study are as follows:

1. To establish a novel process for producing materials with dissimilar layers and distinct properties
2. To determine the mechanical characteristics of the Al/Cu/Al three-layer material subsequent to the ECAR process, encompassing residual stress, microhardness, elongation, and strength.
3. To assess the microstructural attributes of the Al/Cu/Al three-layer material using optical microscope (OP) and scanning electron microscopy (SEM).

1.5 Scope of the Study

At present, there is ongoing investigation into the application of multilayer sheets with tailored mechanical properties and microstructure across various sectors, including the development of industrial machinery, military applications, and furnace technology. This interest stems from the potential to harness a combination of diverse material properties to address concerns such as minimizing structural weight, enhancing mechanical characteristics, reducing costs, and bolstering resistance to corrosion.

In recent years, there has been significant research interest in the field of science and related disciplines regarding the exploration of production techniques and mechanical characteristics of materials possessing nanostructures. The ECAR process has emerged as a viable method for the development of novel materials with targeted properties and reduced thickness.

In this study, the impact of the ECAR process on the three-layered Al/Cu/Al explosive welded sheets will be examined that it is a new process to develop three-layers material with specific properties and nanostructure. The initial step involves the preparation of the sheets, followed by subjecting them to the ECAR process through multiple passes and routes. Subsequently, the mechanical properties and microstructure of the sheets post-ECAR process will be analysed.

Numerous parameters within the ECAR process, including the quantity of rolling passes, the rolling trajectory, the preheating temperature, and duration (particularly for moulds and plates), influence the characteristics and microstructure of the samples. optimisation of the process parameters explosive welding and ECAR process is not included in this scope and focus on improving mechanical properties and microstructure of 3-layer material Al/Cu/Al. The parameters were fixed based on the literature review.

The ECAR process was investigated using a three-layer explosive welded sheet composed of Al/Cu/Al. It is a new process to develop materials with dissimilar layers and specific properties. The study aimed to assess the impact of multiple passes on the samples, and to determine whether the properties were enhanced accordingly. The investigation also examined the mechanical properties and grain size in various routes to identify the routes that have a greater influence on improving mechanical properties and grain size.

To date, the subject has not been explored by researchers. This study examines the mechanical properties and microstructure following the ECAR process on three-layer sheets via the implementation of tensile tests, micro-hardness tests, residual stress tests for mechanical properties, and the utilization of optical microscopy (OM) and scanning electron microscopy (SEM) for microstructural analysis.

1.6 Significance of the Study

1. Severe plastic deformation is a technique used to achieve nanostructure in a variety of metals and alloys. This process can yield different crystallographic structures, leading to the formation of grains on the nanometre scale within the initial larger structure. Consequently, this method enhances the mechanical properties of metals.
2. Nanomaterials, which are defined as materials with at least one dimension ranging from one to one-hundred nanometres, are commonly referred to as nanomaterials. Nanotechnology involves the manipulation and construction of novel materials, tools, and systems by exerting control at the nanometre scale, or at the atomic and molecular levels, and leveraging the unique properties that emerge at these scales.
3. The mechanical characteristics, including hardness, strength, residual stress, elongation, and fracture toughness, play a crucial role in determining the response of materials to incoming forces.
4. Equal channel angular rolling is a severe plastic deformation technique used to process metal sheets and strips, resulting in the formation of an ultra-fine grain structure within the material. This method allows for the continuous

application of significant strains to the material without altering its cross-sectional area, thereby achieving specific material characteristics.

5. The conventional welding of non-homogeneous metals has posed challenges for various industries due to the disparity in their physical properties, resulting in weld defects and the formation of detrimental intermetallic compounds that compromise the mechanical properties of the joint. Consequently, there has been a growing inclination towards solid-state welding techniques in recent years. Explosive welding, a form of solid-state welding, operates on the principle of establishing atomic-scale mechanical bonding at the interface of two metals. This process involves the oblique collision of two mating surfaces at high velocity, induced by the force generated from the detonation of an explosive material, resulting in a highly favourable physical connection.

1.7 Outline of the Study

The introductory chapter provides the theoretical framework for the study, as well as an overview of the development of materials using the ECAR process review and explosive welding. Additionally, this chapter outlines the rationale for conducting the research, as well as the scope and objectives of the study.

Chapter two commences with a comprehensive overview of previous research in the field of explosive welding and the ECAR process as applied to materials. The discussion encompasses various aspects of the explosive welding method, such as its mechanism, properties, and applications. The primary focus of the research is the development of materials using the ECAR process, which encompasses several subtopics including severe plastic deformation and methods, microstructure, the impact of channel looseness of crystals, mechanical properties, hardness, and residual stress, all of which are thoroughly reviewed.

Chapter three investigates the selection of materials and the procedures for preparing the three layers of Al/Cu/Al explosive welding. Subsequently, the study delves into the preparation of the samples and the thermal processing preceding the primary procedure, follows by an exploration of the ECAR process on the explosive welding sheet. Lastly, the analysis encompasses the mechanical and structural tests conducted on the samples.

Chapter four focuses on the outcomes of various mechanical tests, such as uniaxial tensile tests, microhardness, and residual stress tests, to determine the mechanical characteristics of Al/Cu/Al three-layer plates. It then examines the metallurgical findings, including the scanning electron microscopy test, to analyse the grain size and the interfaces of the Al/Cu/Al three-layer plates.

Chapter five as the concluding chapter, provides a summary of the research results, while offering recommendations for future work.

CHAPTER 2

LITERATURE REVIEW

2.1 Overview

This section provides a review of the literature on explosive welding and the ECAR process for materials. It discusses the challenges related to explosive welding and factors affecting mechanical properties and grain size. The chapter also explores the mechanism of explosive welding and the ECAR machine, as well as severe plastic deformation and related methods. Additionally, it covers testing methodologies for mechanical properties and microstructure.

2.2 Explosive Welding Process

2.2.1 Background of Explosive Welding

The damaging impact of explosions was acknowledged with the advancement of explosives, but in the early 1950s, explosives started to be employed in a beneficial manner in industry. This involved using explosions and explosive materials for constructive purposes such as cutting and welding metals, as well as drilling wells and tunnels. Since their discovery, explosives have captivated human interest due to their high energy density that can be readily transported and released.

The fundamental principles of linked blasting have origins dating back to World War I. During this time, there were instances of explosive welding, where a cannonball warhead was fused to a steel target, and the practice of linking missile and bomb warheads to steel structures like tank bodies. Additionally, there were observations of nearby sections being explosively fused together (Meuken & Carton, 2004; Arnett, 2019). Figure 2.1 Illustrates the first published documentation of explosive welding by Leroy Carl in 1944. Figure 2.2 illustrates a schematic image of the explosive welding process.

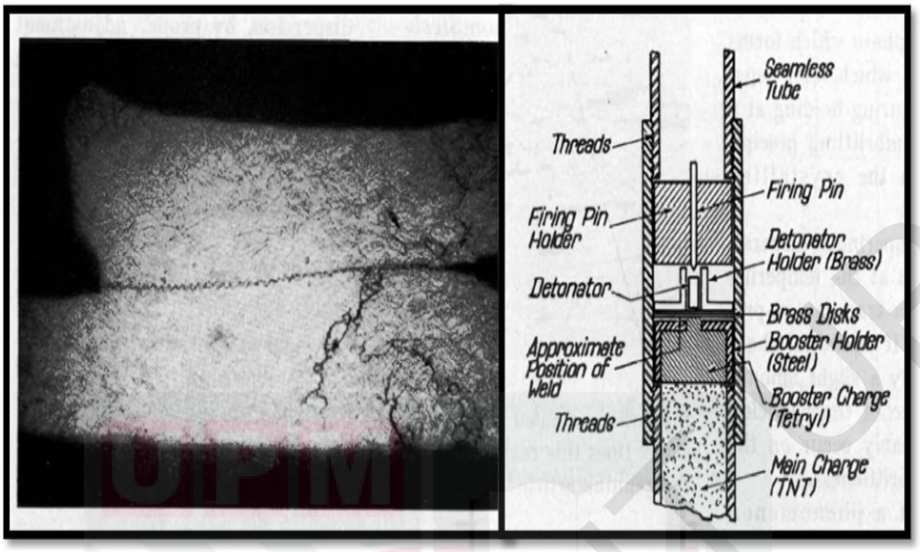

Figure 2.1 : The initial publication of explosive welding by Leroy Carl. The left side displays Carl's welded half-hard brass samples. The right side presents a schematic of the setup where the incident took place, with the brass disks bordered in red by the author (Arnett, 2019)

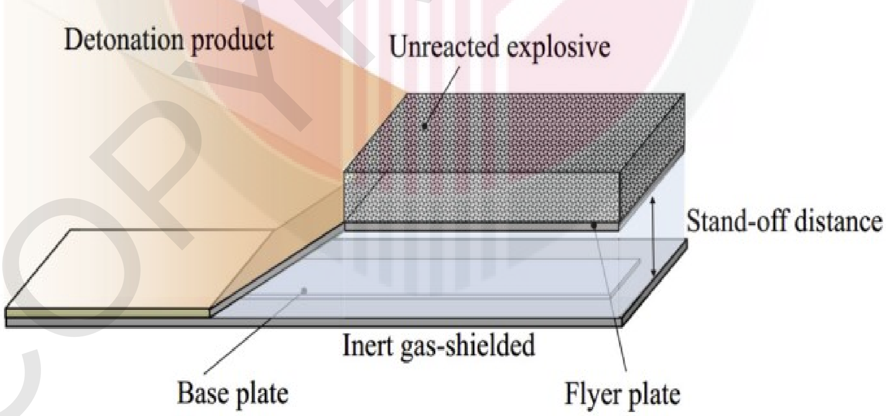

Figure 2.2 : Schematic image of the explosive welding process (Zeng et al, 2019a)

To prevent the damaging impacts of explosions, research into explosive welding was initiated. The energy generated by an explosion was harnessed for connecting metals and joining parts in powder metallurgy, attracting the interest of industrial researchers and practitioners. DuPont extensively documented the experimental findings of this process on a global scale in 1960. Subsequently, in 1962, two scientists named "Philip Jack" and

"Boyce" introduced the theory and technology of explosive welding to the industry. In the same year, the US government utilized explosive coating technology to produce three-layer coins. By 1970, a total of 260 similar and dissimilar connections had been recorded (Bisadi & Meybodi; 2011; Arnett, 2019; Davim, 2021).

Initial research was conducted on flat plate beds, followed by investigations on curved surfaces and pipe fittings both internally and externally. Additionally, external surface connections like cylinders and flag fittings were also examined, particularly the transition from flat to curved surfaces as seen in transformers. The focus was on utilizing this welding technique for these applications. A key challenge lies in comprehending the energy release mechanisms and effectively directing this energy in the intended direction, particularly in the context of materials and design systems that interact with these materials.

Due to their extensive use in military weaponry, information pertaining to these materials was classified within the military industries of various countries. Additionally, due to the rapid nature of explosive interactions, it was extremely challenging to develop tools for experimentally observing these events. The process of explosive welding necessitated a deep understanding of critical factors such as explosive substances, the effects of explosives on metal surfaces, and the behaviour of metals under high-speed explosions (Arnett, 2019; Blazynski, 2012; Davim, 2021).

This was a solid-state welding technique that deployed explosive force to create a metallurgical bond between two pieces. Despite the heat generated by the explosion, there was not enough time for heat to transfer, so the temperature of the pieces did not increase significantly. A high-speed perpendicular struck at the point where the two pieces intersect could make solid metal act like a liquid. The impact of the strike caused the surface layer of the parts to be ejected as a liquid jet, bringing two clean metal surfaces into contact with each other. The surfaces, free of oxide, were forced together and created the bond. (AWS Handbook, 2004; Arnett, 2019).

2.2.2 Mechanism of the Process

During this procedure, the upper plate, referred to as the "flyer plate," is positioned at an incline in relation to the lower plate, known as the "base plate." Figure 2.3 depicts a diagram of the explosive welding process illustrating the angles involved.

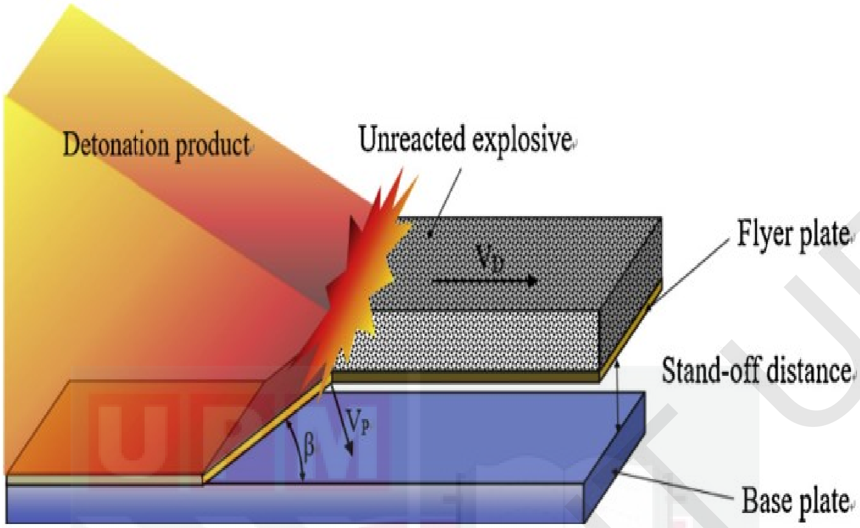

Figure 2.3 : Schematic image of the process that represents the angles
(Zeng et al, 2019a)

The base plate is positioned on a suitable foundation, which can be constructed from either metal or sand. The outer surface of the flying plate is shielded by a protective layer, which could be composed of plastic, cardboard, or a thick coating of plastic paint. An explosive material, such as a plate or powder, is applied to the protective layer, and detonators are activated at the lower end of the explosives. The velocity of the flying plate is determined by the type and quantity of explosives used. The process of explosive welding can be viewed as a two-stage procedure.

In the initial stage, a jet is created, leading to the removal of surface layers. In the subsequent phase, extreme high pressure is applied, causing interference and contact between the intersecting parts. Occasionally, connected waves may be observed at the intersection. The phenomenon can be attributed to the mechanism of wave tension, where a single pressure wave at the collision point between two plates generates reflective waves in both stationary and moving plates. These reflective waves sequentially apply alternating tensions to the front and rear of the collision point, resulting in an unstable surface. If the intensity of these tensions is sufficiently high, surface deformation occurs, leading to collisions of two plates in a small, deformed area (Blazynski, 2012; Arnett, 2019; Davim, 2021).

Numerous factors in the explosive welding procedure, including the speed, pressure duration, distance between plates, welding angle, quantity, and type of explosive, have an impact on the quality of the welding (Zhang & Liu, 2019).

At times, an intermediate layer is employed at the interface to enhance binding properties. For instance, a titanium layer is used at the interface of aluminium and copper to improve the operating temperature, and a silver layer is employed in stainless steel and aluminium connections to guarantee a leak-proof connection (AWS Handbook, 2004; Arnett, 2019; Davim, 2021). The explosive welding method has been extensively researched and is reviewed in the following section.:

Mousavi and Sertangi (2009) performed experiments on explosive welding of AISI 304 / cp-titanium with stainless steel. They utilized analytical calculations to determine the welding ability range, also referred to as the weld window, based on the experimental findings.

Findic (2011) conducted a study on the progress made in explosive welding. The paper reviewed the theories of welding and wave formation, as well as experimental research and numerical studies on explosive welding over the past forty years.

Honarpisheh et al. (2012) examined how the mechanical properties of Al/Cu/Al explosive welded plates were influenced by the cold rolling process. The research aimed to analyse the impact of cold rolling techniques on the mechanical behaviour and interaction of three-layer sheets of aluminium and copper that were joined through explosive welding.

Chu et al. (2017) conducted a study to examine the microstructure and mechanical properties of titanium/steel interfaces created through explosive welding, using both experimental and numerical methods. The interface displayed a wave-like structure, which was a consequence of significant plastic deformation during the explosive welding process. The area where melting occurred due to the trapped jetting was encircled by heavily deformed bulk materials.

Carvalho et al. (2020) investigated the use of carbon steel and niobium interlayers in the explosive welding of aluminum to stainless steel. This work led to the development of the impedance mismatch parameter (IMP), which was a convincing way to organize metallic combinations in a single axis to assess the probability to create typical or curled waves during explosive welding. Researchers Sherpa et al. (2021) looked into how the low velocity of detonation explosive welding (LVEW) procedure affected the Al/LCS interface cladded.

2.2.3 The Process Properties

Welding can produce features not achievable with conventional welding techniques since the process occurs in a solid state and the connection temperature is very low. The principal advantages of this procedure consist of the following:

1. The parts remain in a state of working and casted or annealed structures are not formed.

2. There are no significant changes in the structural components and mechanical characteristics before and after welding. They are utilized to combine dissimilar materials.
3. There is no weld heat-affected zone.
4. There is very little chemical and particle penetration in the sections or along the connection boundaries.
5. The flat and large components can be quickly welded to one another.
6. It is feasible to attach dissimilar elements that have very distinct mechanical and physical characteristics to one another.

The following can also be argued to be the process's primary limitations:

1. The procurement of explosive material is arduous in all countries.
2. It requires large open space or special reactors.
3. It is perilous to work with explosives.
4. It is typically not possible to split and fix connections and reuse the components in the event of calculation problems.
5. The process can be used for cylindrical symmetric parts and sheets (AWS Handbook, 2004; Arnett, 2019; Davim, 2021).

2.2.4 Application of the Process

The explosive welding technique works well for joining materials that are similar and dissimilar. The only prerequisite for this method is that the parts must be sufficiently durable and flexible to avoid bending or breaking while welding. Minimum flexibility requirements are ten percent and minimum breaking energy requirements are thirty joules.

This process is used in the electronic industry to weld thick plate welding, such as components with dimensions of 5 × 13 mm and a thickness of 25-100 mm, as well as 0/5 mm thin components. Tubes and double-layer plates are two of the most crucial parts produced using this process. Refineries, the chemical sector, and equipment used in power generation all make extensive use of the plates and tubes. Other applications are the process of bimetallic part manufacturing methods. By welding one end of these interfaces to one item and the other end to another, it is possible to join disparate parts together.

In the event that two dissimilar pieces of material cannot be joined together because of their unique shapes or other limitations with conventional methods, two pieces of the same material with the proper form and one end welded to one piece and the other end welded to the other piece can be joined together (AWS Handbook, 2004; Arnett, 2019; Davim, 2021).

According to the ASM Handbook (1998) and Weman (2011), the most significant bimetals are the couplings made of aluminium and steel, titanium and aluminium, aluminium/copper-nickel alloy for the shipbuilding industry, aluminium/copper and aluminium/steel for the electronics and transportation industries, aluminium/stainless steel couplings for low temperature pipes, and titanium/stainless steel couplings for the aerospace industry.

2.3 Severe Plastic Deformation (SPD)

Many studies in the fields of materials science and associated disciplines have concentrated in recent years on the mechanical characteristics and production processes of extremely tiny (grain size less than one micron) or nanometer (grain size less than one hundred nanometer) grain sizes. These substances are known as "super metals" due to their unique qualities, which include superior corrosion resistance, high strength at ambient temperature, and super-plastic capabilities at high temperatures and low strain rates.

These materials' ability to alter the usual slide patterns in materials with nanometre grain sizes and to activate the grain boundary sliding mechanism adds to their unique mechanical characteristics. There are numerous proposed methods for creating nanoscale materials as well as various studies about them. The plastic deformation method is one way to make materials with nanometre grain size. The intense strain applied to the sample causes the grain size to be decreased to the nanometre scale, while the mechanical properties of the metal are significantly improved (Yan et al., 2020; Kavyani et al., 2022; Volokitina et al., 2022).

Two broad categories can be used to categorize the field of nanomaterials: nanostructured materials and nano-size materials. Materials classified as nano-size fall into one of three categories: nanoparticles (like carbon nanotubes or nano-silica), nanofibers (like carbon nanofibers), or nano-plates (like mica or clay nano-plates).

Conversely, there are materials that are nanostructured. Materials that are nanostructured have large outward dimensions, yet their constituent structure is tiny. There are two fundamental approaches for creating nanostructured materials: top-down and bottom-up. The first involves working with huge material structures to reduce them to nanometre dimensions, and the second involves starting from scratch and arranging atoms or nanoparticles to form the bulk material.

One of the methods deployed in the top-down methodology is to apply mechanical impart to the material. Among these categories, one of the most crucial processes is severe plastic deformation (SPD) (Valiev et al. 2006).

When a metal undergoes plastic deformation at a low temperature, its internal structure endures changes that enhance its resistance to further deformation. This phenomenon is commonly referred to as work hardening or strain hardening in the field of metallurgy. Work hardening leads to an improvement in the strength and stiffness of the metal, making it more resistant to deformation. However, as the strength of the metal increases, it also loses its ductility and ability to change shape easily. Consequently, the strength of a metal is limited by the amount of mechanical work it can withstand before failure occurs. In certain industrial processes involving metal forming, it may not be possible to achieve the required level of strength due to inherent limitations of the metal itself (Yan et al., 2020; Kavyani et al., 2022; Volokitina et al., 2022).

In certain instances, conventional approaches exhibit limitations in terms of tool capabilities. This implies that as the strain exerted on the material increases, there is a higher likelihood of causing damage to the machine and tools involved. Severe deformity characterizes the manner in which a relatively significant mechanical force can be applied to metal without encountering failure or cracks. The term "severe" denotes that, as a consequence of the measures implemented in this technique, substantial deformation can be achieved in comparison to other conventional metal-forming methods. The intriguing aspect of the severe plastic deformation technique lies in its ability to not only enhance the strength of the metal but also, in many cases, eliminate the loss of ductility and, in other instances, increase its softness.

The distinctive feature that sets SPD apart from other plastic deformation techniques lies in the underlying cause of this unique characteristic. To gain a deeper understanding of this phenomenon, researchers have focused their investigations on metal nanostructures that are formed through severe plastic deformation (Wojtas et al., 2020; Kasaeian et al., 2022; Kayvani et al., 2022; Volokitina et al., 2022).

To date, numerous methods of subjecting metallic materials to severe plastic deformation have been suggested in order to attain nanostructures, each with varying levels of success. The stability and preservation of material appearance throughout the process are shared characteristics and distinctive elements of this technique. Moreover, the limitations on strain application are eliminated, allowing for the attainment of remarkably high strains (approximately eight to ten) in the material.

Applying strain to the sample preserves its integrity while enabling the alteration of its microstructure, reducing grain size to the nanometre scale, and enhancing the mechanical properties of metallic materials. An additional benefit of this technique is the augmentation of particle strength and the refinement of particle structure, all achieved without the need for alloying materials or ceramic particles.

The advantages of severe plastic deformation method are as follows:

- The ability of direct manufacturing of large metal parts with a grain size in the nanometre range.
- The capability of processing via the application of conventional tools and templates.
- The possibility of applying severe plastic strain without altering the dimensions of the samples.

- The absence of restrictions on the strain is significant as it allows for unlimited processing cycles.
- The creation of very fine-grained samples with dimensions suitable for mechanical testing

Despite the advancements achieved in the realm of nanomaterials, there remains a scarcity of data pertaining to the mechanical characteristics of these substances (Wojtas et al., 2020; Kasaeian et al., 2022; Yan et al., 2020; Kavyani et al., 2022; Volokitina et al., 2022).

The methods employed in the field of severe plastic deformation in metallic materials and attaining structures with a grain size of nanometres are outlined below:

- High Pressure Torsion
- Equal Channel Angular Pressing
- Cyclic Extrusion Compression
- Accumulative Roll Bonding

2.3.1 Equal Channel Angular Pressing (ECAP)

Segal et al (1999) introduced the ECAP process, which involves extruding metal into a mould with angled channels. Typically, cylindrical or rectangular samples are used, and as they pass through the channels, a simple shear is applied at the corner of the deformation mould. If the dimensions of the two channels are equal, the sample size remains unchanged before and after the process. This allows for the possibility of re-extruding the sample in the ECAP mould (Figure 2.4).

This technique, known as equal channel angular extrusion (ECAE), is widely regarded as the progenitor of all SPD methods. The die employed in this process features a passageway for introducing the desired material, with an angular alteration positioned at the centre of the channel.

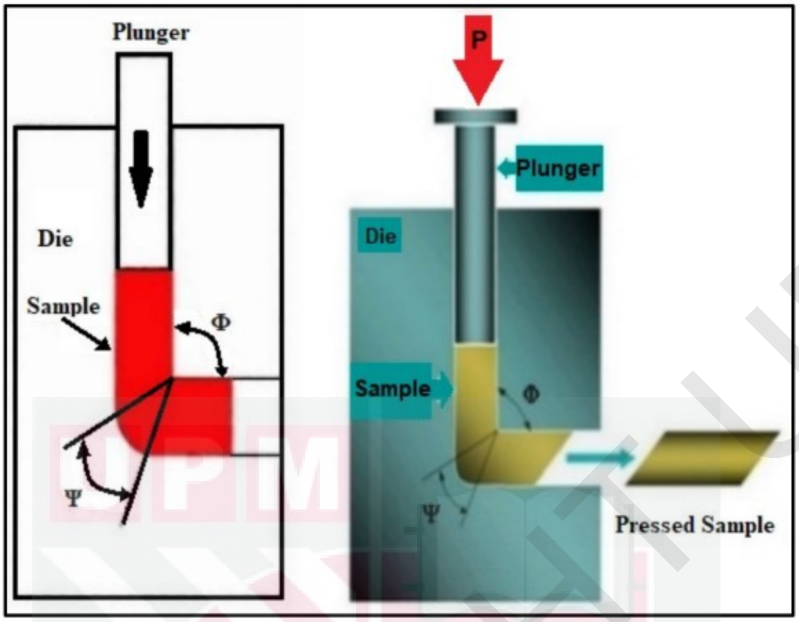

Figure 2.4 : Schematic image of the ECAP process (Baig et al. 2021)

In this way, the metal that is intended for undergoing intense plastic deformation is positioned within the channel and compelled into it from above using a mandrel. The metal components initiate bending and subsequently re-bending as they traverse the channel, ultimately attaining the desired angle. Consequently, the entire part undergoes significant deformation due to this process and emerges from the opposite end.

The determination of the severity of the deformation relies on various factors, including the channel angle, radius, and curvature of the vertex at different angles, as well as the control process parameters. It is important to highlight that due to the bonding of metal components in the moulds and the application of high hydrostatic pressure during the process, there is no risk of component cracking or fracture. This sets severe plastic deformation methods apart from conventional forming methods. The plastic strain applied in each cycle of equal channel angular pressing (ECAP) is determined by the angle and corner radius, which is approximately equivalent to a ninety-degree angle. The strain route in this process plays a critical role, and it has been observed that the rotation of the sample between ECAP cycles can influence the formation of the material's microstructure (Watanabe et al., 2004; Gibbons et al., 2018; Minarik et al., 2021; Baig et al., 2021).

Numerous researchers have conducted studies on this process, and some of their findings are mentioned as follows:

In their study, Dyakonov et al. (2017) investigated the changes in microstructure and the mechanisms responsible for strengthening in commercial-purity titanium when subjected to equal-channel angular pressing (ECAP). Through a comprehensive analysis of the microstructure, the researchers were able to quantify the contributions of different strengthening mechanisms.

They found that during the initial stages of ECAP, the material experienced a rapid strengthening, which could be attributed to a significant increase in dislocation density and the formation of deformation-induced boundaries. However, as the accumulated strain increased further, both the dislocation and grain-boundary density reached a saturation point, resulting in a decrease in the effectiveness of ECAP in terms of hardening at high strains.

Gibbons et al. (2018) investigated the process of microstructural refinement in an ultra-high strength martensitic steel using equal channel angular pressing. Through this technique, the initial grain sizes of the parent austenite were reduced from 188 µm to 14.8 µm, resulting in a corresponding reduction in the size of martensitic laths. As a result of this approach, the steel exhibited impressive mechanical properties, including a yield strength of 1.68 Gpa, ultimate strength of 1.98 Gpa, and an elongation of 16.1%.

Minárik et al. (2021) examined the impact of Zr on the process of dynamic recrystallization in Mg-Y-RE alloys during ECAP processing. The findings of the study revealed that the introduction of Zr in small quantities facilitate the creation of minute secondary phase particles. Consequently, these particles exhibited a reduction in size, accompanied by a denser distribution throughout the alloy.

Alateyah et al. (2021) investigated the improved Corrosion Behaviour of AZ31 alloy achieved through ECAP processing. The experimental results revealed that the implementation of ECAP processing, specifically through 1-P and 2-Bc routes, led to a significant reduction in the corrosion rate compared to the as-annealed counterpart. The corrosion rate decreased to 67.7% and 78.3% of the original value for the 1-P and 2-Bc routes, respectively. These findings highlight the potential of ECAP processing as an effective technique for improving the corrosion resistance of AZ31 alloy.

2.4 Equal Channel Angular Rolling (ECAR)

The ECAR, which is based on the ECAP process, is a method of severe plastic deformation. The key distinction lies in its capability to produce long, slender plates in a continuous manner and with the maximum number of passes. While the ECAP process is significant for generating materials with exceptional mechanical properties, it remains limited to laboratory-scale applications due to its discontinuous nature and inability to utilize thin plates. In order to address these challenges, the ECAR process has emerged as a solution, enabling the application of thin and elongated plastic plates without any dimensional alterations (Kvackaj et al., 2012; Kvackaj et al., 2017; Honarpisheh et al., 2019; Yan et al., 2020).

ECAR operations are carried out within the following dual processes:

- Symmetric rolling
- The formation of sheet in the mould of ECAR

The production of plates is achieved through the implementation of the symmetric rolling process. An illustration of this can be seen in the manufacturing of Magnesium plate (AZ31), which possesses a hexagonal structure and thick base plates. However, it should be noted that this particular process yields weak forming results when conducted at temperatures close to the ambient level (Cheng et al., 2007b).

In the subsequent plate forming process within the ECAR mould, the structure featuring base plates undergoes a reduction and transformation into non-base plates. This alteration enables the production of structures with non-original plates, characterized by delicate granulation and exceptional mechanical properties. This research was conducted on magnesium alloy utilizing the ECAR process. Figure 2.5 shows the schematic of the ECAR process (Bozcheloei et al., 2019).

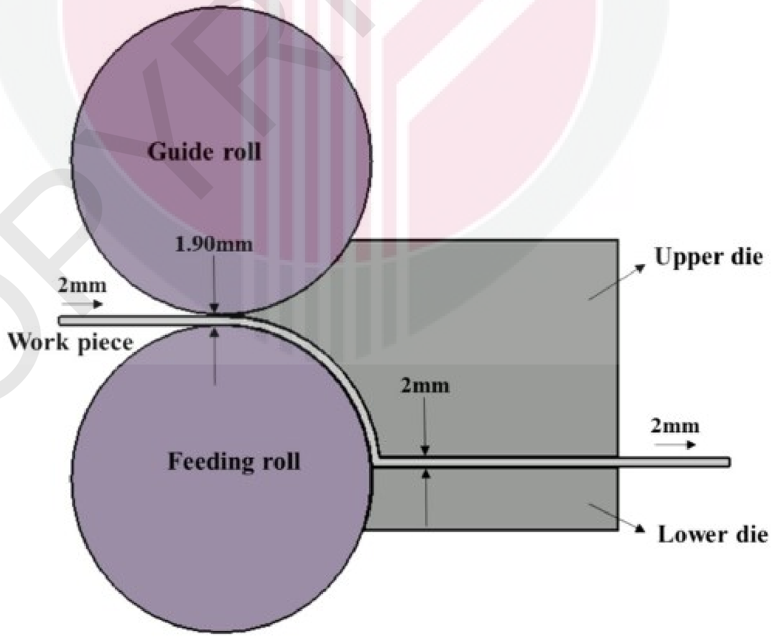

Figure 2.5 : Schematic of the ECAR process (Bozcheloei et al. 2019)

The metal plate is introduced into the ECAR process via the interaction between the rollers and the plate, resulting in the limitation of the maximum feeding force. This limitation is determined by factors such as a sufficient cause coefficient, an appropriate contact area, and the friction between the roller and the plate. In order to minimize the frictional force in the ECAR process, the cross-sectional area of the ECAR exit conduit is intentionally made slightly larger than the entrance duct. The design of the ECAR device aims to enhance shear deformation and create combined plate units. To ensure uniform plate thickness, the channel output gap in the angled orbiting ECAR plastic components is carefully controlled.

Numerous techniques have been employed to fabricate nanometre-scale materials, encompassing a variety of processes that can effectively diminish grain size through the application of severe plastic strain in metallic materials. This approach, aptly named due to its ability to achieve nanoscale dimensions, relies on the direct reduction of sample size from larger dimensions.

These processes have been suggested as novel industrial techniques for manufacturing materials with extremely fine-grained or nanocrystal line structures, and these methods have demonstrated their effectiveness in numerous instances. In light of this, the ECAR process has been identified as a viable means to achieve fine granulation and exceptional mechanical properties. The ECAR process, which involves severe plastic deformation, offers a promising approach to producing metals with grain sizes in the nanometre range. Furthermore, current study has revealed that the ECAR plate formation process may yield structural metal materials with non-base plates, exhibiting intricate granulation and superior mechanical properties (Bozcheloei et al., 2019).

Numerous factors within the ECAR process have been identified as influential parameters on the material or plate's properties and microstructure. These parameters include the number of rolling passes, the rolling path, the looseness between the plate and the channel, the mould structure, and the preheat temperature and time for both the mould and plates. Consequently, these factors have raised concerns among researchers. In terms of ECAR operations on plates, there are various options available, including 1 pass, 2 passes, 3 passes, 4 passes, and 5 passes, as well as two different routes, namely A and C (Honarpisheh et al., 2014). Extensive studies have been fulfilled in this area, some of which are being reviewed. Although the samples encompass four routes, namely A, B, C, and D, the experiments and tests have solely focused on routes A and C. This selection is based on the distance between Gap and Roll, which aligns with the thickness of the samples. To achieve this alignment, the sample is rotated 180 degrees.

After the initial pass in route A, the sample proceeded with a second pass on the same face without any rotation. The subsequent steps were carried out in a similar manner. However, in route C, following the first pass, the sample underwent a 180-degree rotation, and the second pass was executed on it.

Habibi and Ketabchi (2012) conducted an investigation into the fatigue characteristics of pure copper following an angular rolling process utilizing equal channels. The primary focus of their research was to examine the impact of this angular rolling process, specifically with equal ECAR channels, on the fatigue behaviour of pure copper sheets.

In their research, Kvackaj et al. (2012) implemented a comprehensive investigation on the microstructure, mechanical properties, and microhardness of ECAR-purified copper sheets. Through the utilization of electron microscopy, the researchers successfully showcased the capability of this particular process to effectively refine sample particles, achieving a remarkable reduction in size down to four hundred nanometre. The study encompassed a range of one to thirteen passes, providing valuable insights into the transformative effects of ECAR purification on copper sheets.

For the ECAR process, Mahmoodi et al. (2017) investigated the relationship between structural parameters and mechanical properties of Al5083 Sheets. The findings of their research revealed an increase in dislocation density and micro strain, while the crystallite size experienced a decrease.

Honarpisheh et al. (2019) studied the impact of equal channel angular rolling process on the fracture mechanisms of Al-7057 and Al-5052 alloys. The researchers observed that the ECARed Al-7075 samples in route A exhibited a higher incidence of fractures compared to the ECARed samples in route C. Furthermore, they found that the yield and tensile strengths of the alloys increased while the elongation decreased as the number of passes in each pair of sheets increased.

Eisaabadi et al. (2020) conducted an experimental investigation to examine the impact of temperature on the mechanical properties of aluminum sheets manufactured through the equal channel angular rolling process. The findings of their study demonstrated that as the number of ECAR passes increased at a particular temperature, the tensile strength, ultimate tensile strength, and micro-hardness of the sheets also increased. However, it was observed that the rate of increase in these properties was higher during the initial passes compared to the later passes. Conversely, the elongation to fracture decreased as the number of passes increased.

2.4.1 Microstructure

Habibi et al. (2017) studied the fatigue behaviour of nano-grained pure copper following equal channel angular rolling. The researchers utilized various microscopic techniques to analyse the material's characteristics. The scanning electron microscopic micrograph (Figure 2.6 (a)) provided a visual representation, while the atomic force microscopic micrograph (Figure 2.6 (b)) offered a detailed view of the surface. Additionally, the grain-size profile (Figure 2.6 (c)) depicted the sizes of sub-grains ranging from seventy to five hundred nanometre. The grains resulting from the four-pass ECAR process exhibited an irregular, somewhat elongated shape and a distinct orientation. Furthermore, the SEM image of the ECARed specimen revealed the presence of copper particles within the microstructure.

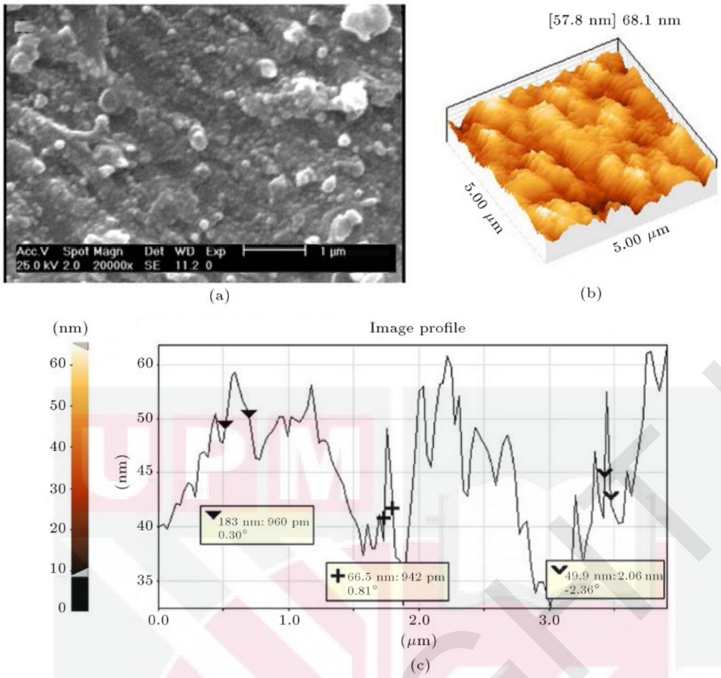

Figure 2.6 : a) SEM pic b) microscopic micrograph c) grain size (Habibi et al. 2017)

Kvackaj et al. (2017) investigated the evolution of microstructure and mechanical properties of copper through the application of equal channel angular rolling. The researchers observed a progressive reduction in grain size, from an initial value of 40 µm, to a final size of 250 nanometre, as the number of rolling passes increased.

In their study, Rahimi et al. (2018) utilized the equal channel angular rolling technique to examine the forming limit diagrams of fine-grained Al 5083. The researchers subjected heated samples to a three-pass ECAR process in route A, and the results are presented in the following figure. The grain size of the samples was determined using the photo tool software. The annealed sample exhibited an average grain size of roughly 45 µm, featuring a heterogeneous structure with angular grains (Figure 2.7 (a)). On the other hand, the grains of the sample subjected to the third pass of ECAR were reduced to 10 µm (Figure 2.7 (b)).

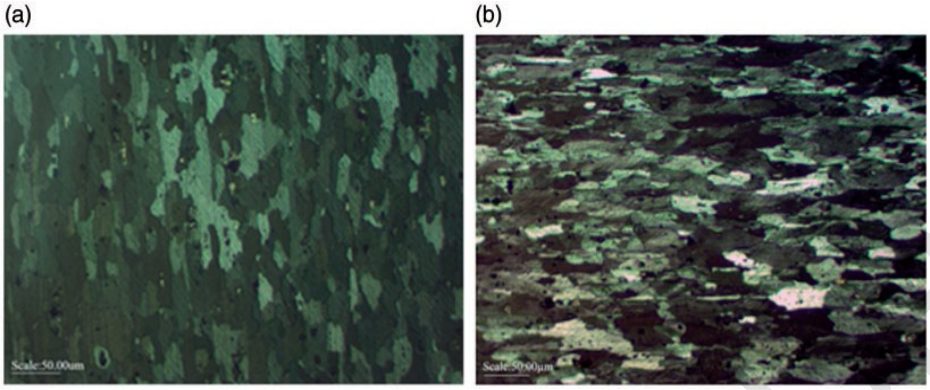

Figure 2.7 : a) before ECAR process b) after 3 passes (Rahimi et al., 2018)

Honarpisheh and Mansouri (2018) conducted an investigation on the mechanical properties of titanium alloy using the equal channel angular rolling process. The initial grain size of the controlled sample was reported to be 10.5 µm. Subsequently, after undergoing the annealing process, the grain size coarsened to 11 µm. As the equal channel angular rolling process progressed, the grain size decreased to 6.5 µm after the first pass, followed by a further reduction to 5.5 µm after the second pass. The third pass resulted in a grain size of 3.5 µm, and finally, after the fourth pass, the grain size reached 3 µm (Figure 2.8).

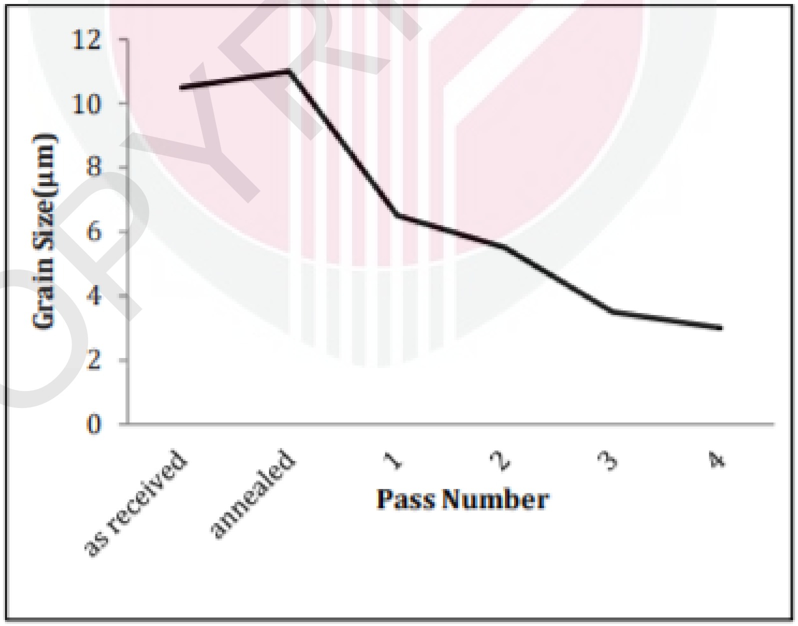

Figure 2.8 : The grain size curve of Ti in different passes
(Honarpisheh and Mansouri 2018)

Mahmoodi and Naderi (2019) examined the microstructure of Al6061 alloy sheets that underwent equal-channel angular rolling, and explored its correlation with mechanical properties. The optical micrographs presented in Figure 2.9 depict both the original sample and the three-pass ECARed samples. It is evident that the ECARed sheets exhibit a finer grain size and a more uniform microstructure compared to the initial sample. Furthermore, an elongated structure predominantly aligned in the ECAR rolling direction was observed following the completion of the third pass.

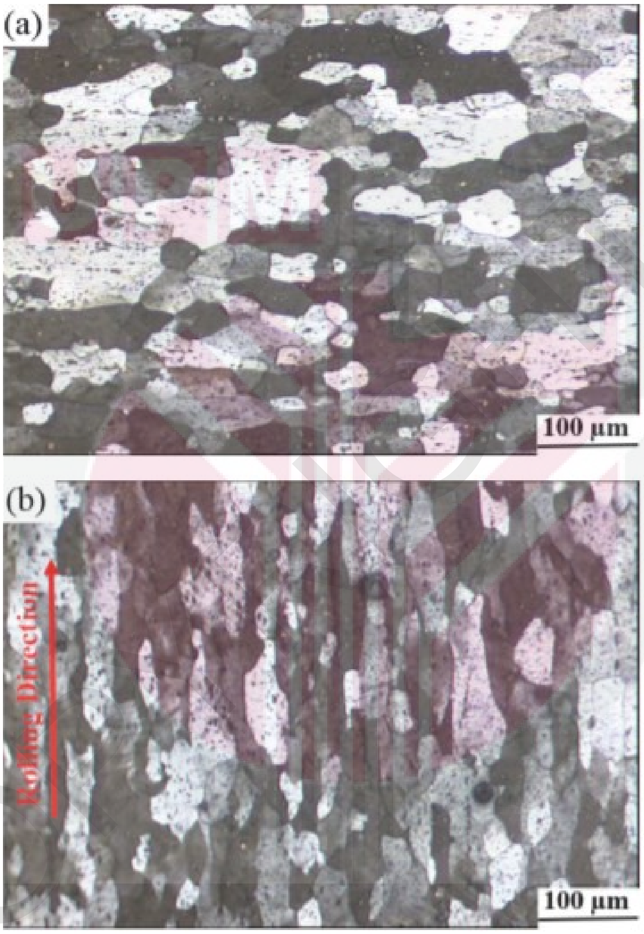

Figure 2.9 : Optical micrographs of the a) initial sample, b) after three passes (Mahmoodi & Naderi, 2019)

The mean size of the grains is roughly 25 µm, exhibiting a disorientation angle exceeding 15°. During the initial stages of the ECAR procedure, dislocations commence their arrangement into sub-grains, which are expected to transform into ultra-fine grains possessing more pronounced high-angle grain boundaries in subsequent passes.

2.4.2 Impact of the Channel Looseness on Crystals

In order to examine the impact of channel looseness between the ECAR mould and plates, Magnesium alloy plates with varying thicknesses of 1.5 mm, 1.7 mm, and 1.9 mm were utilized. The looseness between the two rollers was assumed to be 1.4 mm, 1.6 mm, and 1.8 mm, respectively, for each stated thickness. To analyse the consequences of this looseness, the samples underwent preheating at 350 °C for a duration of 5 minutes in a furnace prior to the commencement of the operation (Cheng et al., 2007a).

When the thickness of the sheet is small and its width is large, the strain in the transverse direction cannot be taken into account. In this process, there is no lubrication between the sheet and the rollers. The coefficients of friction between the rollers and the plate were calculated to be 0.4 for the hot process of magnesium alloy, and the coefficient of friction between the channel and the frame plate was estimated to be 0.12. Magnesium alloy is sensitive to changes in strain rate and heat during hot extrusion. The experimental results are presented in equation 2.1 (Cheng et al., 2007a).

$$\dot{\varepsilon}_s = A_1(\sigma_s)^n \exp\left(\frac{Q}{RT}\right) \quad \textbf{(2.1)}$$

where A_1 remains constant. n represents the degree of work hardening; Q denotes thermal energy and R signifies the constant for gases.

$A1=2.3\times10^{-8}$

n=8.43

Q=112000

Figure 2.10 illustrates transformation in the mould during one ECAR operation.

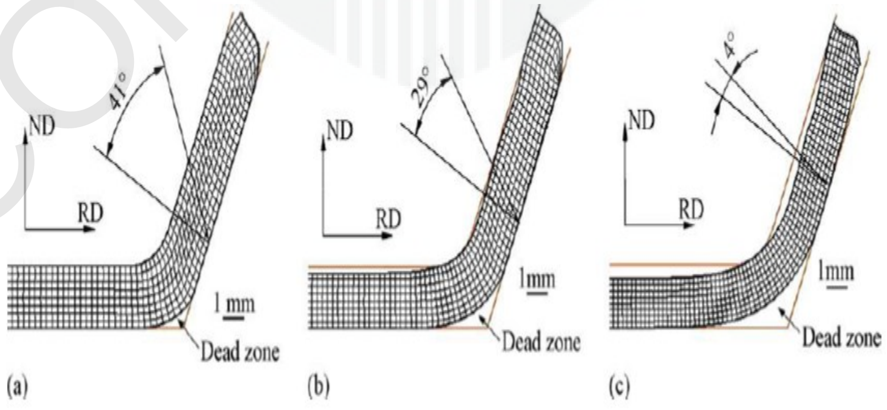

Figure 2.10 : FEM-predicted grid distortions for different channel clearance in ECAR process: (a) c = 1.00; (b) c = 1.13; (c) c = 1.29 (Cheng et al., 2007a)

The dissimilarity in shear deformation and shear strain caused by changes in the looseness of the mould is evident in Figure 2.10. In figure (a), where there is approximately 1 mm of looseness, the cutting angle measures around 41 degrees. The alteration in shapes observed in the figure signifies that the shear deformation is not evenly distributed across the thickness, particularly in the plate (Lee et al., 2002).

The presence of diagonal levels radius has multiple effects on the shear deformation and strain cut in a plate. Firstly, it increases the shear deformation zone while simultaneously reducing the strain cut. Additionally, it leads to non-uniform shear deformation at the upper level of the plate. Although it is possible to eliminate this radius by considering r = 0, it is crucial to note that this would result in the production of plates. In Figure 2.11, it can be observed that as the gap between the plate and the mould widens, the shear strain decreases and the cutting form becomes more consistent. Moreover, both the top and lower layers of the plates undergo non-uniform changes, and the dead zone expands accordingly (Cheng et al., 2007a).

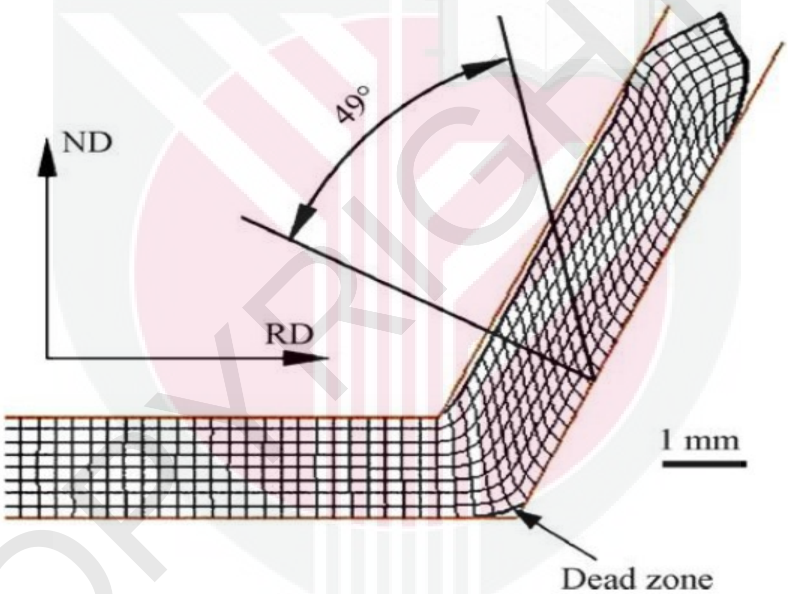

Figure 2.11 : Grid distortions for ECAR processing with an oblique radius of 0 mm were predicted by FEM (Cheng et al., 2007a)

Shear deformation occurs when the clearance is 1 mm, as depicted in Figure 2.11. Once the temperature falls below 225 °C, the base plates initiate slipping, leading to the deformation of the twins. Twinning serves as a significant mechanism for plastic deformation in certain metallic materials, exerting a shear force capable of causing atomic displacements. When the arrangement of atoms in one grain can be obtained by reflecting across a shared plane from another grain, they are considered twinned. The crystal structure of both grains remains identical.

If the temperature is high and additional slip plates are in operation, the base plate undergoes shear deformation and aligns itself parallel to the cut during ECAR operation. Consequently, the grain directions are altered. As a result, the base plate becomes weakened and extraneous plates are formed.

Due to the heightened shear strain and diminished angle resulting from ECAR operations, the cutting angle has the potential to be diminished. Therefore, it can be inferred that the orientation of crystal directions can be controlled through the introduction of looseness (Pérez-Prado et al., 2005).

Nevertheless, it is comprehensible that the ECAR methodology encounters heightened challenges when the looseness attains a value of 1. In instances where the looseness surpasses one, the thickness of the plate can be augmented subsequent to traversing the corner of the ECAR mould. This augmentation is necessitated by the intricate strain imposed on the plate as a result of the complex exertion of strain.

The augmentation of thickness results in an elevation of friction, which, in turn, can induce shrinkage in the specimen. However, a certain degree of slackness is necessary for the fabrication of plates. Consequently, the cutting angle could be reduced to facilitate the loosening process, which subsequently hampers the precise regulation of crystal orientations. Hence, it is imperative to carefully evaluate the appropriate level of slackness and establish a strong correlation between the loosening and crystal orientations.

The AZ31 plate can undergo an operation to enhance its grain structure, resulting in a finer grain. This process involves annealing the plate at a temperature of 264 °C for a duration of one hour, as illustrated in figure 2.12 of the study conducted by Cheng et al. in 2007b. To further improve the grain structure, it is possible to increase the number of ECAR passes and subsequently anneal the final product.

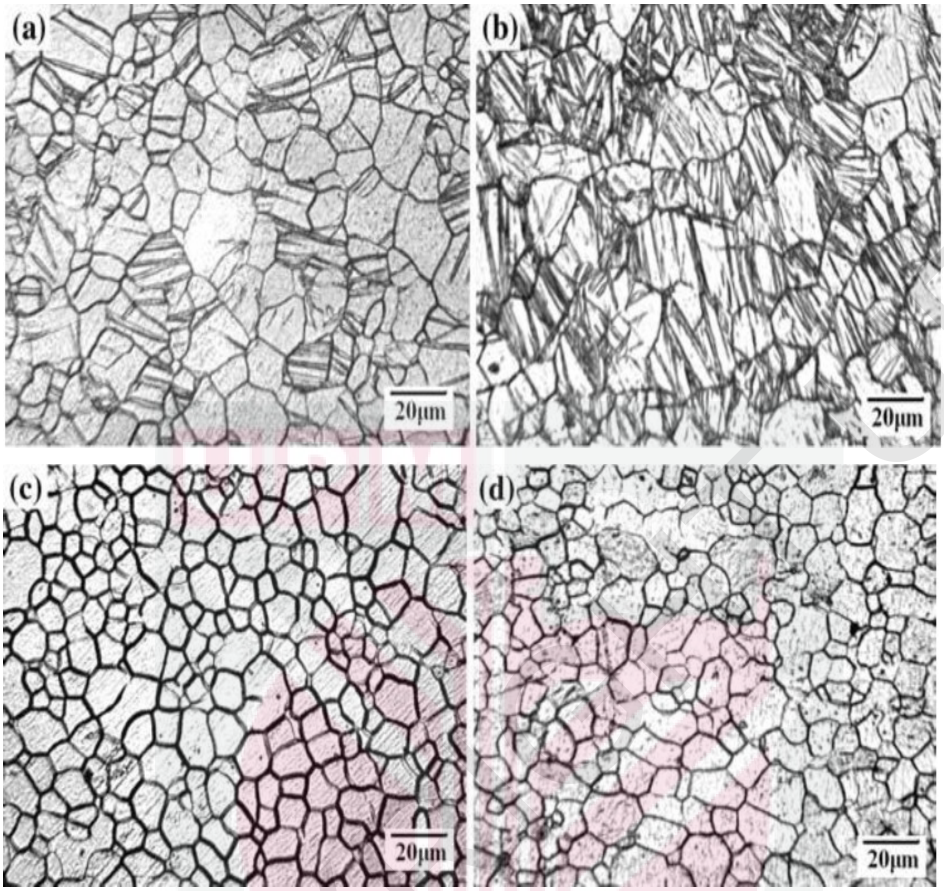

Figure 2.12 : Microstructure (AZ31) (a) normal sample before annealing (c) normal sample after annealing (b) non-annealing ECAR sample (d) an acted ECAR sample (Cheng et al. 2007b)

2.4.3 Mechanical Properties

Azimi and colleagues (2012) conducted a comprehensive investigation into the mechanical properties and microstructure evaluation of Al 1100 during multiple passes of the ECAR process. In Figure 2.13, the tensile properties of the original prototype and ECAR sample are illustrated, considering various passes and paths. The SPD process, implemented through the ECAR technique, leads to a notable enhancement in both tensile strength and yield stress, while simultaneously causing a decrease in elongation. ECAR tensile properties against various passes are illustrated in Table 2.1 and Figure 2.14.

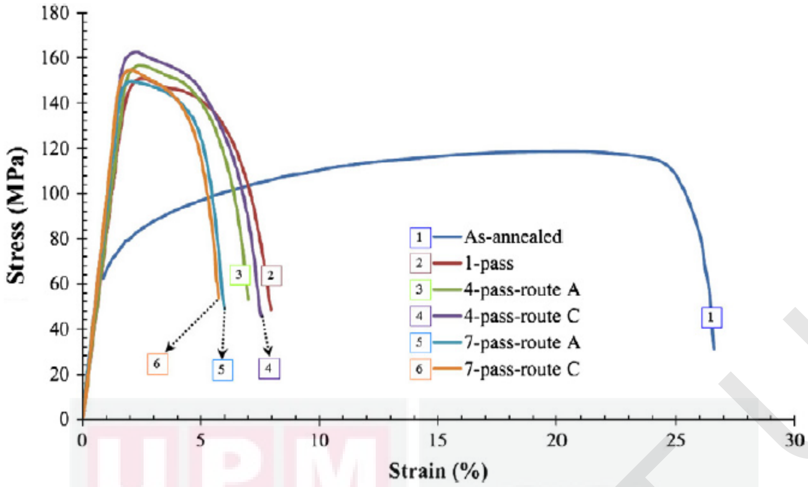

Figure 2.13 : Aluminium stress-strain diagram (Azimi et al. 2012)

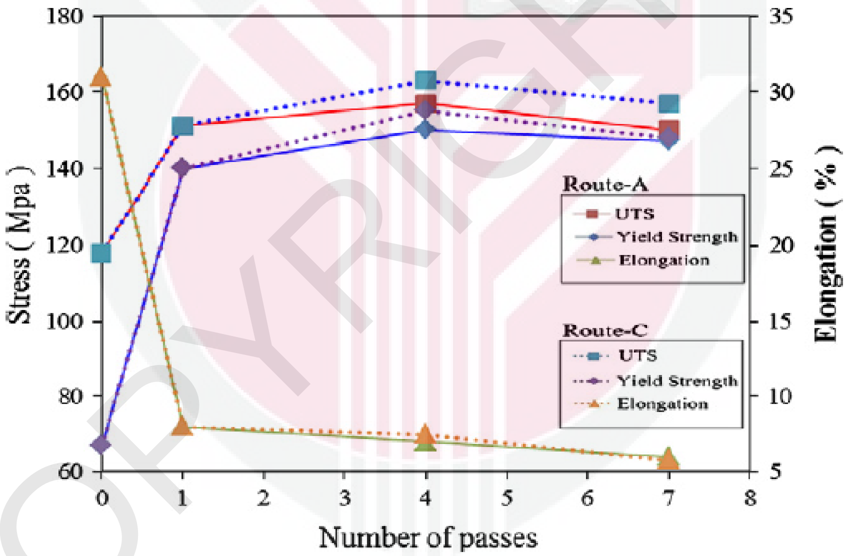

Figure 2.14 : Stress-strain diagram by number of passes (Azimi et al. 2012)

Table 2.1 : Stretching properties for different of passes

Process parameters	YS (MPa)		UTS (MPa)		E (%)		Microhardness (Hv)	
	Route-A	Route-C	Route-A	Route-C	Route-A	Route-C	Route-A	
							At the surfaces	At the middle of thickness
1 pass	140	-	151	-	8	-	38.8	36.6
4 passes	150	155	157	163	7	7.5	42.3	37.2
7 passes	147	148	150	157	6	5.8	45.2	38.4
As-annealed	67		118		31		25.5	

(Azimi et al. 2012)

It is evident from the results that following the initial pass, the yield strength and ultimate tensile strength exhibited an increase from 67 to 140 and 118 to 151 Mpa, respectively. Conversely, the percentage of elongation experienced a decrease from 31% to 8%. These notable alterations in the mechanical properties can be attributed to the occurrence of strain hardening and dislocation resonance processes, which are induced by the implicit dislocation borders.

During the initial pass, ECAR implemented wider intervals to segregate the grains, leading to the formation of fine grains with a substantial dislocation density ratio. This phenomenon greatly influences the strength subsequent to the first pass. At this stage, the dislocation density within and outside the primary coarse grain escalates, accompanied by the formation of numerous low-angle grain boundaries. Following the fourth pass, both the yield strength and ultimate tensile strength experience enhancements, reaching 150 and 157, respectively. However, the elongation diminishes to 7%, which is 1% lower than that observed after the first pass.

Honarpisheh et al. (2014) conducted an investigation into the mechanical properties of an explosive-welded Al-Cu bimetal using ECAR routes. The authors examined the stress-strain behaviours of Al-Cu bimetals, specifically those subjected to two and eight passes in routes A and C. These findings were obtained through a tensile test and are illustrated in Figure 2.15.

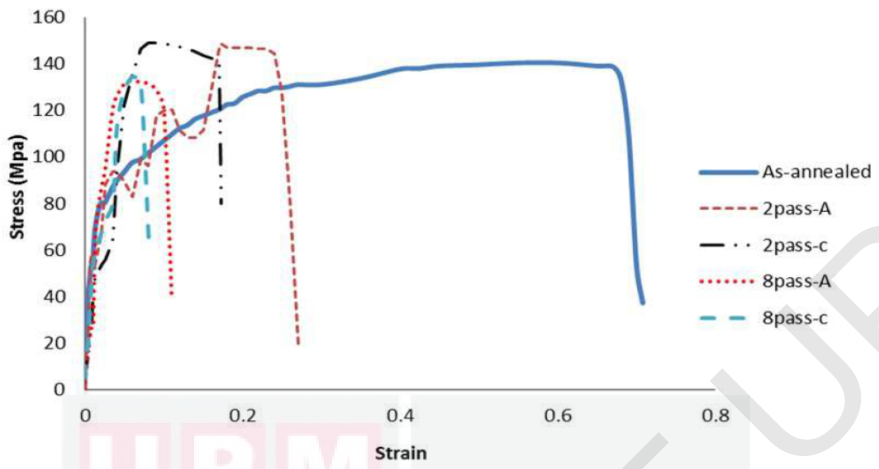

Figure 2.15 : Stress-strain chart on Al/Cu in different passes
(Honarpisheh et al. 2014)

As it is illustrated, the stress-strain curves exhibit enhanced strength and decreased elongation after undergoing the ECAR process. Moreover, in the second and eighth passes, the tensile strength in route C surpasses that in route A. Notably, the investigation reveals a substantial increase in tensile strength after the initial pass.

Strain hardening and dislocation strengthening are two crucial factors in enhancing the strength of materials. In the context of ECAR testing, two models can be examined to understand the process of sample strengthening. The first model suggests that the stress required to induce dislocation loops, originating from Frank-Read sources, within a collection of larger grains with a critical semicircle structure, governs the plastic flow in a nanocrystal line material. On the other hand, the second model proposes that material strengthening during significant deformations can be attributed to two mechanisms. The first mechanism is dislocation strengthening, which arises due to the presence of incidental dislocation boundaries. The second mechanism is grain strengthening. (Honarpisheh et al., 2014).

The Hall-Petch relationship (Honarpisheh et al. 2014) leads to the strengthening of boundaries through the formation of geometrically essential borders. These borders are created due to variations in slip systems operating in nearby grains or local strain differences within each grain. It is worth mentioning that the eighth pass of the ECAR procedure does not have a notable impact on the strength and elongation of the sample. Figure 2.16 illustrates the changes in yield and tensile strength for routes A and C as the ECAR pass number increases.

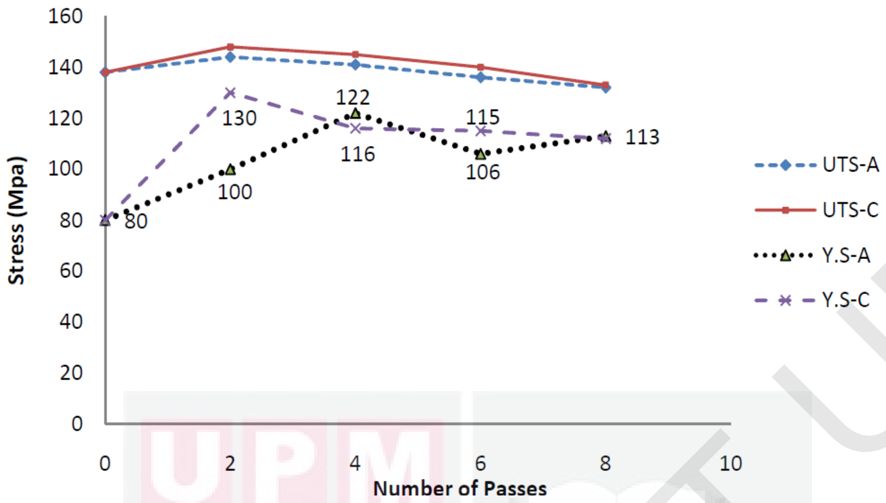

Figure 2.16 : Yield and tensile strength chart in different passes and different routes (Honarpisheh et al. 2014)

Kotobi and Honarpisheh (2017) utilized uncertainty analysis to determine the residual stresses in Al-1060 strips that underwent equal-channel angular rolling and were measured using the slitting method. The findings of the tensile test conducted are illustrated in Figure 2.17. It was observed that the one-pass ECARed sample exhibited a yield strength (YS) of 132 MPa and an ultimate tensile strength (UTS) of 143 MPa, whereas the control sample had YS and UTS values of 113 MPa and 128 MPa, respectively. Furthermore, the elongation value decreased from 10.3% in the control sample to 7.3% in the one-pass sample. These results indicate that the ECAR process has an impact on the mechanical properties of the sample.

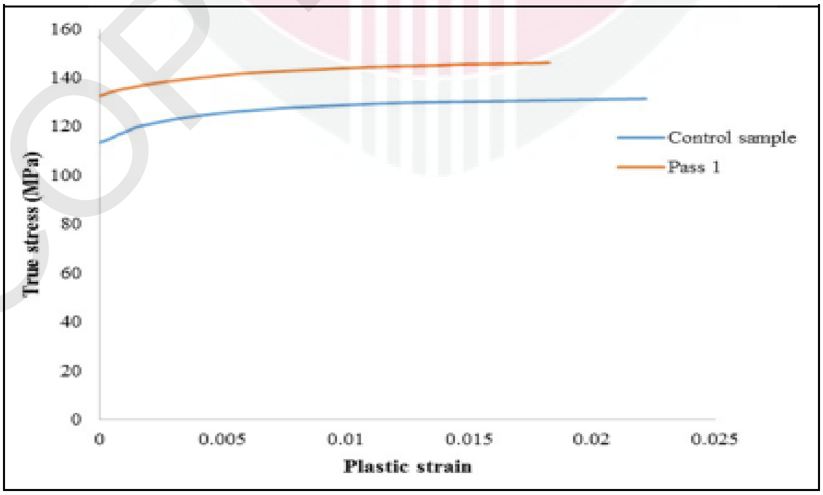

Figure 2.17 : Stress–Strain curves of control and 1-pass samples (Kotobi & Honarpisheh 2017)

Sedighi et al. (2017) conducted a comprehensive study on the mechanical properties and fatigue life of ECARed AA5083 aluminium alloy. The investigation involved multiple passes of rolling, and the results revealed interesting findings regarding the yield strength of the alloy. Upon the completion of the first pass of rolling, the yield strength of the sample exhibited a significant increase of 54%. This trend was observed consistently for the second and third passes as well, although the rate of increase in yield strength gradually decreased. Comparing these values to the yield strength of annealed sheets, which was measured at 145MPa, it is evident that the rolling process had a substantial impact on enhancing the mechanical properties of the alloy. Specifically, after the first pass of ECAR, the yield strength rose to 223MPa. Subsequent passes further elevated the yield strength to 230MPa and 286MPa for the second and third passes, respectively. Furthermore, the stress-strain curve analysis revealed interesting behaviour during the second pass of rolling. The curve exhibited a smooth transition between the elastic and plastic regions, indicating the alloy's ability to deform plastically without undergoing significant structural damage (Figure 2.18).

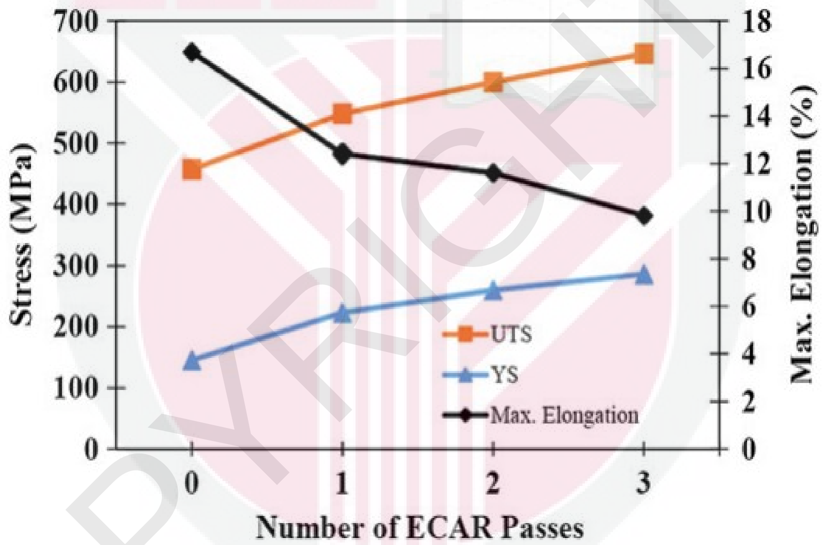

Figure 2.18 : Variations in multi-pass ECAR for Y.S, U.T.S, and elongation (Sedighi et al. 2017)

Honarpisheh and Mansouri (2018) examined the mechanical properties of titanium alloy during the equal channel angular rolling process. The stress-strain diagram obtained from their experimental analysis demonstrated noteworthy changes. Following the initial pass, both the ultimate tensile strength and yield strength exhibited a significant increase. As the process continued with a second pass, the trend of improvement persisted, albeit at a slower pace compared to the first pass. Surprisingly, after the third pass, the tensile strength did not show any further enhancement; instead, it experienced a decrease before eventually rising again during the fourth pass, reaching higher values (Figure 2.19 and Figure 2.20).

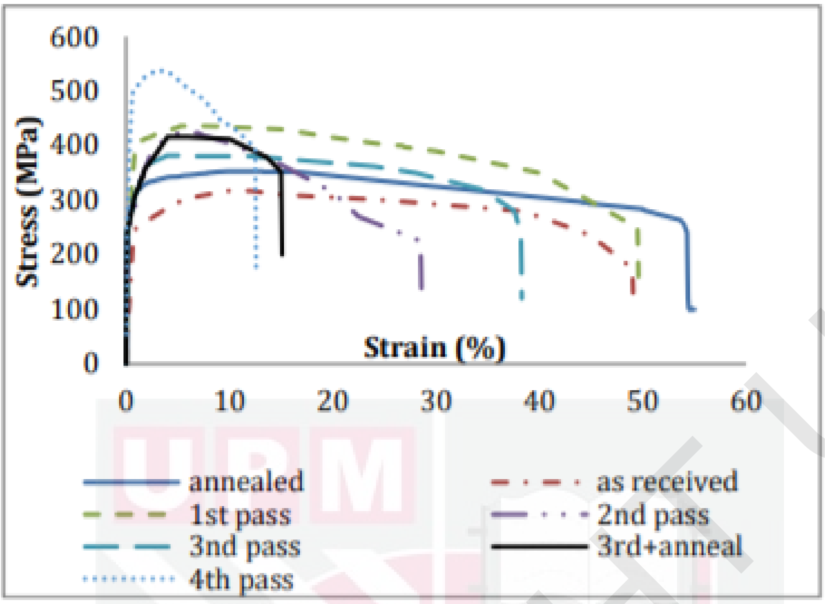

Figure 2.19 : The stress-strain curve obtained in various passes
(Honarpisheh and Mansouri, 2018)

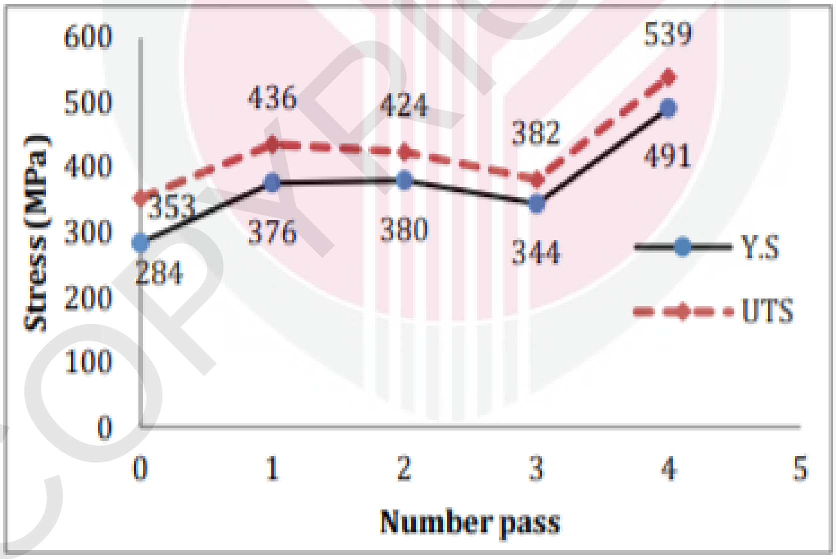

Figure 2.20 : Yield and ultimate tensile strength curve in different number of passes
(Honarpisheh and Mansouri, 2018)

In their study, Honarpisheh et al. (2019) examined the impact of the equal channel angular rolling process on the fracture mechanisms of Al-7057 and Al-5052 alloys. Figure 2.21 illustrates the findings by focusing on the yield stress, tensile strength, and elongation of Al-7075 samples for routes A and C, as well as Al-5052 on route C. Upon analysing the results, it is evident that the yield strength of the Al-7075 sample reached 253 MPa after the first pass. This increase in yield strength can be attributed to the work-hardening mechanism. In route A, the tensile strength remains unchanged until the fourth pass, but it reaches its maximum value after the fifth pass, showing a 13% increase. On the other hand, route C exhibits the highest tensile strength, with a subsequent decrease observed after the fifth pass. For the Al-5052 sample, the tensile strength increases by 7% after the first pass and further increases to 21% after the second pass. However, the tensile strength decreases from the third to the fifth pass. Similarly, the yield strength shows a steep increase after the first pass, followed by a decreasing rate in subsequent passes. The yield strength improves by 52% and 48% in the Al-7075 and Al-5052 samples, respectively. The researchers attribute the significant increase in yield stress to the work-hardening phenomenon observed in all samples after the first pass. They suggest that the formation of sub-grains contributes to the enhanced strength of highly deformed aluminium alloys. Notably, the Al-7075 sample in route A achieves the highest strength after the fifth pass, with a 70% increase compared to the annealed sample. Additionally, the strength of route C increases by approximately 80% after the fourth pass. Comparing the results of routes, A and C for the Al-7075 alloy, it is evident that route C exhibits greater strength values. This difference may be attributed to the 180° turn in each step of route C, leading to a more homogeneous and coaxial strain distribution compared to route A. Figure 2.21 illustrates how the yield strength of the Al-5052 sample increases to 74% compared to the annealed sample.

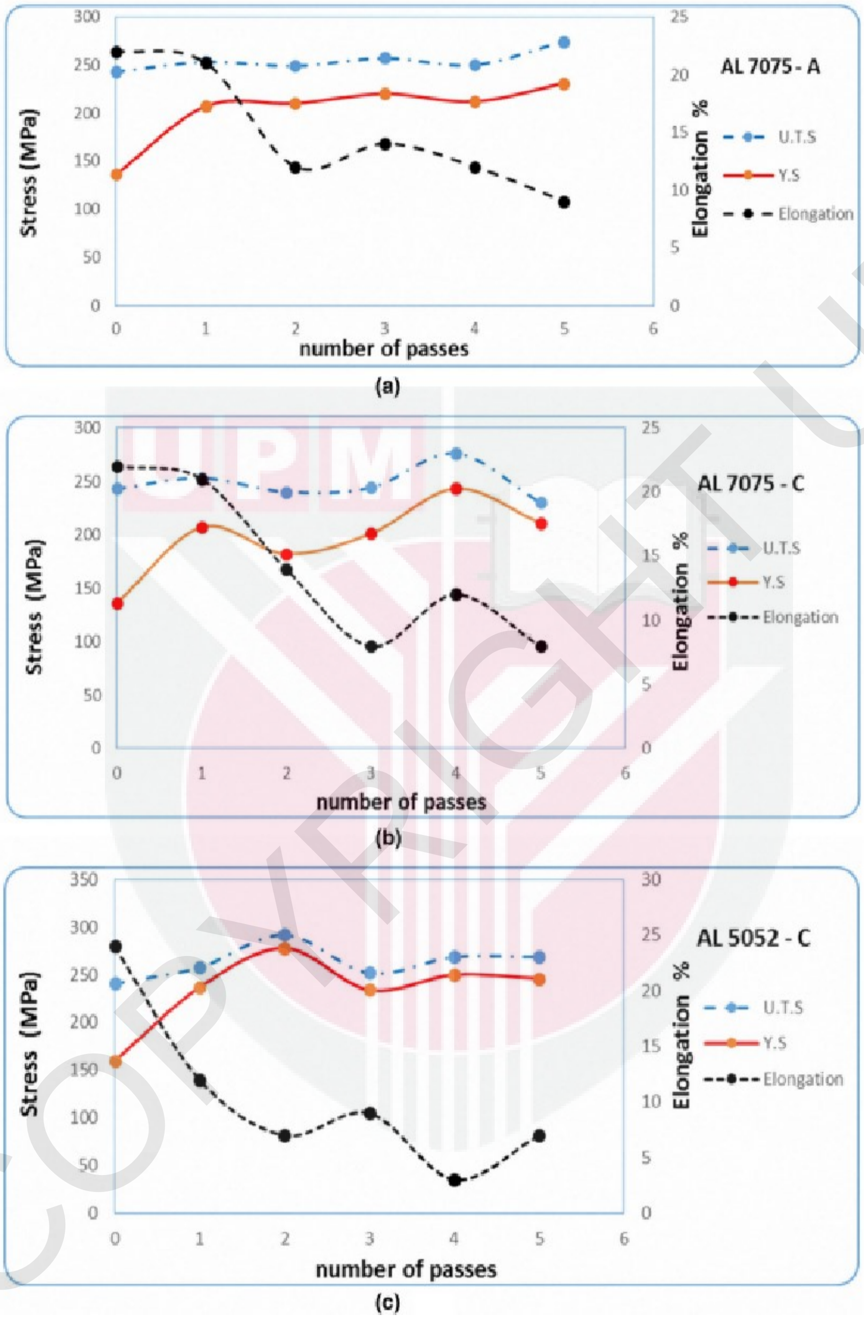

Figure 2.21 : Variations in yield and ultimate tensile strength and elongation for samples: (a) Al-7075 in the route A, (b) Al-7075 in the route C, and (c) Al-5052 in the route C (Honarpisheh et al. 2019)

2.4.4 Hardness Measurement

Cheng et al. (2007b) reported that ECAR processing significantly improves the flexibility of a magnesium alloy plate at room temperature. Figure 2.22 illustrates the correlation between sample orientation and strain hardening power, which is determined using equations that accurately represent the real stress-strain relationships. In comparison to a standard steel plate suitable for deep drawing, which typically exhibits a strain hardening value ranging from 0.2 to 0.5, prototypes of the magnesium alloy plate exhibit a relatively lower strain hardening value of approximately 0.165.

Prototypes exhibit a limited degree of flexibility, amounting to only 20% and process of deep drawing at room temperature in a cold state finds limited applications. The strain hardening exponent for ECAR samples stands at 0.304 on average, signifying an enhanced capability for deep drawing in these specimens; nevertheless, the underlying mechanical factor responsible for this improvement lies in the alteration of crystallographic orientation.

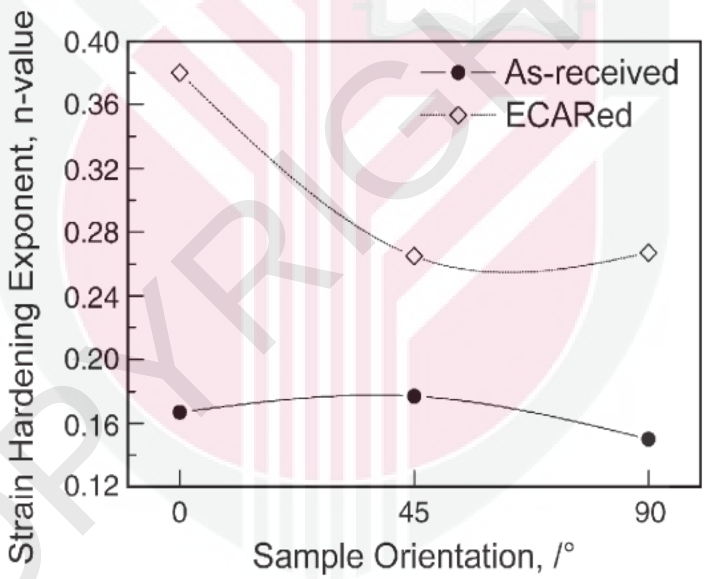

Figure 2.22 : Strain hardening chart in different angles (Cheng et al. 2007b)

Figure 2.23 illustrates that the sample subjected to zero-degree strain exhibits isotropy, characterized by an anisotropic ratio of 1/29. Conversely, in the ninety-degree direction, a significant degree of stress anisotropy is observed, with a value of 3.36 at ambient temperature.

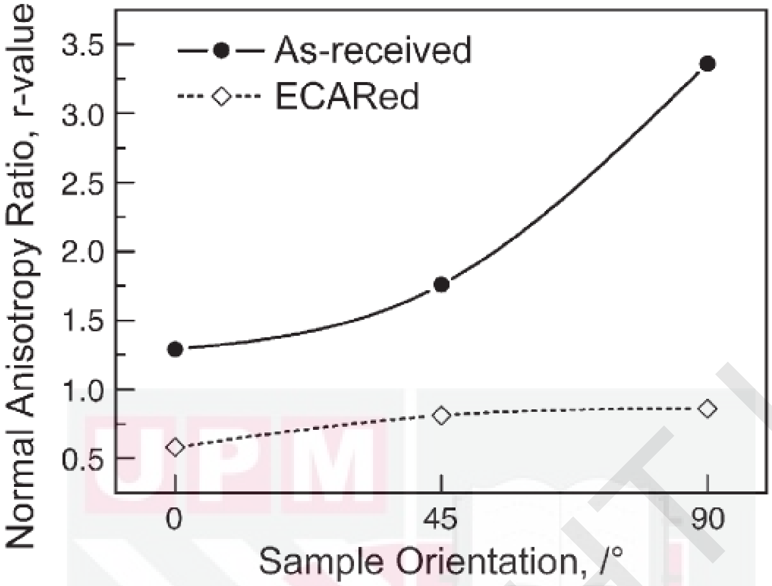

Figure 2.23 : Graph of heterogeneous changes in terms of various angles (Cheng et al. 2007b)

Habibi and Ketabchi (2012) examined the fatigue characteristics of pure copper following a rolling procedure utilizing equal channels. Figure 2.24 illustrates the division of the temperature stability curve into four distinct regions. The micro hardness level remains constant at temperatures below room temperature, up to 210 °C, with a marginal rise observed at exceedingly high temperatures. The augmentation of microhardness can be attributed to the formation of cellular structures through the arrangement of dislocations.

Different processes of severe plastic deformation can lead to an observed rise in microhardness after undergoing annealing at low temperatures. The microhardness experiences a decrease in the range of 210 to 250° due to the recrystallization of new grains without internal dislocation. Moving on to the third region on the thermal stability chart, which spans from 250 to 350 degrees, a consistent decline in microhardness is observed. This decline can be attributed to the growth of grains within the material being studied.

The microhardness remains relatively stable in the fourth section of the chart, indicating a consistent value. Additionally, this section is distinguished by rapid growth in material gain. By analysing this graph, it is possible to estimate the recrystallization temperature. After undergoing eight ECAR passes, the recrystallization temperature of pure copper is estimated to be approximately 230 °.

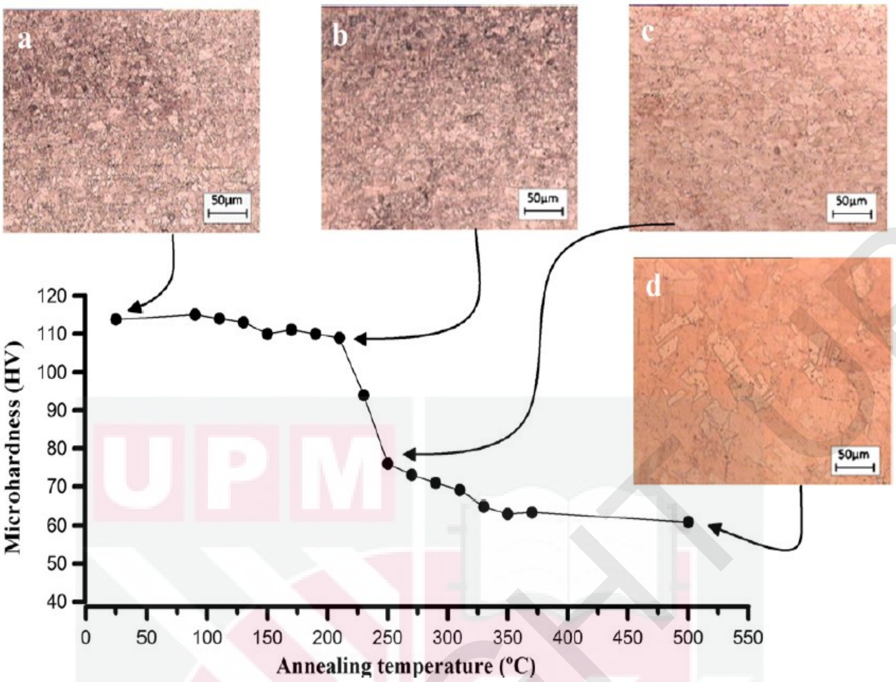

Figure 2.24 : Micro hardness chart according to temperature
(Habibi and Ketabchi 2012)

Honarpisheh et al. (2014) studied the mechanical properties of an explosive-welded Al/Cu bimetal using the ECAR process across various routes. The authors presented their findings in Figure 2.25, which illustrates the changes in hardness based on the number of ECAR passes for routes A and C.

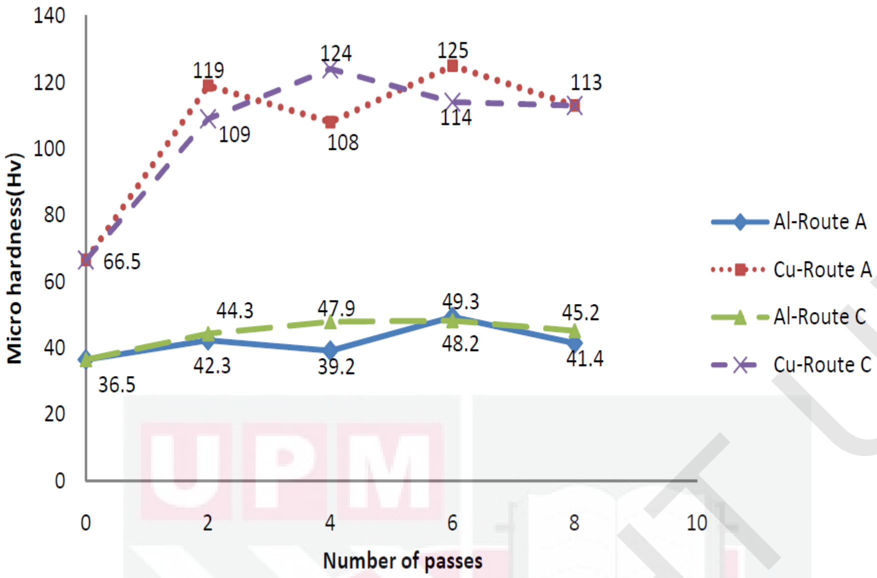

Figure 2.25 : Microhardness chart on Al and Cu in different passes and routes (Honarpisheh et al. 2014)

After undergoing two cycles of the ECAR process, it can be observed that the microhardness values in the Cu and Al layers experience an increase. Specifically, the microhardness in the Cu layer rises to 119 Hv from an initial value of 66.5 Hv, while the microhardness in the Al layer increases to 109 Hv from 44.3 Hv. Similarly, the microhardness in the Al layer increases to 42.3 Hv from 36.5 Hv.

The significant increase in microhardness during the first pass is attributed to strain hardening rather than grain refinement. This can be attributed to the formation of sub-grain boundaries (Honarpisheh et al., 2014).

However, subsequent passes do not exhibit significant variations in microhardness. It is worth noting that the rate of microhardness improvement reaches a saturation point in the subsequent passes. This behaviour may also be observed in other SPD processes. The strengthening observed in the subsequent passes is likely due to a rapid increase in dislocation density, followed by dislocation reorganization into sub grains (cells) and grain refinement (Honarpisheh et al., 2014).

Honarapisheh et al. (2018) conducted another study to examine the residual stress and mechanical properties of St12 (steel) strips that underwent equal-channel angular rolling. The microhardness of the HV samples is illustrated in Figure 2.26. Upon analysing the results, it was observed that after the initial ECAR process, the microhardness of the samples significantly increased from 117 HV in the control sample to 174 HV. Furthermore, the microhardness exhibited a change in slope, indicating a shift towards a tensile behaviour. This notable increase in hardness following a single pass of ECAR may be a consequence of strain hardening.

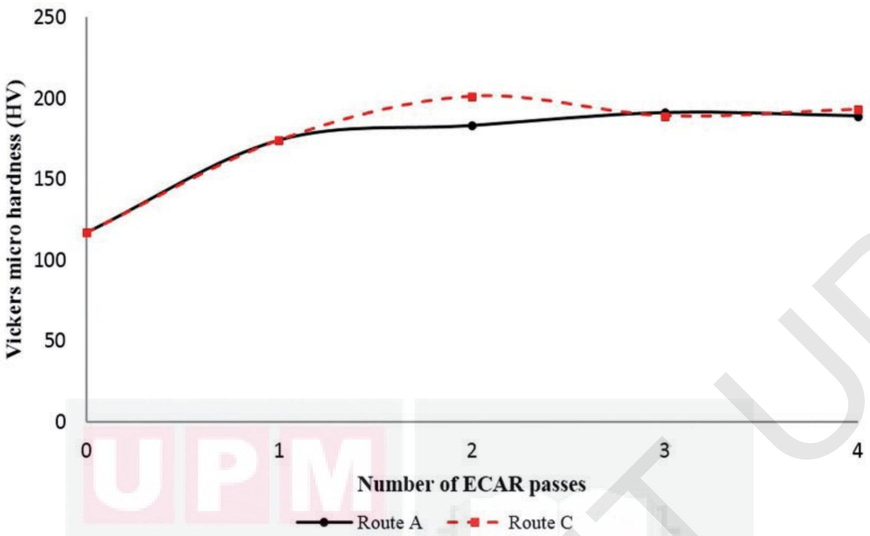

Figure 2.26 : Microhardness graph on ST12 in different passes and routes (Honarpisheh et al. 2018)

Rahimi et al. (2018) made enhancements to the Fine-grained Al 5083 forming limit diagrams that were initially created using equal channel angular rolling. The microhardness values of the ECARed samples were examined across the sheet thickness, as depicted in Figure 2.27. It is evident that there is a significant increase in the micro-hardness values after the first pass of the ECAR process, with an approximate 37% rise compared to the annealed samples. The third pass resulted in the highest level of microhardness, exhibiting a 73% increase in comparison to the annealed sample. However, the values slightly declined after the fourth pass due to the presence of large cracks on the sheet surface.

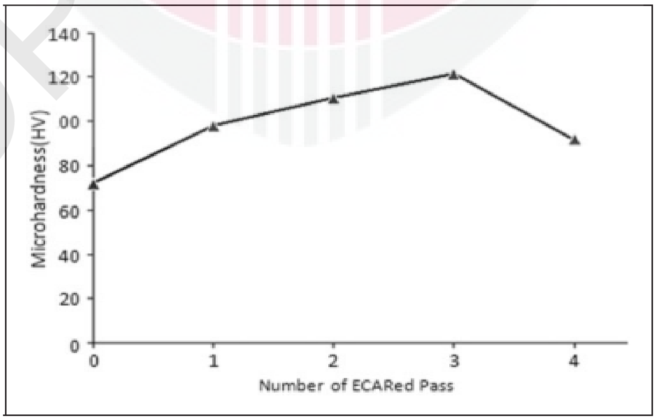

Figure 2.27 : Microhardness variations determined by the number of ECARed passes (Rahimi et al. 2018)

Honarpisheh et al. (2019) investigated the influence of annealing heat treatment on the bond strength of explosive welded copper/steel after the ECAR process. The researchers analysed the changes in hardness for three different bonding zones between copper and stainless steel, based on the number of ECAR passes. The graphs presented in Figure 2.28 clearly demonstrate an increasing slope, indicating the impact of ECAR on hardness enhancement. According to the findings of the study, the steel region exhibited the highest hardness value of 262 HV, followed by the weld bond at 143 HV, and the copper region at 135 HV. To further understand the effects of thermal treatment, the component was annealed during this particular pass (four), as it yielded the highest hardness rate across all locations.

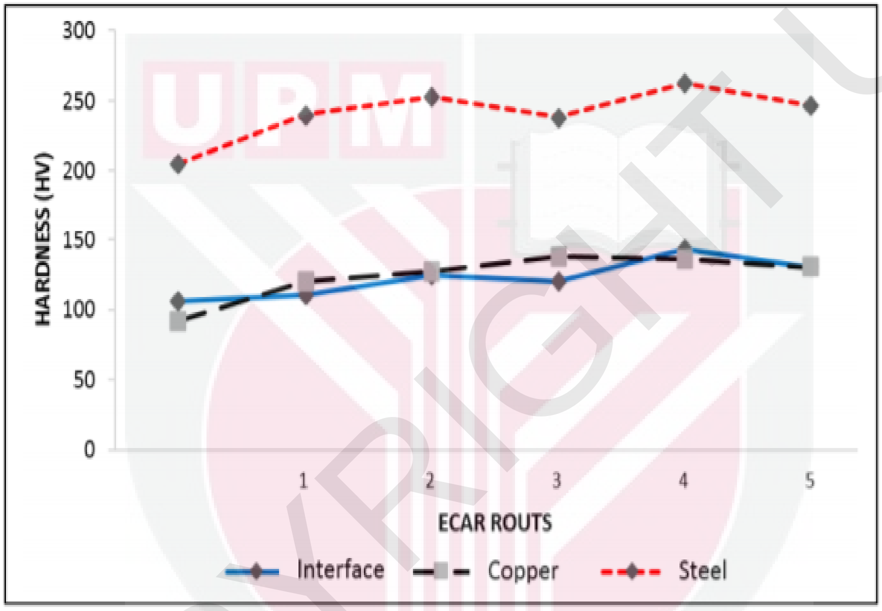

Figure 2.28 : The two-layer sheet's hardness in different passes
(Honarpisheh et al. 2019)

2.4.5 Residual Stress

Kotobi and Honarpisheh (2017) used uncertainty analysis to examine the residual stresses in Al-1060 strips that were rolled, using the equal-channel angular rolling technique. The authors utilized the slitting method to measure these residual stresses.

The images demonstrate the close agreement between the series expansion of each sample, at a chosen order, and the measured strain data. Figure 2.29 illustrates the profiles of residual stresses across the thickness of the control sample, as well as the one-pass and two-pass samples.

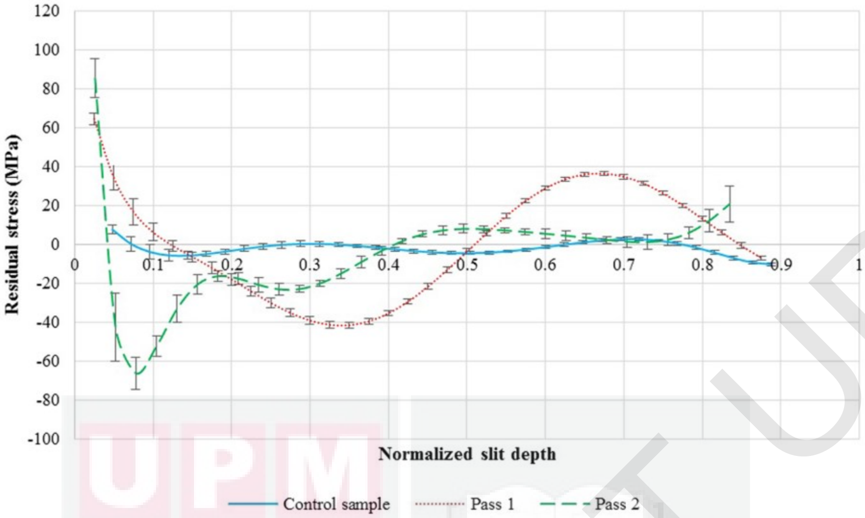

Figure 2.29 : Residual stress graph on Al-1060 after 1 and 2 pass
(Kotobi and Honarpisheh, 2017)

Figure 2.29 illustrates the inclusion of total uncertainty bars with each increment in slit-depth. Meanwhile, Figure 2.30 presents the overall variation, the highest levels of residual tensile and compressive stresses, and the RMS total ambiguity for each individual sample. In the control sample, the most prominent tensile residual stress measured 7.59MPa. However, upon implementing ECAR, the maximum compressive and tensile residual stresses increased to 64.4 and 41.56 MPa, respectively, after the initial pass. Notably, the one-pass ECARed sample exhibited the highest ratio of tensile residual stress to yield stress at 48.8%. Consequently, the ECAR process demonstrated a significant capability to elevate the maximum magnitude of residual stress within the component.

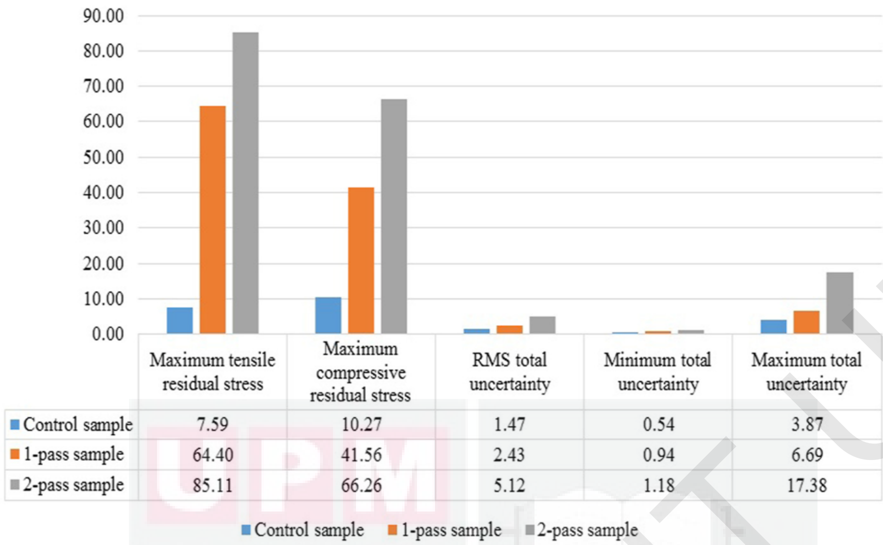

	Maximum tensile residual stress	Maximum compressive residual stress	RMS total uncertainty	Minimum total uncertainty	Maximum total uncertainty
Control sample	7.59	10.27	1.47	0.54	3.87
1-pass sample	64.40	41.56	2.43	0.94	6.69
2-pass sample	85.11	66.26	5.12	1.18	17.38

Figure 2.30 : Residual stress chart on Al-1060cafter one and two pass (Kotobi and Honarpisheh, 2017)

Honarapisheh et al. (2018) examined the residual stress and mechanical properties of St12 strips that underwent equal channel angular rolling. Figure 2.31 presents the residual stress profiles across the thickness of the samples, both before and after stress relieving. Prior to the ECAR process, the samples were subjected to stress relieving in a furnace at a temperature of 720°C for a duration of thirty minutes. This step aimed to alleviate the residual stresses that had accumulated during the previous manufacturing process.

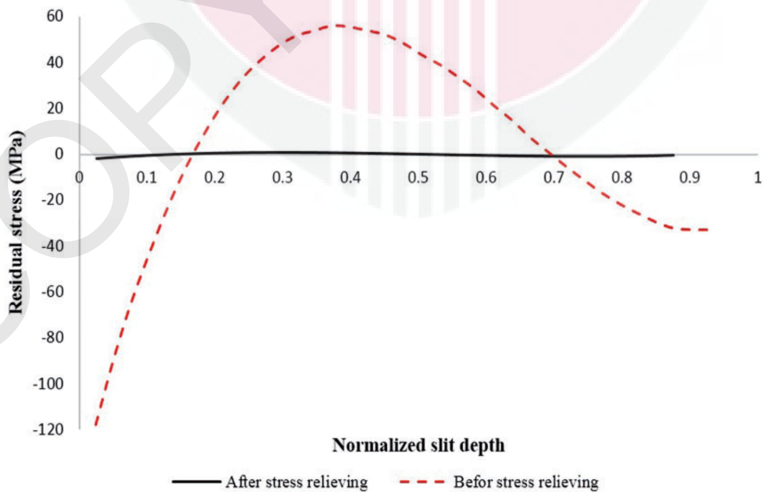

Figure 2.31 : Residual stress chart on ST12 after and before stress relieving (Honarpisheh et al. 2018)

The recorded data reveals that the maximum values for tensile and compressive residual stress were approximately 60 MPa and 120 MPa, respectively. These values can be attributed to the specific production method employed and the preparation of the sample.

In Figure 2.32, the residual stress distribution across the thickness of the sample is illustrated after undergoing a single pass through the ECAR process. It is evident that following this process, the highest tensile and compressive residual stresses escalated to approximately 125 MPa and 135 MPa, respectively. This increase can be attributed to the exposure of the material to non-uniform severe plastic deformation during the ECAR process.

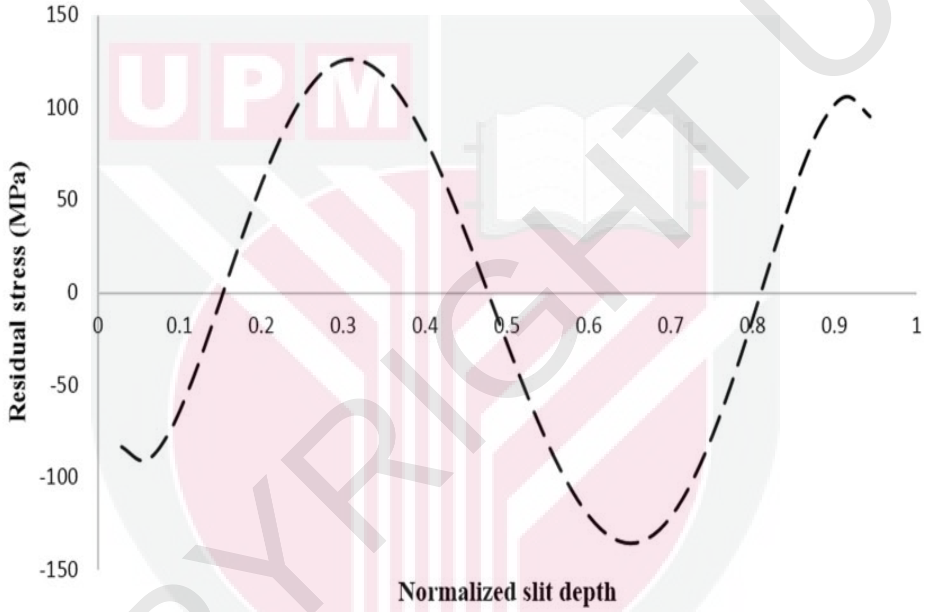

Figure 2.32 : Residual stress graph over the sample's thickness following one ECAR process pass (Honarpisheh et al. 2018)

Figure 2.33 illustrates the residual stress profiles of samples that underwent two ECAR passes. The sample that underwent two ECAR passes in route A demonstrated maximum residual stresses of approximately 200 MPa and 280 MPa, respectively. These values surpass the maximum tensile and compressive residual stresses observed in route C.

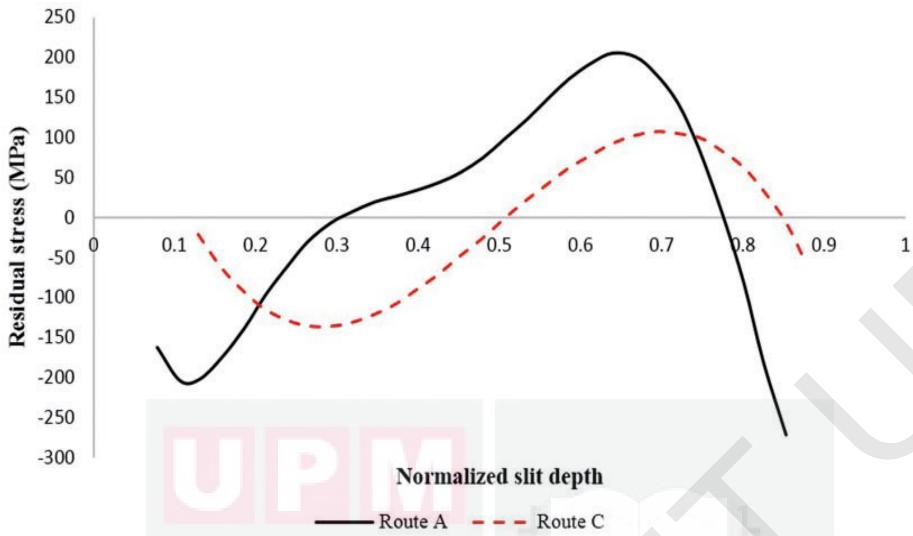

Figure 2.33 : Residual stress graph over the sample's thickness after second ECAR process pass (Honarpisheh et al. 2018)

2.5 Summary

In this chapter, various aspects pertaining to the mechanism of explosive welding process, severe plastic deformation and its methods, factors influencing the ECAR process, mechanical properties, and microstructure were thoroughly examined. The ECAR process, which is a type of severe plastic deformation method, has been effectively utilized to produce ultra-fine grain materials. One of the challenges faced by the industry is the scarcity of dissimilar multilayer sheets that possess low thickness, ample size, strength, and high hardness. However, this predicament has been successfully addressed through the implementation of the ECAR process. Additionally, the presence of nanostructured materials is another significant concern. While some researchers have investigated single-layer and double-layered sheets, the scarcity of multi-layered sheets with nanostructures remains a pressing issue in various industries.

In the ECAR process, a material with distinct mechanical properties and grain size can be produced by altering various parameters such as the number of rolling passes, preheat temperature, time, and so on, and incorporating additional layers. In this particular project, a three-layer Al/Cu/Al sheet was utilized in two different routes, namely A and C, to examine the mechanical properties and microstructure. To investigate the mechanical properties, residual stress, tensile test, and microhardness test were conducted, while optical microscope and SEM pictures were employed to analyze the microstructure in both routes A and C. The findings revealed significant changes in the mechanical properties and microstructure in both routes. It has been suggested that one of the two routes exhibits more favorable outcomes, which will be further discussed below.

Furthermore, various industries require multilayer sheets with distinct mechanical properties, high strength, and hardness. These requirements have been extensively investigated in the following sections. For this particular project, multilayer sheets were fabricated using explosive welding, and the effectiveness of the ECAR process on the samples was thoroughly assessed, resulting in the resolution of all associated issues.

According to the data presented in Table (2.2), the research focused on utilizing the ECAR technique to develop materials primarily employed one-layer and two-layer sheets. The investigation specifically examined the properties of an Al/Cu/Al sheet consisting of three layers, which underwent the ECAR process to achieve desired material characteristics. Notably, Table (2.2) encompasses all relevant articles published since 2010, discussing the development of novel materials using the ECAR method.

Table 2.2 : A comprehensive overview of the ECAR research conducted since 2010

Authors/ Researcher	Journal	Year	Research work/ Title	Findings
Khaled, M. H., Elkholy, A. N. M., & El-Abden, S. Z.	Zaštita materijala	2022	Mechanical characteristics of AL-1050 and Al-6061 alloys deformed using equal channel angular rolling process	The results showed that for AL-6061 without the annealing process in the first pass, it was a higher stress than the pass after the annealing process, and also the grains were fine in the first pass.
Eisaabadi, B. J., Sedighi, M., & Hashemi, R.	Iranian Journal of Manufacturing Engineering	2020	Experimental study of the effect of temperature on mechanical properties of aluminium sheets produced by equal channel angular rolling process.	The results revealed that by increasing number of ECAR passes at a specific temperature, tensile strength, Ultimate tensile strength and micro-hardness increased in a way that increasing rate at initial passes is more than last passes, while the elongation to fracture decreases.
Bozcheloei, J. E., Sedighi, M., & Hashemi, R.	The International Journal of Advanced Manufacturing Technology	2019	The effect of temperature on the mechanical properties and forming limit diagram of Al 5083 produced by equal channel angular rolling	The results showed that by applying the ECAR process at a specified temperature, the mechanical and microhardness properties of the samples improved, while elongation to fracture reduced.
Honarpisheh, M., Entezami, S. S., & Akhavan, S.	Metallography, Microstructure, and Analysis	2019	Effect of Equal Channel Angular Rolling Process on the Fracture Mechanisms of Al-7057 and Al-5052 Alloys	The results showed that performing thermal treatment at different temperatures caused the formation of intermetallic compounds in the weld bond, which would increase the hardness of this region. Also, increasing the annealing time increased the thickness of the weld bond.

Table 2.2 : Continued

Authors/ Researcher	Journal	Year	Research work/ Title	Findings
Mahmoodi, M., & Naderi, A.	Iranian Journal of Materials Forming	2019	Microstructure and its Relationship to Mechanical Properties in Equal Channel Angular Rolled Al6061 Alloy Sheets	Results showed the ECAR process strongly increases the yield strength and microhardness due to an increase in the dislocation density over a wide range of strain.
Honarpisheh, M., Haddadi, A. A., & Mansouri, H.	Journal of Modern Processes in Manufacturing and Production	2019	The Effect of Annealing Heat Treatment on the Bond of Explosivewelded Copper/Steel after the ECAR Process	The results showed that performing thermal treatment at different temperatures caused the formation of intermetallic compounds in the weld bond, which would increase the hardness of this region. Also, increasing the annealing time increased the thickness of the weld bond.
Honarpisheh, M., & Mansouri, H.	Manufacturing Engineering	2018	Investigation of Mechanical Properties of Titanium Alloy in the Equal Channel Angular Rolling Process	Results show that the tensile strength and hardness increased after first pass of ECAR process.
Nemati Chari, R., Mollaei Dariani, B., & Fallahi Arezodar, A.	Journal of Engineering Manufacture	2018	Numerical and experimental studies on deformation behavior of 5083 aluminum alloy strips in equal channel angular rolling.	The investigation of mechanical properties demonstrated that increasing number of equal channel angular rolling passes leads to a considerable increase in yield stress, ultimate tensile strength and hardness. In contrast, elongation was dramatically reduced.
Authors/ Researcher	**Journal**	**Year**	**Research work/ Title**	**Findings**
Rahimi, H. R., Sedighi, M., & Hashemi, R	Journal of Materials: Design and Applications	2018	Forming limit diagrams of fine-grained Al 5083 produced by equal channel angular rolling process.	Tensile strength and hardness increased and elongation decreased. Also, the average grain size was 45 µm, and after the third equal channel angular rolling pass, this amount was reduced to 10 µm.
Honarpisheh, M., Haghighat, E., & Kotobi, M.	Journal of Materials: Design and Applications	2018	Investigation of residual stress and mechanical properties of equal channel angular rolled St12 strips.	The results showed significant increase in the yield strength, ultimate tensile strength, and micro hardness of the samples in both routes. But the elongation decreased. Considerable magnitude of residual stress was created through the thickness of equal channel angular rolled samples such that the maximum tensile residual stress of some samples raised to about half of the corresponding yield strength. The maximum magnitude of residual stress in route C was smaller than that in route A.
Habibi, A., Ketabchi, M., & Eskandarzadeh, M.	Scientia Iranica	2017	Fatigue behavior of nano-grained pure copper processed by equal channel angular rolling.	The result showed after 4 passes of this process, grains with a diameter of about 70- 500 nm were formed.

Table 2.2 : Continued

Authors/ Researcher	Journal	Year	Research work/ Title	Findings
Sedighi, M., Monshi, P., & Joudaki, J.	Fatigue & Fracture of Engineering Materials & Structures	2017	Investigation of mechanical properties and fatigue life of ECARed AA5083 aluminium alloy.	Results show that the tensile strength and hardness of samples increases with increasing the pass of rolling. Also, the maximum elongation of samples decreases.
Mahmoodi, M., Naderi, A., & Dini, G.	Journal of Materials Engineering and Performance	2017	Correlation between structural parameters and mechanical properties of Al5083 sheets processed by ECAR.	The results showed that the dislocation density and micro strain were increased, and crystallite size was decreased during ECAR process.
Kvačkaj, T.et al.	Materials Characterization	2017	Microstructure evolution and mechanical performance of copper processed by equal channel angular rolling	It was found that the grain size gradually decreased from ~ 40 μm to ~ 250 nm with increasing the number of passes and tensile strength is increased.
Mahmoodi, M., & Naderi, A.	Iranian Journal of Materials Forming	2017	Microstructure and its Relationship to Mechanical Properties in Equal Channel Angular Rolled Al6061 Alloy Sheets	The results showed that the dislocation density and micro strain were increased, and crystallite size was decreased during ECAR process.
Authors/ Researcher	Journal	Year	Research work/ Title	Findings
Kotobi, M., & Honarpisheh, M	The Journal of Strain Analysis for Engineering Design	2017	Uncertainty analysis of residual stresses measured by slitting method in equal-channel angular rolled Al-1060 strips.	The results showed in route C the important role of both measurement and model uncertainties in the calculation of total uncertainty. The maximum tensile residual stresses of the control, 1-pass and 2-pass samples were 7.59, 64.4 and 85.11 MPa, respectively.
Mahmoodi, M., & Lohrasbi, S	The Journal of Strain Analysis for Engineering Design	2017	Investigation of residual stresses distribution in equal channel angular rolled aluminum alloy by means of the slitting method	According to the finite element results, the residual stresses were created in the sample because of different plastic strain deformation at the same times in different locations.
Ostovari Moghaddam, A., Mazinani, A., & Ketabchi, M.	Transactions of the Indian Institute of Metals	2017	Effect of accumulative roll bonding and equal channel angular rolling on microstructural and mechanical properties of Cu–Al–Mn shape memory alloys.	The results showed the grain size is not reduced to a large extent after 5 passes of ECAR and post-deformation annealing, but tensile strength increases significantly. Also, the microhardness test showed a significant increase (43%) in the microhardness of the alloy at the first two passes. This significant increase at initial passes of ECAR is attributed to strain hardening introduced by the process.

Table 2.2 : Continued

Authors/ Researcher	Journal	Year	Research work/ Title	Findings
Sedighi, M., Monshi, P., & Joudaki, J	Sharif Journal of Mechanical Engineering	2016	INVESTIGATION OF MECHANICAL PROPERTIES AND FATIGUE LIFE OF AL-5083 SHEETS PROCESSED BY EQUAL CHANNEL ANGULAR ROLLING	Results show that the ultimate tensile strength (UTS) of samples increases with increasing the pass of rolling. Also, the maximum elongation of samples decreases and the hardness of samples increases at higher pass of rolling
Hakimian, H., Sedighi, M., & Asgari, A	Mechanics & Industry	2016	Experimental and numerical study on the ECARed magnesium AZ31 alloy.	Results indicate that the microhardness after 8th pass ECAR has been increased about 45%. Also, the average grain size has been decreased about 94% after 8th pass ECAR.
Entezami, S. S., & Honarpisheh, M	Bulletin de la Société Royale des Sciences de Liège	2016	A study on the hardness of 7075 and 5052 aluminum alloys in the equal channel angular rolling process	The results of hardness test showed that by increasing the number of passes, surface hardness and hardness in the direction of thickness for ECARed Al 7075 alloy were increased 63% and 46% in the route A, respectively and 51% and 30% in the route C respectively. Also, the hardness in the direction of thickness and surface hardness in Al-5052 alloy were increased 41% and 64%, respectively.
M. Honarpisheh, M. Dehg hani, E. Haghighat	Procedia Materials Science	2015	Investigation of Mechanical Properties of Al/Cu Strip Produced by Equal Channel Angular Rolling	The microhardness of samples after the first passes of the ECAR process significantly increased and remained constant until 6 passes. After that, a slight decreasing was observed. Images of optical microscopy and SEM show the improvement of microstructure of samples at the first pass rather than the next passes.
Authors/ Researcher	**Journal**	**Year**	**Research work/ Title**	**Findings**
Honarpisheh, M., Aghili, M. R., & Kotobi, M.	Journal of Modern Processes in Manufacturing and Production	2015	Experimental investigation of thermal conductivity of aluminum alloy 3003 produced by equal channel angular rolling process.	the results, the thermal conductivity of samples increased up to definite pass and raised to its maximum value, then had an oscillatory trend up to tenth pass. Although this improvement of the thermal conductivity wasn't significantly, the improvement of yield and ultimate strength, and micro-hardness of the samples in passes associated with the maximum thermal conductivity, were meaningful and so, this ECARed alloys can be used in harder situation.
Honarpisheh, M., Dehghani, M., & Ghaffari, S	Journal of Modern Processes in Manufacturing and Production	2014	Investigation of ECAR Routes on Mechanical Properties of Explosive-Welded Al-Cu Bimetal.	Results show that the yield and tensile strength in the route C are higher than route A and the yield strength led to the largest value in the fourth pass in the route A and in the second pass in the route C.
Ballóková, B., Kvackaj, T., Hvizdos, P., & Besterci, M.	Acta Metall-Slovaca Conference	2013	Fracture analysis and local mechanical properties of copper processed by ECAR	An ECAR is a useful method providing a structural refinement to the submicrometer range. The OFHC copper, with initial grain size 10-40 µm, processed by 13 passes contains typically ultrafine grains with the diameter ~ 0.5 µm

Table 2.2 : Continued

Authors/ Researcher	Journal	Year	Research work/ Title	Findings
M. Mahmoodi , M. Sedi gi, D.A. Tanner	Materials and Design	2012	Investigation of through thickness residual stress distribution in equal channel angular rolled Al 5083 alloy by layer removal technique and X-ray diffraction	The yield strength of the annealed Al 5083 sample was increased after the ECAR passes and the RS values were compressive at the top surface and tensile at the bottom surface.
Azimi A,tutunchilar S,Faraji G, Besharati MK.	Materials and Design	2012	Mechanical properties and micro structural evolution during multi-pass ECAR of Al1100–O alloy	Applying ECAR up to seven passes on the as-annealed Al 1100 alloy considerably increased the ultimate and yield strength and decreased the elongation.
Habibi A, ketabchi M.	Materials and Design	2012	Enhanced properties of nano-grained pure copper by equal channel angular rolling and post-annealing	Hardness values which are affected by grain size highly increased until 8-pass due to significant grain refinement occurred by ECAR process, and then slightly reduced at final passes of process due to saturation in high level of accumulated strain.
Kvačkaj, T. et al.	Micron	2012	TEM studies of structure in OFHC copper processed by equal channel angular rolling	It was found that ECAR is a tool used for the purpose of achieving significant structural refinement resulting in a final grain size *d* ~ 400 nm and the strength significantly increased at the 1st pass, from initial 220 to 380 MPa.
Authors/ Researcher	Journal	Year	Research work/ Title	Findings
Sedighi, M., & Mahmoodi, M.	Materials and Manufacturing Processes	2012	Residual stresses evaluation in equal channel angular rolled Al 5083 by IHD technique: investigation of two calculation methods.	The result showed the equal channel angular rolled sample can reveal maximum residual stress of nearly 45% of its yield strength.
Hassani, F. Z., Ketabchi, M., & Hassani, M. T.	Journal of materials science	2011	Effect of twins and non-basal planes activated by equal channel angular rolling process on properties of AZ31 magnesium alloy.	The result showed elongation to failure was increased from 8% of as-received material to 19% after two passes of process and then decreased. Also, hardness values showed an increase of about 53% at eighth pass.
Hassani-Jabali, F. Z., & Ketabchi, M	AIP Conference Proceedings	2011	Controlling The Temperature Of Equal Channel Angular Rolling Process to Obtain Nano-grain Structure in AZ31 Magnesium Alloy.	After 10 passes of process significant grain refinement was occurred and the grains about 40 nm were achieved in grain boundaries of previous larger grains.
Asiyeh Habibi, Mostafa Ketabchi, Mohammad E skandarzadeh	Journal of Materials Processing Technology	2011	Nano-grained pure copper with high-strength and high-conductivity produced by equal channel angular rolling process	Results showed that the size of grains were decreased significantly to about 14–70 nm and at the 8th pass, hardness values increased by 53%.
F.Z. Hassani, M. Ketabc hi	Materials Science and Engineering: A	2011	Nano grained AZ31 alloy achieved by equal channel angular rolling process	Results showed that the size of grains were decreased significantly to about 14–70 nm and at the 8th pass, hardness values increased by 53%.

CHAPTER 3

METHODOLOGY AND MATERIALS

3.1 Overview

In this chapter, an analysis is conducted on the substances employed and the procedure for preparing the three layers of Al/Cu/Al explosive welding. Subsequently, the investigation focuses on the preparation of the sample and the heat treatment procedure carried out prior to the ECAR process. The ECAR process is then applied to the explosive welding sheet, and finally, an examination is conducted on the mechanical and microstructural aspects of the samples. Figure 3.1 illustrates the comprehensive flowchart of the explosive welding and ECAR process in routes A and C, highlighting the involvement of in this study and numbers in Figure 3.1 refer to objectives.

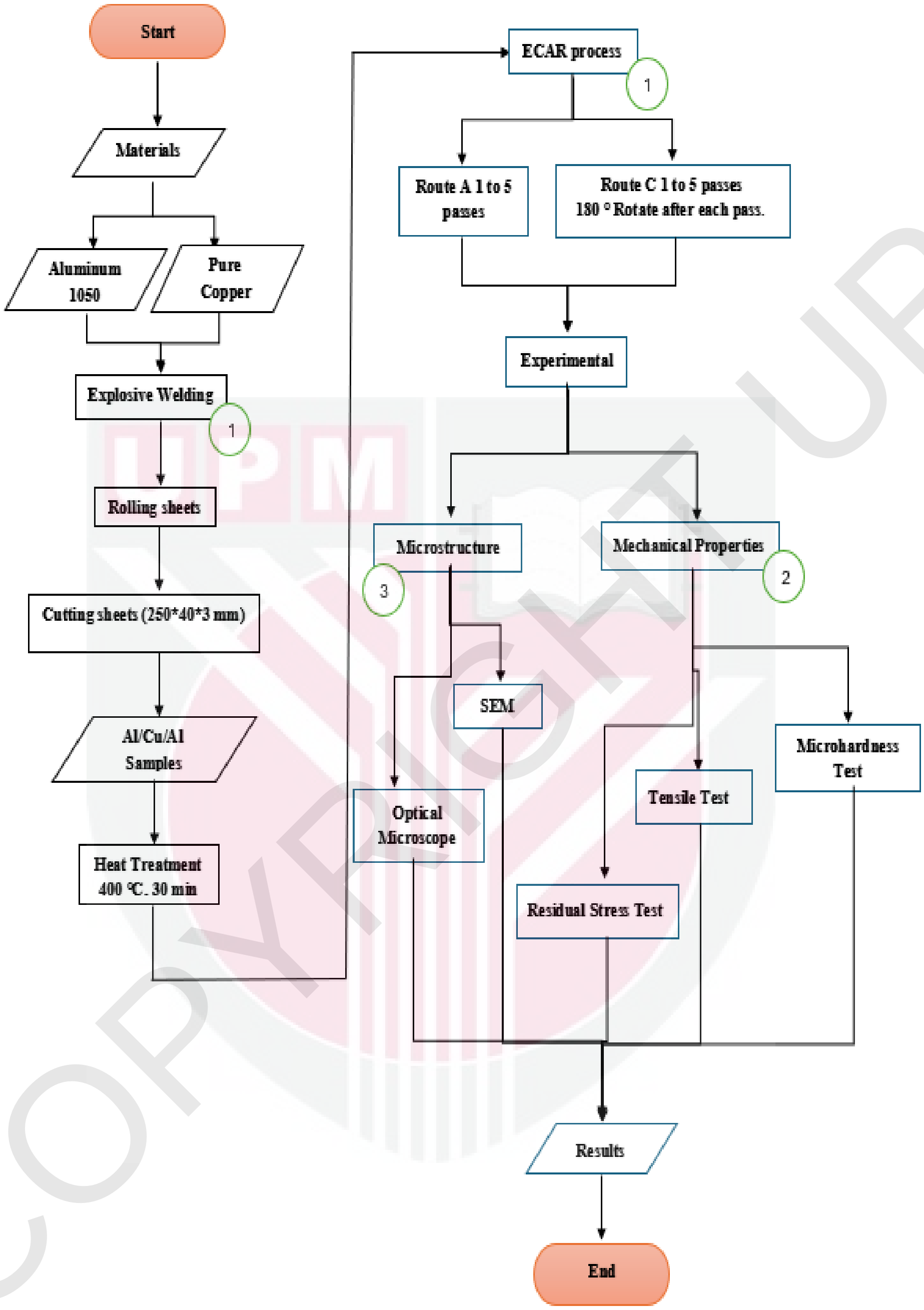

Figure 3.1 : Flowchart outlining the explosive welding and ECAR process in routes A and C

3.2 Raw Material

In this study, Aluminium 1050 and pure copper sheets with dimensions of 1000 × 1000 × 3 mm for Aluminium and 1000 × 600 × 2 mm for copper were utilized. These sheets were obtained from Arak Co., located in Tehran, Iran. The chemical composition analyses of Aluminium 1050 and pure copper is illustrated in Table 3.1.

Table 3.1 : Chemical composition of Al1050 and pure Cu Chemical composition of pure Cu alloy (wt.%)

Zn	Pb	Sn	P	Mn	Fe	Ni	Si	Cr	Al	S	
<0.01	<0.01	<0.01	<0.02	<0.01	<0.01	<0.05	<0.01	<0.002	Trace	None	
Ag	Co	Be	Cu								
Trace	0.02	<0.001	Base								
Chemical composition of Al 1050 alloy (wt.%)											
Si	Fe	Cu	Mn	Mg	Cr	Ni	Zn	Ti	Be	Ca	Li
0.09	0.18	0.01	0.02	Trace	0.02	0.01	0.03	0.01	Trace	Trace	Trace
Pb	Sn	Sr	V	Na	Bi	Co	Zr	B	Ga	Cd	Al
0.01	0.01	Trace	0.01	Trace	0.02	0.01	0	0	0.01	0	Base

These metals underwent resizing before being subjected to surface cleaning and sanding, resulting in their removal. Table 3.2 presents certain mechanical and metal characteristics of these two alloys.

Table 3.2 : Physical and mechanical properties of aluminium 1050 and pure copper

properties	*Al 1050*	*Cu (C10100)*
Density (kg/m3)	***2.71***	***8.94***
Melting Point (o C)	***650***	***1083***
Modulus of Elasticity (GPA)	***71***	***115***
Electrical Resistivity (Ω. m)	***2.66 x10-8***	***1.68 x10-8***
Thermal Conductivity (W/m. K)	***222***	***391***
Thermal Expansion (x10-6 /K)	***24***	***17.3***
Hardness (%)	***57.98***	***106.9***

The study utilized a powder type explosive known as AMATOL, which is a combination of TNT and ammonium nitrate. This explosive has a detonation velocity of 2500 m/s, indicating the speed at which the detonation waves propagate through the explosive material. Additionally, it has a density of 800 kg/m3. In order to initiate and regulate explosions, C4 has also been employed. The explosive material used in this study has a thickness of 14 mm, with a spacing of 10 mm between the plates.

When compared to other explosive materials, this particular one exhibits a lower susceptibility, as highlighted by Zhang et al. (2019) and Arnett (2019).

In order to carry out the process of explosive welding between aluminium 1050 and pure copper plates, the procedure involved placing the aluminium plate initially on the concrete plate, followed by the copper plate, and finally the aluminium flyer plate with a predetermined distance. These plates were then positioned on the base plate using wooden sticks.

Once the explosive materials have been meticulously prepared and accurately measured, typically ranging from 2 to 2.5 kilograms, they are delicately positioned on the flyer plate. This plate, serving as a crucial component, is enclosed within a dried wooden box. It is important to emphasize that the stop gap is determined by the thickness of the flyer plate, as highlighted by Blazynski (2012), Arnett (2019), and Davim (2021). Figure 3.2 provides a schematic depiction of the plate layout.

The project utilized AL 1050 and pure copper as the materials of choice. Initially, the desired thickness for the project was set at three mm, based on the specifications of the device being used. However, during the explosive welding process, the sample was unfortunately destroyed due to the intensity of the explosion. As a result, thicker sheets were employed in order to produce viable samples. These sheets were explosively welded at thicknesses of four, five, six, and seven mm. However, these attempts also resulted in torn and unusable samples. Consequently, a thickness of eight mm was ultimately selected. The decision to use eight mm thickness was influenced by several factors. Firstly, since the top and bottom sheets were made of aluminium, they experienced a greater intensity of explosion and impact. Secondly, considering the materials available in the market, a thickness of three mm was chosen for the aluminium sheet, while the copper sheet was set at two mm. If both sheets were of equal thickness, a total thickness of nine mm would have been required. However, this would have necessitated the use of more explosive materials, increasing the risk of tearing or even failure to weld the samples. Hence, the decision was made to opt for an eight mm thickness for the sample. Specifically, the aluminium 1050 sheets used at the top and bottom were each three mm thick, while the pure copper sheet placed in the middle was two mm thick.

The dimensions of the Al/Cu/Al plate obtained through explosive welding are 1000 × 600 × 8 mm. The material used for this process, which matches the input of the mould and the machine's rolling rollers, has a thickness of three mm. Consequently, in order to achieve sheet thicknesses ranging from eight mm to three mm, the sheet needs to undergo rolling. In the reducing process, seven rolling passes were utilized. A schematic image of the arrangement of the plates prior to the explosion can be observed in Figure 3.2 and also three layers Al/Cu/Al sheet explosive-welded sheet in Figure 3.3.

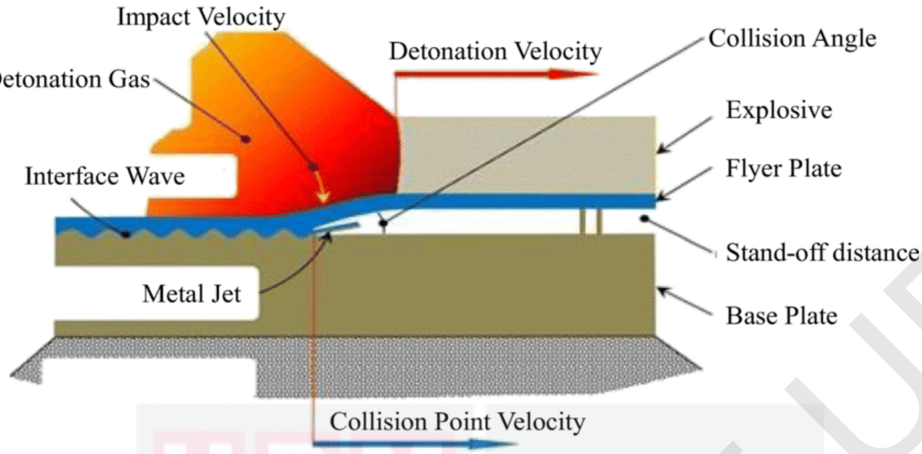

Figure 3.2 : Schematic image of the layout of the plates before the explosion (Zeng et al., 2019 b)

Figure 3.3 : Three layers Al/Cu/Al explosive welded sheet

3.3 Heat Treatment of Explosive Welding Samples before the ECAR Process

Prior to the ECAR process, the construction of the samples was carried out in order to examine the impact of the heat treatment procedure on the mechanical properties and interface of the Al/Cu/Al explosive welded multilayers.

To begin with, all the samples were subjected to annealing by being placed in a furnace. The temperature of the furnace was set at 400 °C for a duration of thirty minutes. Subsequently, the specimens were left inside the furnace for a whole day to cool down along with the furnace temperature. This process was conducted using AZAR furnaces F11L 1250, located in Tehran, Iran (Figure 3.4).

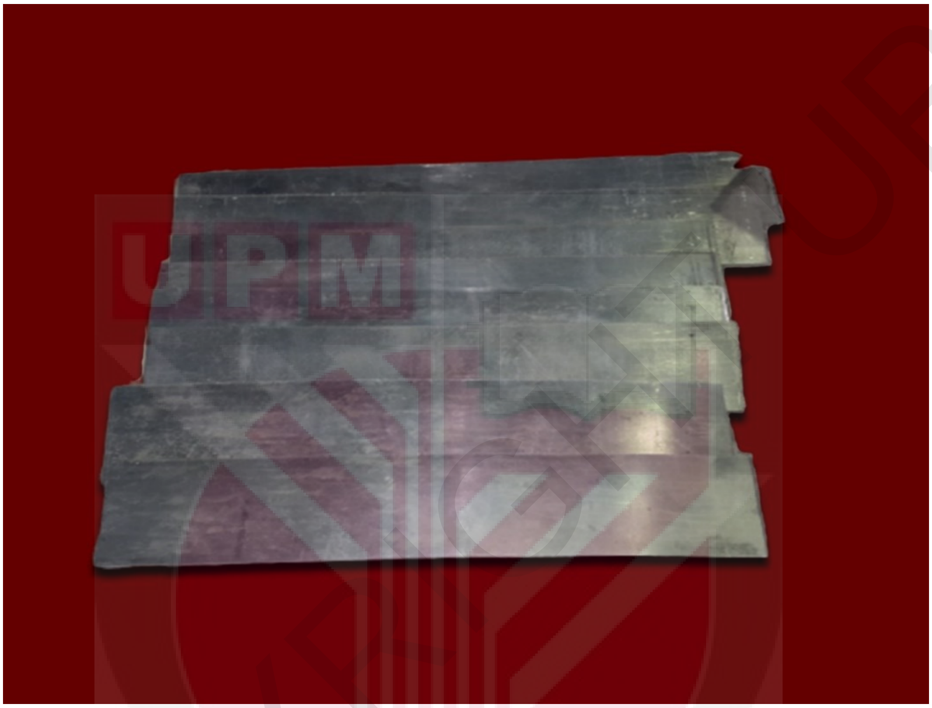

Figure 3.4 : Sample after heat treatment

3.4 ECAR Machine

Figure 3.5 illustrates the ECAR machine utilized in this particular process, consisting of two rollers with a diameter of 105 mm each. These rollers possess an angular shape with a curvature angle measuring 115°. The moulds and rollers employed in this device are made of SPK, which is a type of steel known as X210Cr12 with the roller's rolling speed of 6.4 m/s.

This steel variant contains significant amounts of carbon and chromium. Apart from its resistance to abrasive and adhesive wear, this alloy offers high compressive strength and satisfactory dimensional stability, making it suitable for applications in tools and forming dies. The chemical composition analyses of SPK are presented in Table 3.3.

Table 3.3 : Chemical composition (wt %) of SPK

C	Si	Mn	P	S	Cr
1.9 - 2.2	0.1 - 0.6	0.2 - 0.6	max 0.03	max 0.03	11 - 13

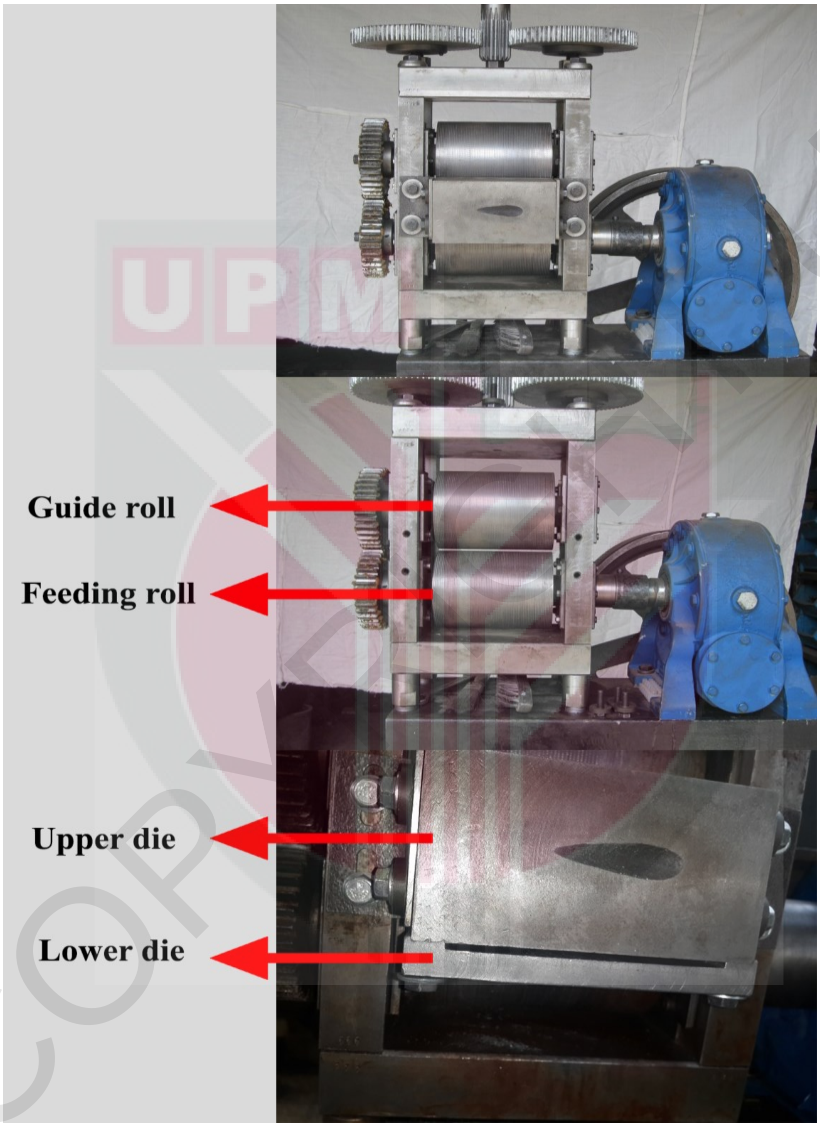

Figure 3.5 : ECAR device utilized in this project (University of Kashan, Iran)

3.5 Sheet Deformation Process Using ECAR

To examine the impact of ECAR process parameters on the mechanical characteristics of explosive welding samples, rectangular specimens measuring 250 × 40 × 3 mm were extracted from a three-layer sheet of explosive welding Al / Cu / Al (Figure 3.6).

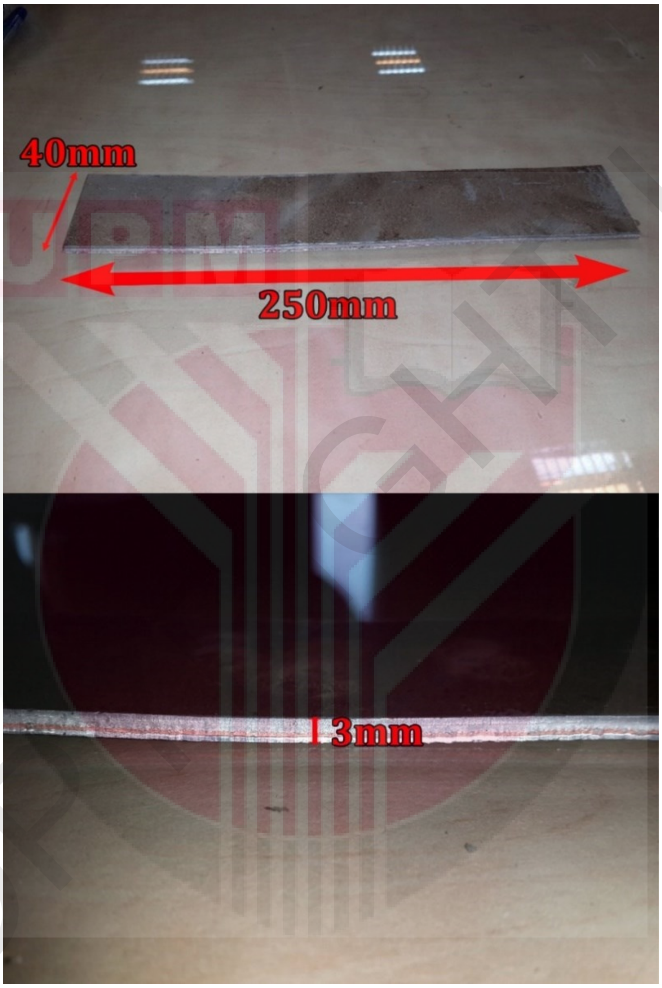

Figure 3.6 : Samples prior to ECAR process

To commence, the initial step involves adjusting the distance between the two rollers in order to accommodate the insertion of the sheet within the span of the rollers. This adjustment is facilitated by the lever connected to the gears located at the top of the device. Subsequently, the thickness of the sheet is reduced to 2.95 mm by manipulating the chapters and applying pressure to ensure a proper fit within the channel opening. When the sheet is positioned between the mould and the roller within this specific range, the relatively small distance between the two components subjects the sheet to significant strain. Consequently, this strain enhances both the strength and thinness of the seeds. It is important to highlight that in cases where there exists a gap between the mould and the roller, no substantial deformation occurs, resulting in only a marginal increase in the sheet's dimensions (Figure 3.7).

Upon entering the fracture area, the mechanical properties of the sheet revert back to their initial state, while simultaneously undergoing a conversion in thickness to three mm.

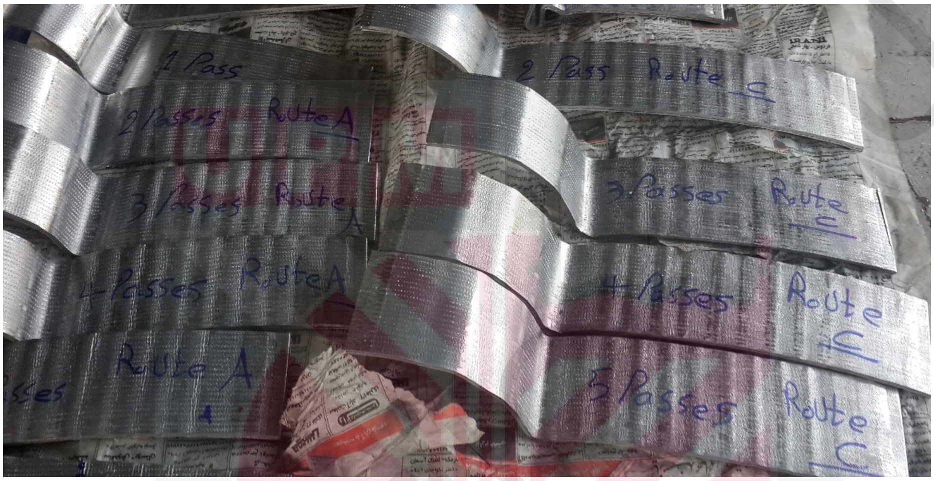

Figure 3.7 : Samples after ECAR process.

The ECAR operation is carried out under ambient conditions, specifically at a temperature of 30°C. The samples undergo a varying number of passes, ranging from one to five, following two distinct routes labelled as A and C. This alteration in the slip line band of the sheet necessitates the use of different routes. However, after the fifth pass, the sixth pass cannot be conducted due to the observed increase in strength and hardness, coupled with a decrease in elongation. Consequently, when the sample is placed in the ECAR machine, it fails to enter the channel. This occurrence can be attributed to the heightened hardness and reduced ductility of the sample. Prior to each step, the surface of the roller is meticulously sanded, and the sample is thoroughly cleaned. Subsequently, the samples are prepared in accordance with the American society for testing and materials (ASTM) standard for testing purposes.

3.6 Routes A and C

The project involved conducting experiments and tests on samples that were divided into four routes: A, B, C, and D. However, for this particular project, the focus was on routes A and C. This decision was made due to the distance between gap and roll, which aligns with the thickness of the samples. To achieve this alignment, the samples were rotated 180 degrees.

In route A, the sample underwent multiple passes without any rotation. The same face was used for each pass until the fifth pass was completed. On the other hand, in route C, the sample was rotated 180 degrees after each pass. This rotation was performed before the second pass, and then again before the third pass, and so on until the fifth pass. The purpose of conducting tests in both routes A and C was to compare the results of mechanical properties and granulation size. The aim was to determine if testing in these two routes had any impact on improving mechanical properties and reducing grain size, or if the results were similar. After the ECAR process was performed on the samples, tests were conducted on all the samples to identify which routes had more significant changes in mechanical properties and grain size. Figures 3.8 and 3.9 provide a schematic representation of the ECAR routes.

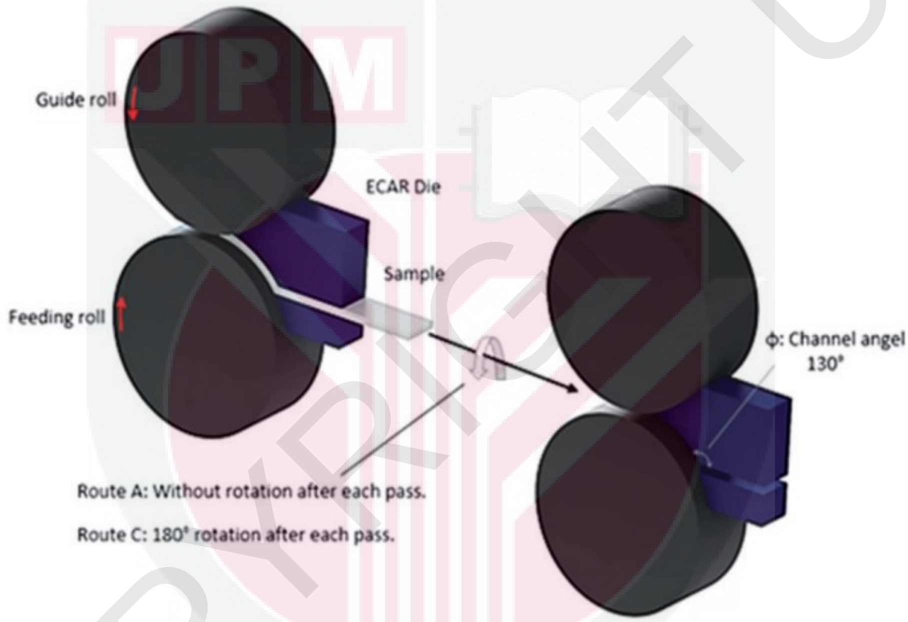

Figure 3.8 : A schematic of ECAR routes (Rahimi et al. 2018)

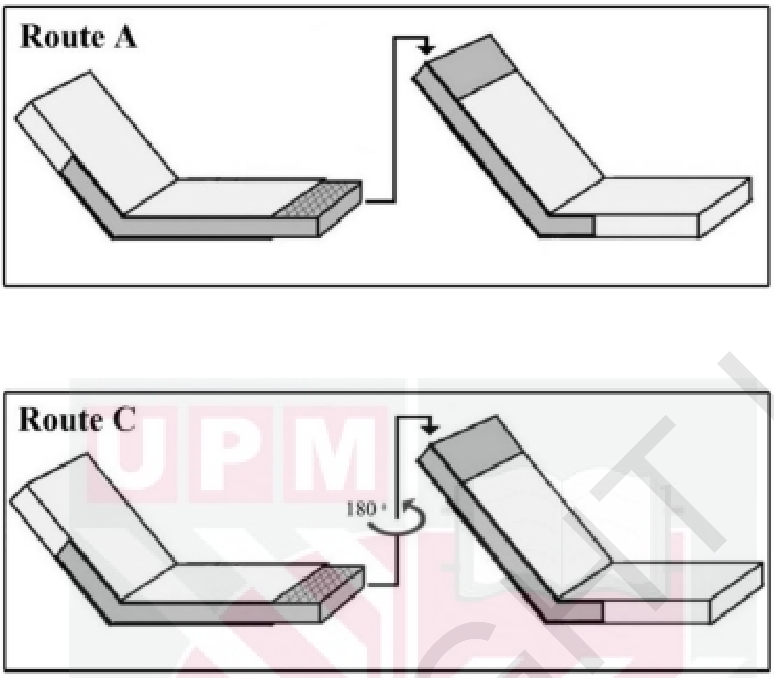

Figure 3.9 : A schematic of ECAR routes (Honarpisheh et al. 2019)

3.7 Mechanical Properties of ECAR Samples

In this section, various tests were conducted to assess the mechanical properties of ECAR samples with different passes on routes A and C. These tests included the tensile test, micro hardness test, and evaluation of residual stress. The results obtained from these tests provided valuable insights into the mechanical behaviour of the samples.

3.7.1 Tensile Test

The tensile test is a destructive test that involves subjecting a sample to a unidirectional tensile force until it reaches failure. During this test, the elongation of the sample is also measured simultaneously with the applied load.

The universal or general-purpose type of testing machine is commonly used for conducting tensile tests. In this study, an INSTRON 3366 (Norwood, MA) universal testing machine with a maximum allowable load of 50kn was utilized. This type of testing device consists of two fixed blocks, one of which can be adjusted to accommodate the length of the sample, while the other is responsible for applying the force. These testing machines are available in two variants:

hydraulic and electromagnetic. The primary objective of these tests is to generate a stress-strain curve.

Al/Cu/Al undergoes uniaxial tensile testing in compliance with the ASTME8 standard. The ECAR process is followed, wherein the samples are precisely wire-cut into a dumbbell shape. These samples are in the form of a sheet, and there are two possible arrangements for the specimens in the tensile test formats. The jaws used in the testing apparatus are cone-shaped, and the first and last sheets have their two ends pierced and inserted into the pin. One side of the specimen is fixed, while the other side is stretched (Figure 3.10).

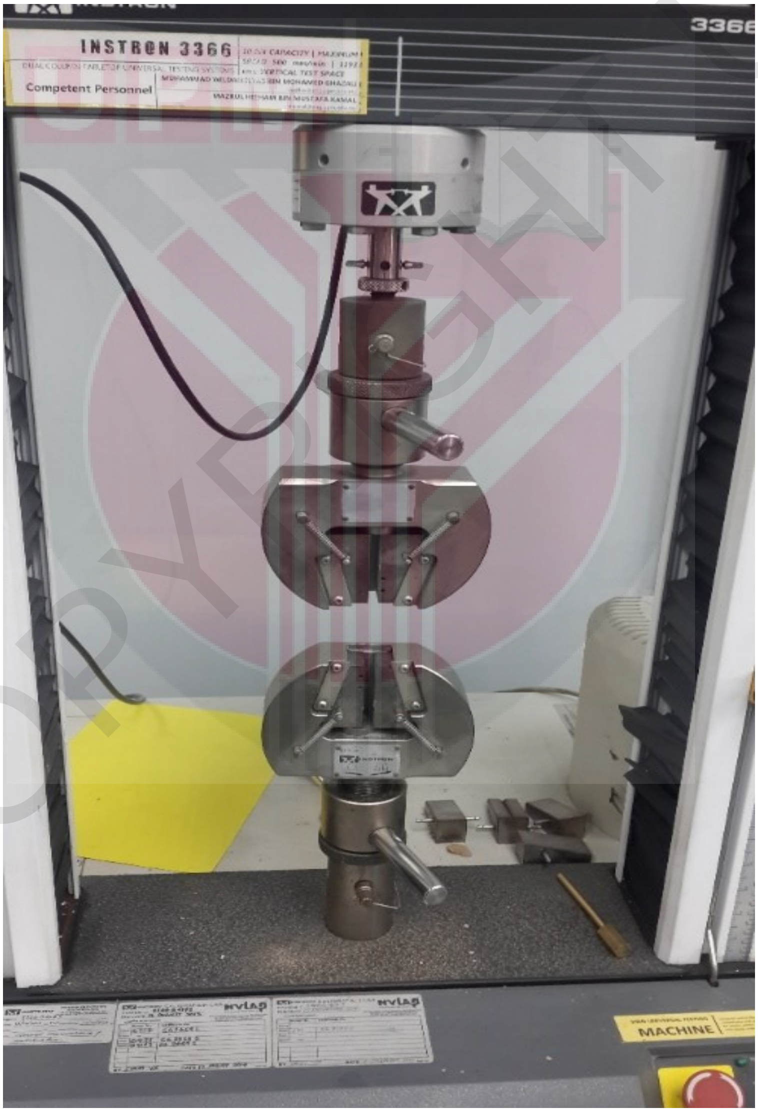

Figure 3.10 : Tensile test machine (Mechanical Engineering Laboratory, UPM)

Tensile test specimens were fabricated in order to assess the impact of the ECAR process on mechanical properties, including yield strength, ultimate strength, and percentage of elongation at a speed of five mm/min. The samples prior to the tensile test are depicted in Figure 3.11.

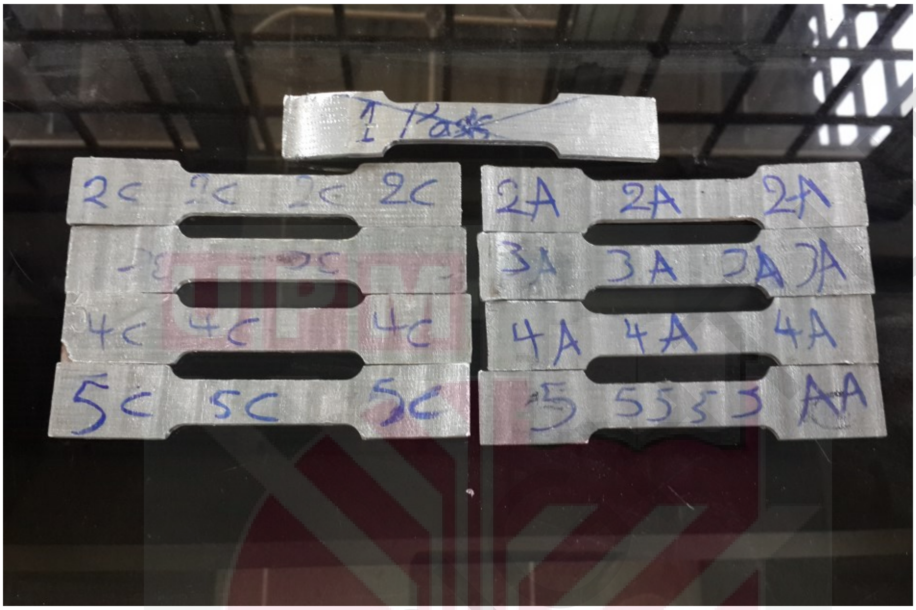

Figure 3.11 : Dumbbell form specimens for uniaxial tensile testing

3.7.2 Hardness Measurement

The HV Microgravity Test is a widely utilized ASTM E92 micro hardness test. This test involves applying a minimal amount of force, typically measured in grams. To carry out these tests, specialized metallurgical microscopes are employed. These microscopes are specifically designed for the purpose of examining materials at a magnification of twenty to two hundred and can focus on specific grains of the material. A small diamond pyramid is placed on a dedicated lens page, which is capable of injecting a low-power diamond pyramid onto the targeted grain. The force applied during the test typically falls within the range of one to a hundred grams. Subsequently, the HV test method (CB THV-1, Shandong, China) is used to accurately measure the diameter of the resulting dent, which takes on a squared form (Figure 3.12).

Figure 3.12 : Micro hardness test machine (Mechanical Engineering Laboratory, UPM)

The hardness of each ECAR sample with different passes was determined by cutting the ECAR samples cross-sectional. In order to facilitate the polishing and sanding process, the samples were mounted and then polished using sheets ranging from 120 to 3000. The hardness test was conducted using a 300-gram load and a force applied for ten seconds, and the obtained results were reported as HV hardness.

To assess the enhancement in mechanical properties and surface hardness, the samples were subjected to a HV hardness tester. The subsequent chapter provides a comprehensive analysis and conclusion of the test outcomes.

3.7.3 Residual Stress

Residual stresses refer to the stresses that persist in a solid material even after the initial stresses have been removed. The measurement of residual stresses involves various techniques, which can be classified into three main categories: destructive, semidestructive, and non-destructive. In this project, the contour method (Mituyoyo Crysta-Apex 122010, Kawasaki, Japan) (Figure 3.13) is employed as a destructive technique to examine residual stress.

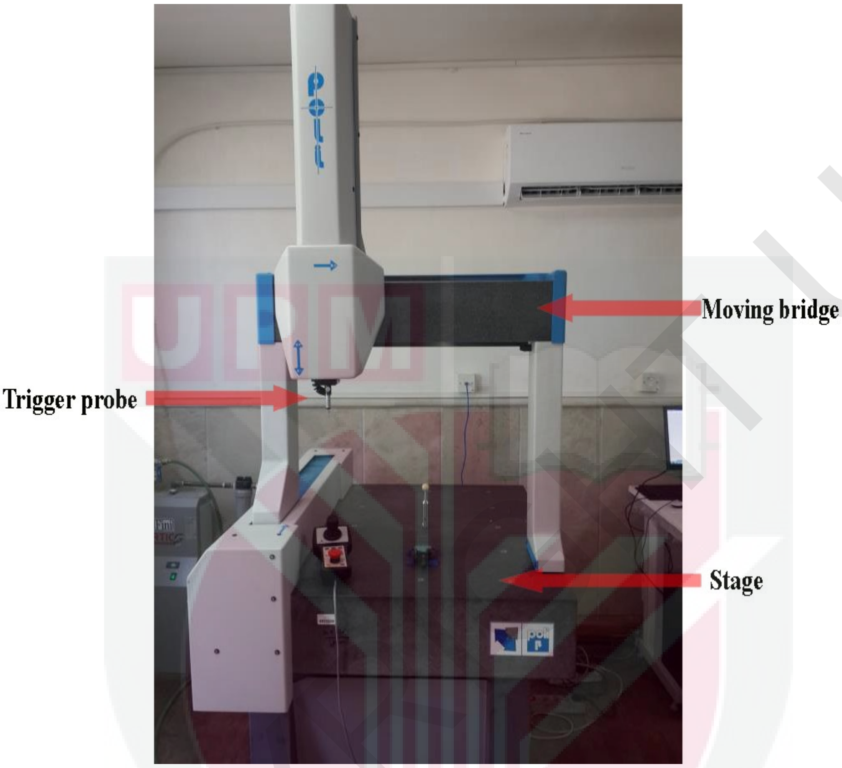

Figure 3.13 : Residual stress machine (Mechanical Engineering Laboratory, University of Kashan, Iran)

The utilization of destructive techniques results in significant and irreversible alterations to the specimen, rendering it unsuitable for further use. In such cases, either a mock-up or a spare specimen must be employed. Among these destructive techniques is the contour method, which is employed to determine the magnitude of residual stresses formed perpendicular to the surface of the cut. Prime introduced the contour method in 2001 as a compliance technique for assessing residual stress levels (Prime, 2001; Prime et al., 2004).

The contour method, a recently developed technique, is employed to calculate residual stress across a cross-section. This method operates on the principle that when a section containing residual stress is bisected along a straight line, the resulting free surface undergoes deformation as the stresses perpendicular to the surface are released through the cutting process. What sets the contour method apart from other destructive procedures is its remarkable capability to comprehensively map the normal component of residual stresses on a cut surface, all while utilizing a relatively simple and cost-effective approach. Moreover, the experimental steps involved in this method can be carried out utilizing apparatus and machinery that are already readily available in the majority of industrial and academic research facilities (Prime, 2001; Prime et al., 2004; Gadallah et al., 2020).

The conventional contour method is implemented through a series of four steps. Firstly, the welded specimen is cut in two equal parts. Then, the shape of the relaxed surface is acquired. Subsequently, data processing takes place. Finally, stress computation is performed. By employing an elastic finite element model, the deformations of the cut surface can be observed and utilized to accurately determine the initial residual stress that acts perpendicular to the cut plane. One notable characteristic of the contour method is its ability to generate a comprehensive two-dimensional map of the residual stress component normal to the cross section (Woo et al., 2008; Carlone & Palazzo, 2013; Gadallah et al., 2020).

The investigation of residual stress on an Al/Cu/Al three-layer sheet during a five-pass ECAR process, in relation to the pass number in different routes A and C, was conducted in accordance with ASTM E837-13a.

First step involved dividing the samples into two equal parts, each measuring 70 × 40 × 3 mm, with utmost precision using a wire cut machine from the vertical section. This particular method was chosen due to its superior surface smoothness and minimal stress loss compared to alternative techniques. The second step of this technique involves measuring surface contours in the cut section, which are caused by minor distortions. These are usually measured using coordinate measuring machines (CMM) with a touch probe (Figure 3.14). In principle, any surface profile measurement method that provides adequate accuracy for the expected surface displacement can be used. The measurement step was the most time-consuming step in the contour technique.

The third step of this technique is data analysis. This is the method used to transform a 3D surface contour into a 2D stress field, i.e. filtering the raw data array and superimposing the surface contour into a finite element method (FEM). The raw data measured by the CMM yields a combination of stress release distortions. for this reason, the data array must be filtered and smoothed before it can be applied to the model and used the MATLAB software to determined formula for each samples before finite element model for each sample in stress software. The formula is not same for all samples and determined according to data measured by contour machine for each samples. The fourth step is the finite element method (FEM) to collect residual stress results. Finite element analysis needs to model samples in stress software to investigate residual stress and ABAQUS is one of the software to investigate stress and used in this study. The ABAQUS software was employed to 2D simulate each sample, with the MATLAB-derived formula being incorporated for each respective sample. Upon executing the simulation, the residual stress for each sample was successfully determined which results are mentioned in Chapter 4.

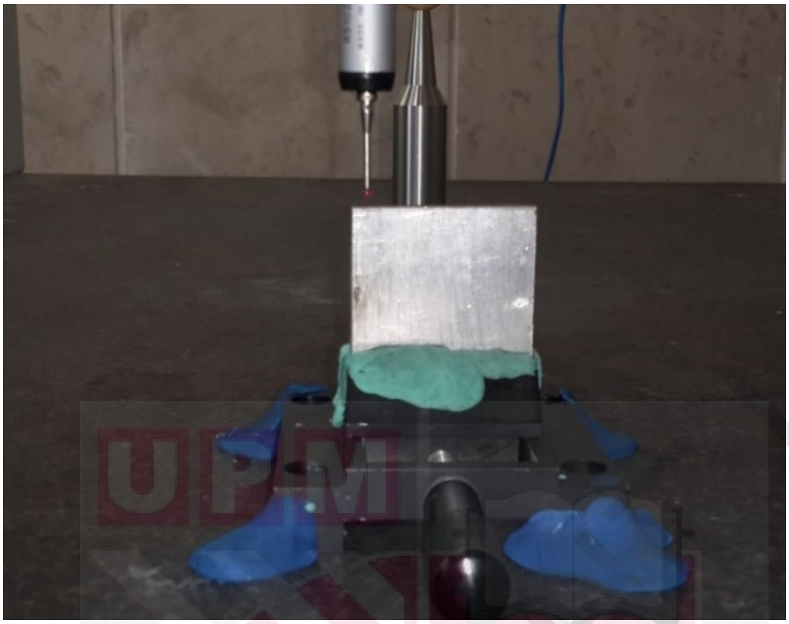

Figure 3.14 : Contour measurement (Mechanical Engineering Laboratory, University of Kashan, Iran)

The investigation of residual stress in each sample utilized in ABAQUS software was conducted. Within the ABAQUS, the formula and numerical values obtained for each residual stress sample in ECAR samples were employed to generate the residual stress by modelling a three-layer Al/Cu/Al sheet.

3.8 Microstructure Examination

SEM (scanning electron microscopy) was employed in two instances to conduct more precise scanning. A comprehensive analysis of the interfacial samples of explosive welding was conducted, along with an investigation into the grain size and morphology before and after the ECAR process.

3.8.1 Sample Preparation

Before capturing images with scanning electron microscopes (SEMs), it is necessary to etch the samples. The etching process involved cooling the samples initially, followed by the application of 120 to 4000-polished sand blades on their surfaces. Subsequently, the surface of the samples underwent etching for a duration of thirty to thirty-five seconds. The etch solution used varied depending on whether the samples were made of aluminium or copper. For aluminium, the etch solution comprised of 92ml distilled water, 5ml hydrofluoric acid, and 15gm ammonium pyrosulphate. On the other hand, the etch solution for copper consisted of 100ml distilled water, 30ml hydrochloric acid, and 5gm Ferric chloride.

Following the etching process, the samples were prepared for metallographic studies using the FEI Nova Nanosem 230, a scanning electron microscope from the United States (Figure 3.15).

Afterwards, images (scanning electron micrographs) of the two surfaces of the samples and the interface interval between them are captured in order to ascertain the dimensions of the aggregate and its interconnected area.

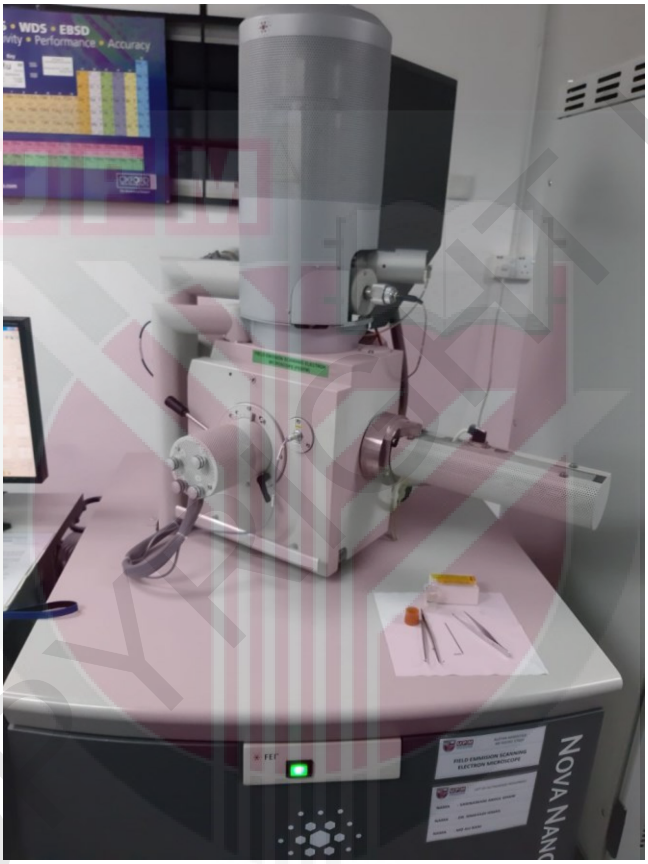

Figure 3.15 : SEM machine (Department of Chemical Engineering Laboratory, UPM)

Explosive welding has brought about the emergence of interconnected areas undergoing transmutation. The high explosion energy possessed by the two alloys is a significant factor that can trigger potential reactions between them. Additionally, the explosion generates plastic seals, which form an intermediate layer within the joint. The thickness of this intermediate layer is directly proportional to the stopping distance and collision speed. Detailed information regarding the parameters, both fixed and variable, for explosive welding and the ECAR process can be observed in Tables 3.4 and 3.5.

Table 3.4 : Parameters setting for explosive welding

Parameters	Value
Al 1050 sheet dimension	1000*1000*3 mm
Pure Copper sheet dimension	1000*600*2 mm
Velocity	2500m/s
Density	800 kg/m3
Explosive	C4
Explosion material thickness	14mm
Explosion material weight	2.5 kg
Space between plates	10mm

Table 3.5 : Parameters setting for ECAR process

Parameters	Value
Number of rolling passes	5
The looseness between plate and channel	1
Mould structure	SPK (x210cr12
Heat temperature	400- 30 min
Rolling speed	6.4 m/s
Curvature angle	115
Specimens dimension	250*40*3 mm

3.9 Summary

The primary emphasis of this chapter revolved around the materials employed, which was subsequently followed by an analysis of the devices utilized in this study. The subsequent phase involved an investigation into the mechanical properties and aggregate size of the materials, along with the examination of the connection area of the three-layer aluminium/copper/aluminium sheet. Several tasks were completed, including conducting tensile strength tests, HV micro hardness assessments, evaluating residual stress, and studying the interfaced areas after the ECAR operation. Additionally, the size of the grain was examined through scanning with an electron microscope.

CHAPTER 4

RESULTS AND DISCUSSION

4.1 Overview

In this chapter, an effort has been made to establish a consensus regarding the behaviour of Al/Cu/Al three-layer plates by conducting various tests to evaluate their mechanical properties. These tests include the uniaxial tensile test, micro hardness test, and residual stress test. The results obtained from these tests provide valuable insights into the performance and behaviour of the materials. Additionally, the metallurgical aspects are examined through scanning electron microscopy to analyse the grain size and intersections of the Al/Cu/Al three-layer plates. The findings are presented in well-defined graphs and thoroughly reviewed and compared to enhance the comprehensibility and clarity of the performance analysis.

4.2 Mechanical Properties of Explosive Welded Al/Cu/Al Plates

4.2.1 Tensile Strength of ECAR Specimens

The mechanical properties of the explosive welded plates were evaluated via a tensile test. This test aimed to determine the yield stress, which indicates the point at which deformation occurs, the ultimate strength, which represents the maximum tensile stress the sample can withstand, and the elongation, as per the ASTM E8 standard. To conduct the test, samples with different numbers of passes (ranging from one to five) and two different routes (A and C) were prepared using the ECAR process.

Figure 4.1 presents the engineering stress-strain curve of the ECAR samples with varying numbers of passes in route A. This curve was obtained through tests conducted on the samples. Additionally, Figure 4.2 illustrates the relationship between the yield strength and tensile strength as the number of passes in route A's ECAR process increases.

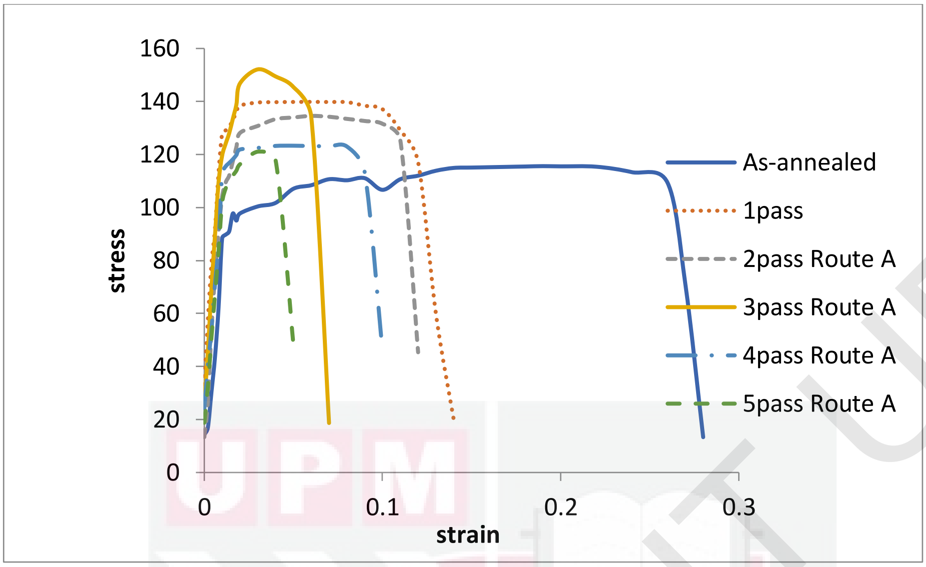

Figure 4.1 : Tension-strain chart of ECAR samples with different number of passes in route A

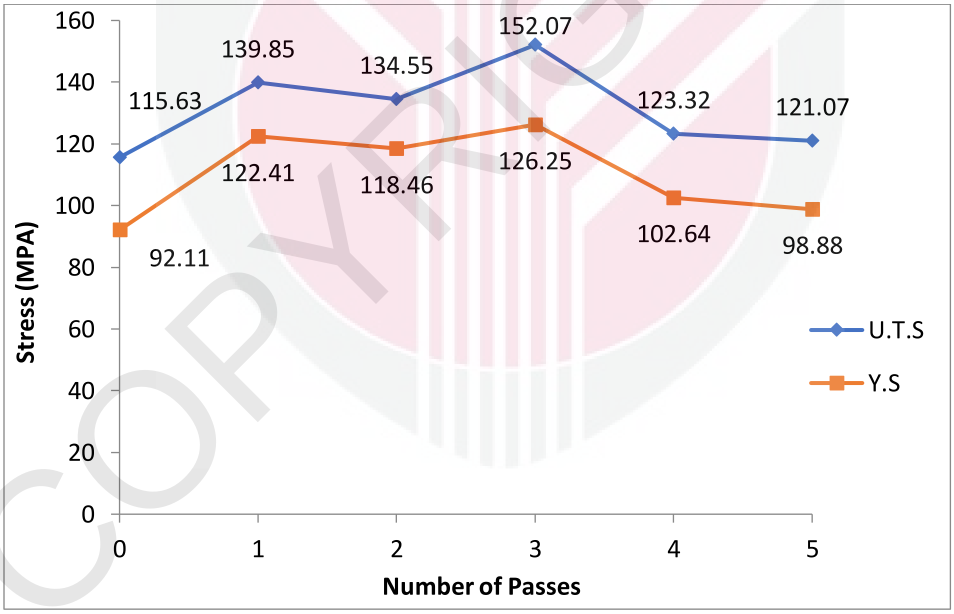

Figure 4.2 : The yield and tensile strength chart of the number of ECAR process passes in route A

The comparison and description of the tensile strength structure of different passes can be derived from Figure 4.1 and Figure 4.2. This section focuses on the analysis of five distinct passes, each exhibiting varying behaviours in the sample.

The results are as follows: The ECAR samples displayed noteworthy enhancements in both tensile and yield strengths after a single pass, reaching values of 139.85 and 122.41 MPa, respectively. The increase in strength can be attributed to the work hardening mechanism. Furthermore, the significant disparities in mechanical properties, such as yield strength, ultimate strength, and elongation at break, observed after the first pass can be attributed to the strain hardening or dislocation reinforcement mechanisms. These mechanisms arise from the presence of implicit dislocation boundaries with small disorientations.

The plate strength exhibited a minor decline to 134.55 and 118.46 MPa following the second passes. Subsequently, during the third pass, the tensile strength and yield strength of the specimen reached their peak levels at 152.07 and 126.25 MPa, respectively. However, there was a decrease in elongation. The enhancement in strength observed in subsequent passes of the process can primarily be attributed to the evolution of the grain structure (microstructural modification) rather than the formation of fine grains. The occurrence of variations in tensile strength in metals subjected to severe plastic deformation can be attributed to factors such as the increased density of dislocations, work hardening by dislocations and grain refinement, strain hardening, the application of large strains, and cold working. Upon reaching the fourth pass, the plate strength decreased, measuring 123.32 and 102.64 MPa, while the elongation increased. In the fifth pass, the plate strength experienced a slight decrease to 121.07 and 98.88 MPa, but the elongation exhibited a significant reduction (figure 4.5). The hardening stress in higher passes decreases considerably, and the yield strength and ultimate strength converge to identical values.

These findings are consistent with the results obtained in previous studies. Sedighi et al. (2017) also observed that the yield strength of aluminium alloy sheets increased by 54% after the first pass of rolling in an ECAR process. Similarly, Honarpisheh and Mansouri (2018) found that the tensile strength of titanium alloy samples increased after undergoing an ECAR process pass.

The research findings conducted by Honarpisheh et al in 2019 demonstrate that the application of the ECAR process on Al 7057 samples leads to an enhancement in their tensile strength. Remarkably, this improvement becomes evident after the initial pass and reaches its maximum value after the fifth pass. One of the primary objectives of this project is to investigate the impact of the ECAR process on Al/Cu/Al sheets as a novel material for enhancing mechanical properties, specifically the yield strength and tensile strength. The study successfully achieved this goal, yielding results that align with the initial expectations. Figure 4.3 provides a comprehensive analysis of the sample behaviour based on elongation criteria at various passes along path and route A. Additionally, Figure 4.4 illustrates the engineering stress-strain curve of ECAR specimens with different numbers of passes in route C. Furthermore, Figure 4.5 demonstrates the relationship between the number of ECAR process passes in route C and the corresponding increase in yield strength and tensile strength.

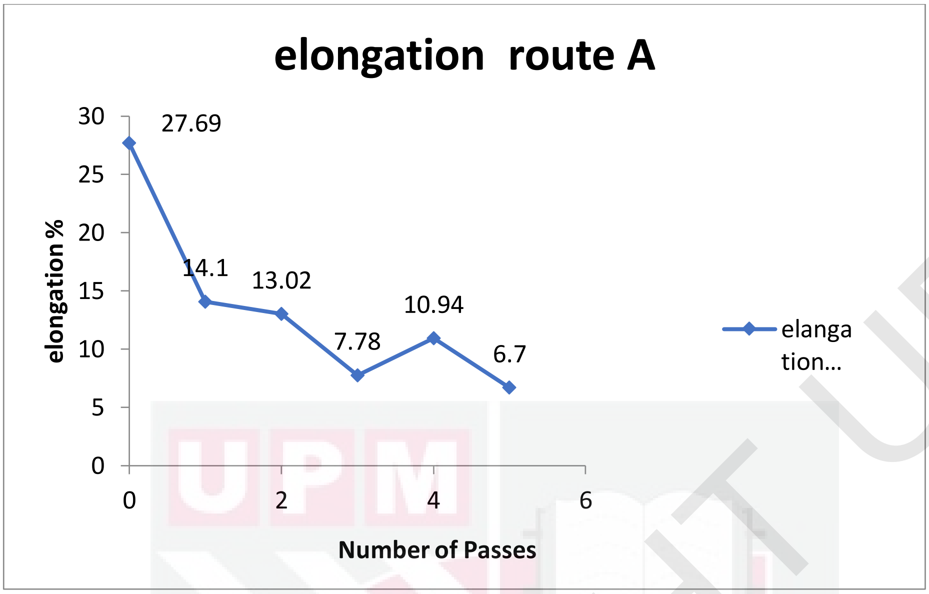

Figure 4.3 : Elongation of the samples at different passes in route A

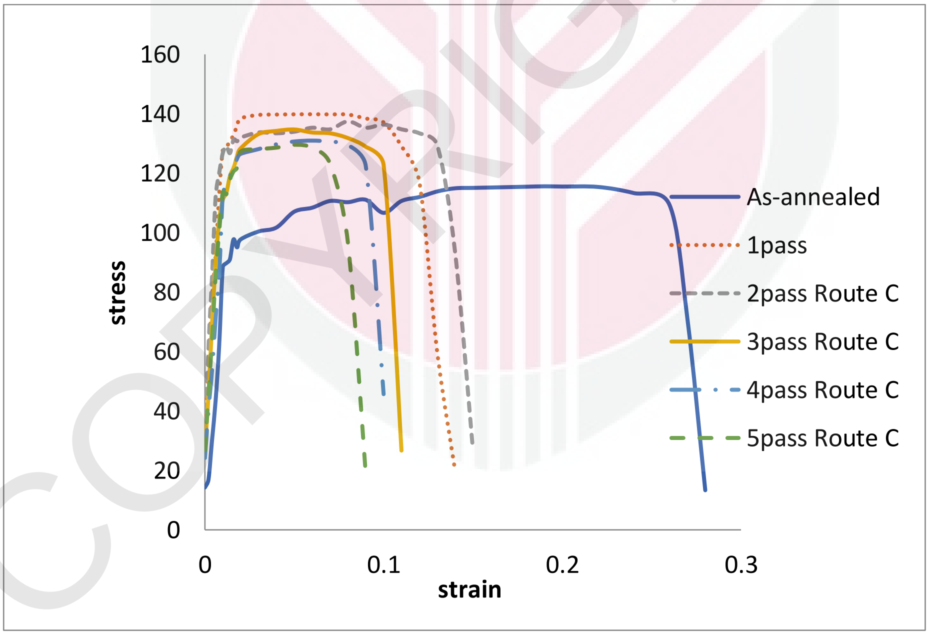

Figure 4.4 : Tension-strain chart of ECAR samples with different number of passes in route C

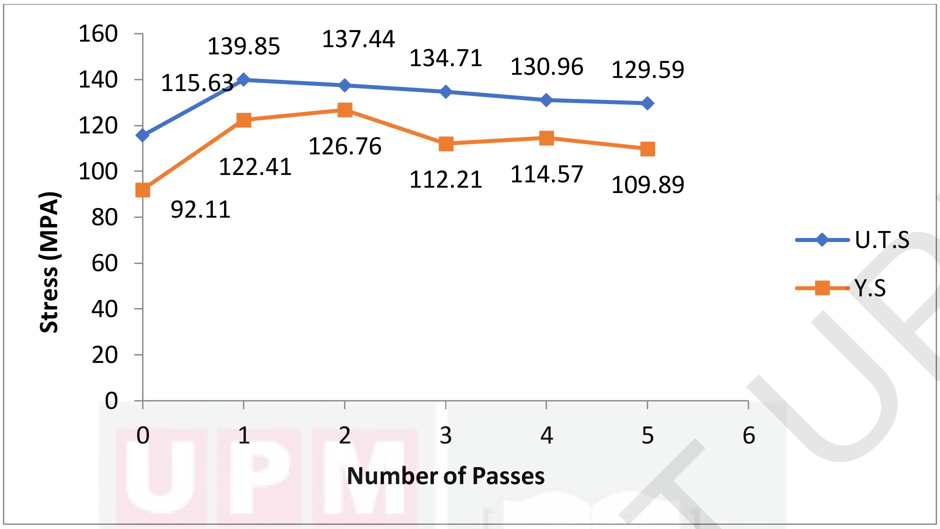

Figure 4.5 : The yield and tensile strength chart of the number of ECAR process passes in route C

According to figures 4.4 and 4.5, the highest stress experienced by the specimens was 139.85 MPa after one pass, while the yield strength was 122.41 MPa. The initial pass of ECAR resulted in the disruption of large, elongated grains and the formation of sub-grains with relatively high dislocation densities. This process played a crucial role in strengthening the metallic materials. During this stage, the dislocation density within the primary coarse grains and at their boundaries increased, led to the formation of a significant fraction of low-angle grain boundaries. After the second pass, the tensile strength of the plate experienced a slight reduction, reaching 137.44 MPa, while the highest yield strength was 126.76 MPa. The plate's strength continued to decrease slightly during the third pass, reaching 134.71 MPa for tensile strength and 112.21 MPa for yield strength, despite a minimal change in elongation. In the fourth pass, the plate's tensile strength and yield strength decreased further, reaching 130.96 MPa and 114.57 MPa, respectively. However, the elongation increased. By the fifth pass, the plate's strength slightly decreased to 129.59 MPa for tensile strength and 109.89 MPa for yield strength, accompanied by a decrease in elongation (Figure 4.8). The stress-strain charts demonstrated that the yield and tensile strength were approximately comparable in the upper passes. However, as the number of ECAR passes increased, the strain hardening decreased.

The results obtained from the tensile test conducted on the specimens in route C clearly demonstrate that the ECAR process has significantly enhanced the tensile strength of the specimens. These findings are consistent with previous studies conducted on the subject matter. The ECAR process involves subjecting the sheet to large strains, which in turn leads to an increase in the dislocation density within the initial grains' boundaries. This process causes a transformation in the grain boundary from a low angle to a high angle by increasing the number of passes in both routes A and C. The high angle grain boundary acts as a barrier against the movement of dislocations, thereby reducing their mobility.

Consequently, dislocations accumulate and form boundaries between adjacent grains, ultimately resulting in the formation of grain boundaries with large angles. The cold work and the subsequent increase in dislocations cause these dislocations to become entangled and locked together, leading to an overall increase in hardness.

The findings presented by Honarpisheh et al. (2014) demonstrate that the implementation of the ECAR process on two-layer samples of Al1050 /pure Cu explosive welding leads to an enhancement in strength, which aligns with the results of this study. This investigation was carried out using ECAR routes A and C. However, the outcomes indicate that the tensile strength of route C surpasses that of route A. In a separate study conducted by Honarpisheh et al. (2019), the effect of equal channel angular rolling process on the fracture mechanisms of Al-7057 in routes A and C, as well as Al-5052 in route C, was examined. The results obtained in this project are consistent with the findings of Honarpisheh et al., indicating that the tensile strength of Al-7075 samples increases in routes A and C following the ECAR process, with route A exhibiting a greater tensile strength than route C.

According to the results obtained from the tensile test conducted on the samples in route C, it was anticipated that the ECAR process would enhance the tensile strength while decreasing the elongation. These observations were also noted in route A. Additionally; Figure 4.6 illustrates the diagram depicting the elongation of the samples at various passes in the route C direction.

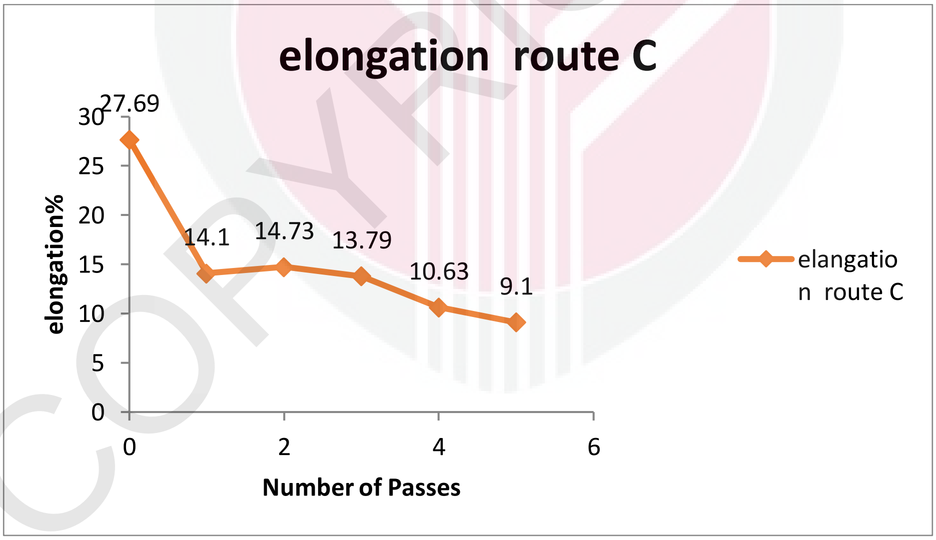

Figure 4.6 : Elongation of the samples at different passes in route C

Figures 4.7 and 4.8 illustrate the variations in yield strength and tensile strength of ECAR samples considering different numbers of passes in routes A and C.

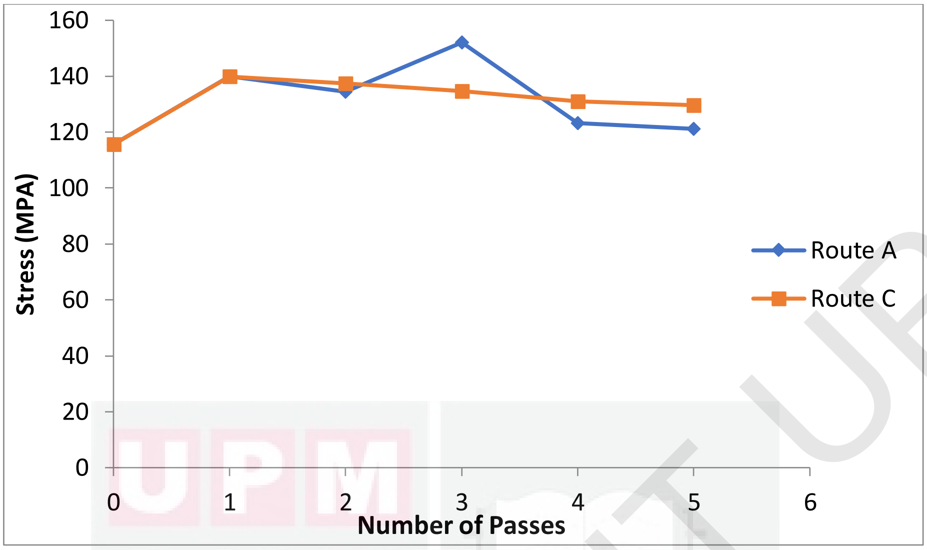

Figure 4.7 : Tensile strength of samples from the ECAR with various numbers of passes in routes A and C

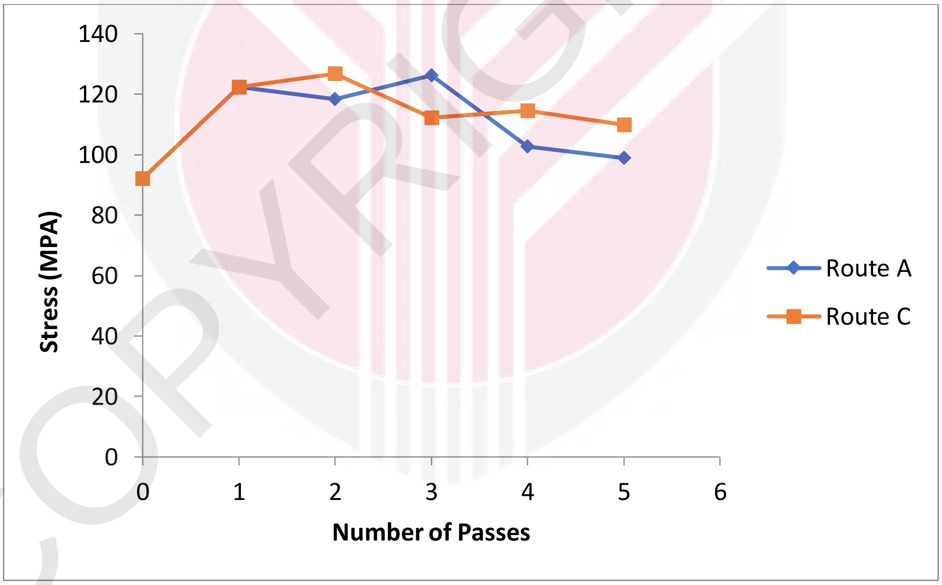

Figure 4.8 : Yield strength of samples from the ECAR with various numbers of passes in routes A and C

The tensile test results of Al/Cu/Al samples subjected to explosive welding and ECAR process in different passes and routes (A & C) were examined. It was observed that route A exhibited slightly higher yield strength and tensile strength compared to route C. The length increase remained unchanged.

In route C, the rotation of the specimens by 180 degrees after each pass resulted in a uniform plastic strain. This is the reason why the tensile strength in route A is higher than in route C. Improving the mechanical properties, including tensile strength, has been a key challenge addressed in this project. The results of the tensile testing were as expected. Furthermore, the lack of similar studies on three-layer explosive welded sheets has posed another challenge in comparing the results with previous research.

4.2.2 Analysis of Hardness

One aspect examined following the ECAR procedure on materials involves assessing the hardness of samples post-process. The hardness of these samples is influenced by two factors: grain size and dislocation density. When the density of dislocations and twin dislocations is high, increasing the number of passes leads to an increase in hardness. The changes in micro hardness observed in copper align with the level specified by ASTM E92 and are depicted in Figure 4.9.

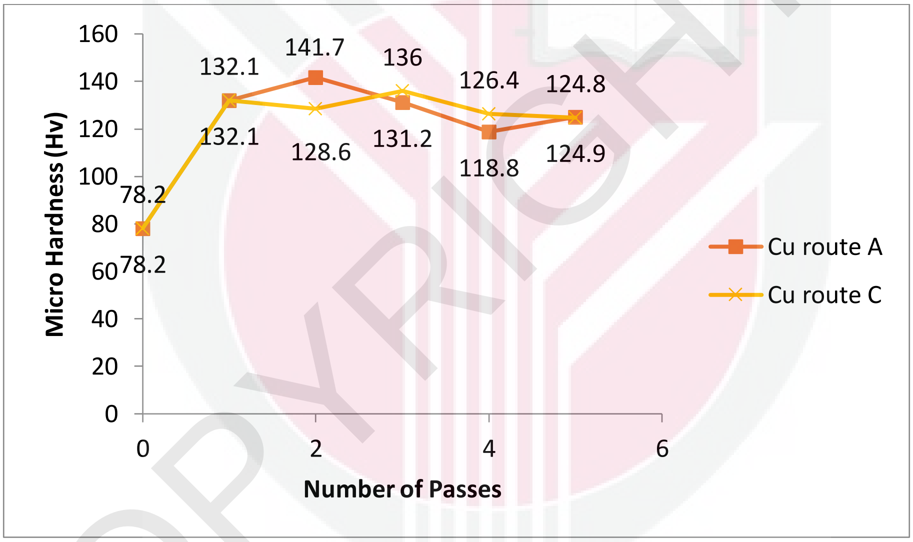

Figure 4.9 : The hardness chart on copper according to the various numbers of passes in routes A and C

The ECAR specimens in route C displayed a microhardness of 132.1 HV during the initial pass, indicating a significant 68% increase. Rather than being attributed to grain refinements, this rapid rise in microhardness is believed to be the result of strain hardening caused by the formation of sub-grain boundaries. In the subsequent pass, the microhardness decreased to 128.6 HV. The microhardness then reached its peak at 136 HV during the third pass, representing a remarkable 73% increase compared to the original sample. However, there was a slight decrease in microhardness by the fifth pass, with values of 126.4 HV and 124.8 HV recorded for the fourth and fifth passes, respectively. Despite this decrease, the microhardness remained 43% higher than that of the primary sample.

Furthermore, route A exhibited a microhardness of 132.1 HV during the initial pass, constituting approximately 68% of the overall microhardness. As the first pass progressed, the microhardness experienced a significant increase due to the heightened density of dislocations caused by strain hardening. This resulted in a steep rise in microhardness. Subsequently, during the second pass, the microhardness reached its peak at 141.7 HV. However, the presence of extensive cracks on the surface of the sheet led to a decrease in hardness during the third and fourth passes, measuring 131.2 HV and 118.8 HV respectively, accounting for 51 percent. Nevertheless, following the fifth pass, the hardness exhibited an increase, reaching 124.9 HV.

Analysis of the results reveals that these findings align with the outcomes made by other researchers. Furthermore, Rahimi et al. also corroborated these aforementioned findings in their study conducted in 2018, where they observed similar trends on the AL5083 sheet. Notably, a substantial enhancement in hardness was observed following a single pass.

This result is also in line with the findings of Honarpisheh et al. (2019), indicating that the ECAR process applied to the two-layer CU/ST explosive welding specimen had a notable impact on enhancing the hardness of the specimens. Additionally, the study revealed another noteworthy aspect concerning the mechanical properties, specifically micro-hardness. As anticipated, the hardness of the samples exhibited an increase in both directions, as observed in the results. In Figure 4.10, the hardness of aluminium is depicted based on the number of passes and various routes.

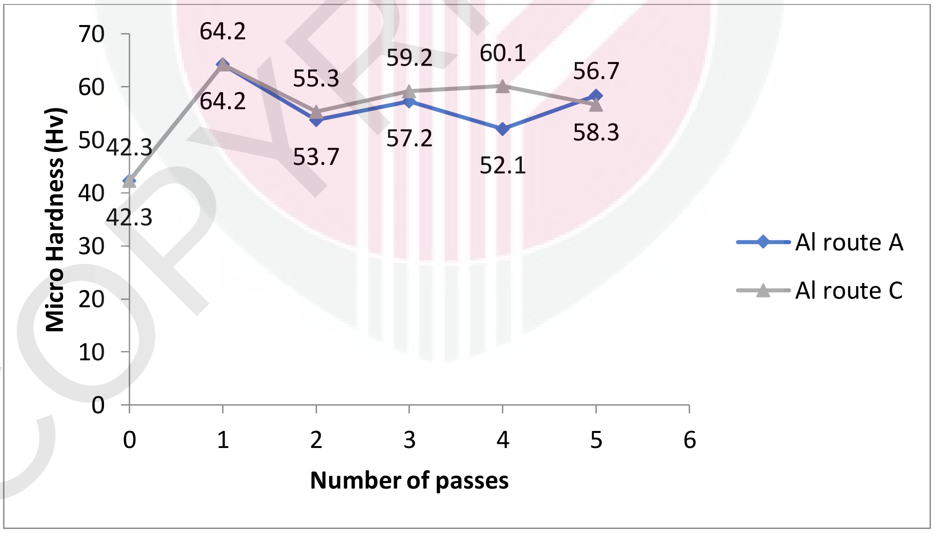

Figure 4.10 : The hardness chart on aluminium according to the various numbers of passes in routes A and C

The microhardness increase of the aluminium plate in route A of the ECAR specimens reaches its maximum of 64.2 HV at the first pass, which is 51% higher than the primary sample. Subsequent passes of ECAR do not result in significant variations in microhardness. However, the rate of microhardness enhancement becomes saturated in the following passes of ECAR. This phenomenon may also occur in other SPD processes. The rate decreases to 53.7 HV on the second pass and then increases to 57.2 HV on the third pass. On the fifth pass, the hardness increases to 58.3 HV, which is 37% higher than the primary sample.

In the initial pass of route C, the micro hardness increase reaches its peak at 64.2 HV, which is 51% higher than the primary sample. The subsequent passes exhibit strengthening due to the rapid increase in dislocation density, followed by the rearrangement of dislocations into sub-grains (cells) and grain refinement. In the second pass, the hardness reaches 55.3 HV. As the number of passes increases, there is a slight increase in hardness, but this does not vary significantly from pass to pass. The third pass records a hardness of 59.2 HV, while the fourth pass shows a hardness of 60.1 HV. However, the hardness decreases during the fifth pass, reaching 54.3 HV.

Cheng et al., 2007 demonstrated through their research that the application of the ECAR process on magnesium alloy samples leads to an increase in hardness. Similarly, Honarpisheh et al., 2018 found that the ECAR process enhances the hardness of ST12 samples, with noticeable effects observed even after the first pass. It can be observed that the ECAR process has the potential to increase the hardness of specimens across various materials, with maximum benefits achieved through multiple passes.

It is widely recognized that the ECAR process enhances the hardness of AL / CU / AL samples through various passes and routes (A & C). Similar to the findings from the tensile test, the results obtained in route A surpass those in route C. The findings indicate that the initial increase in hardness can be attributed to the hardness resulting from straining due to the formation of grain boundaries, rather than grain refinement. Additionally, there are no notable alterations in hardness observed after the first pass, and this phenomenon can also occur in other severe plastic deformation (SPD) techniques.

4.2.3 Residual Stress

Residual stress results in routes A and C shown in figures 4.11 and 4.12. It is evident that the residual stress increases after explosive welded and heat treatment before the ECAR process on the samples. This increase in residual stress is primarily observed during the first pass. The underlying cause for this phenomenon can be attributed to the manufacturing method of the material and the preparation of the sample.

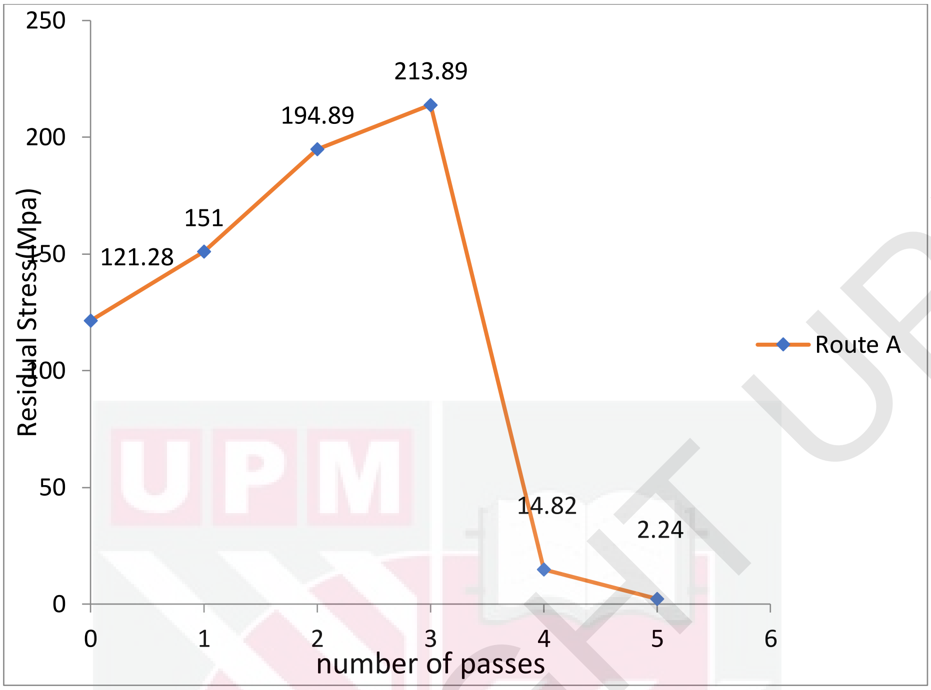

Figure 4.11 : The residual stress chart of passes in route A

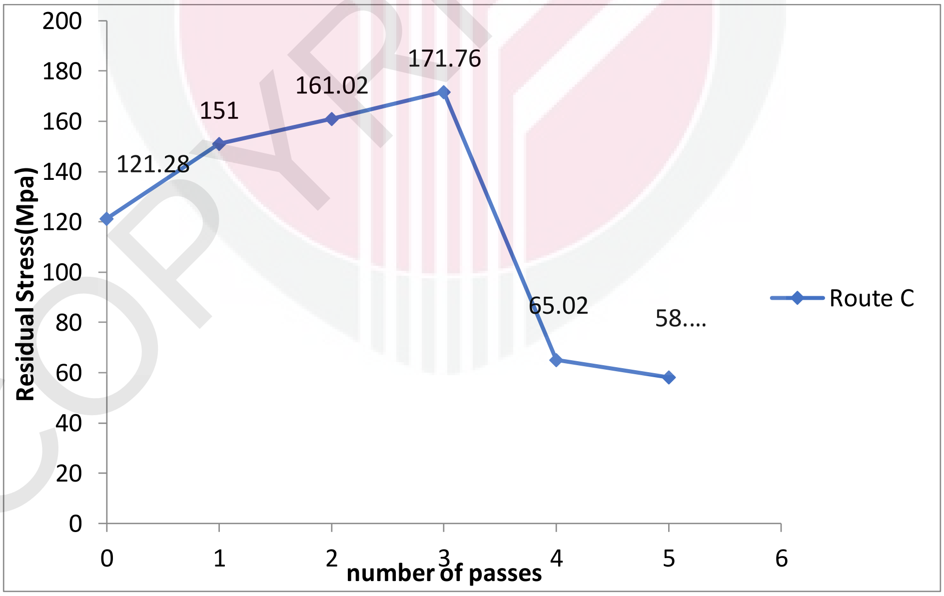

Figure 4.12 : The residual stress chart of passes in route C

After one pass of the ECAR process, it can be observed that the residual stress increased to 151 MPa. Similarly, in route A, the residual stress after two passes of the ECAR process on the sample was 194.89 MPa, while in route C it was 161.02 MPa. The ECAR process has the potential to significantly increase the maximum magnitude of residual stress in the part. During each pass of the ECAR process, the strip was passed through a mould and subjected to SPD. The third pass in route A exhibited the highest level of residual stress, and similarly, the third pass in route C also showed the highest level of residual stress.

The maximum residual stress was recorded at 213.89 MPa for route A and 171.76 MPa for route C. This disparity can be attributed to the non-uniform severe plastic deformation experienced by the material. The residual stress profile of the third pass ECARed sample closely resembles that of plastic bending operations. It is likely that the initial flat sheet acquired some curvature during the ECAR process due to the bending and unbending actions performed on it within the ECAR mould. Subsequently, after the fourth and fifth passes, the residual stress decreased to 14.82 MPa and 2.24 MPa for route A, and 65.02 MPa and 52.13 MPa for route C.

According to the research conducted by kotobi et al., in 2017, it was found that the ECAR process applied to the AL-1060 sample resulted in an increase in residual stress. The process was carried out in two passes, and the residual stress showed a significant increase after the first pass. Similar observations have been documented in other alloys, suggesting that the ECAR process plays a crucial role in elevating residual stress (Honarpisheh et al., 2018). However, after multiple passes, the ECAR process is released from the samples due to the failure in granulation of the trapped waste stress. Consequently, this issue leads to a significant reduction in residual stress within the sample. These scientists used the Slitting method for reaching residual stress, which is different from the Contour method, and used FEM to investigate residual stress but model samples in another stress software and did not used ABAQUS software.

Via the conduction of tensile strength, micro hardness, and residual stress tests, and the subsequent analysis of the acquired data, it was evident that the ECAR process exerts a substantial influence on enhancing the mechanical properties in both routes A and C. This outcome aligns with the objectives of the project and is consistent with previous research and investigations. Nevertheless, the scarcity of studies involving comparable alloys and three-layer exploded welding sheets has posed a challenge in this regard.

4.3 Microstructure Analysis

4.3.1 Analysis of the Intersection

In Figure 4.13, the scanning electron microscope and optical microscope images depict the intersection of the samples where the ECAR process was conducted in two different passes, namely routes A and C. The images reveal the emergence of new phases within the confined regions of the intersection.

This intermediate phase is a characteristic feature of explosive welding, which arises due to localized heat generation and the presence of high shear stress at the intersection (Honarpisheh et al., 2012). Despite the presence of copper, one of the bonded metals in the middle, which possesses an exceptionally high heat transfer coefficient, the occurrence of this phenomenon cannot be completely ruled out and may still manifest in certain sections of these intermediate phases (Yan & Lenard, 2004).

The findings presented by Honarpisheh et al., 2014 exhibit resemblances to our results, with the exception that their study focused on a two-layer sheet composed of AL / CU. Consequently, the intermediate phase is positively correlated with the amount of kinetic energy transformed into heat. Evaluations derived from the examination of explosive welding specimens through scanning electron microscope (SEM) and optical microscope (OM) reveal the existence of both aluminium and copper elements at the intersection of the sample (Honarpisheh et al., 2012).

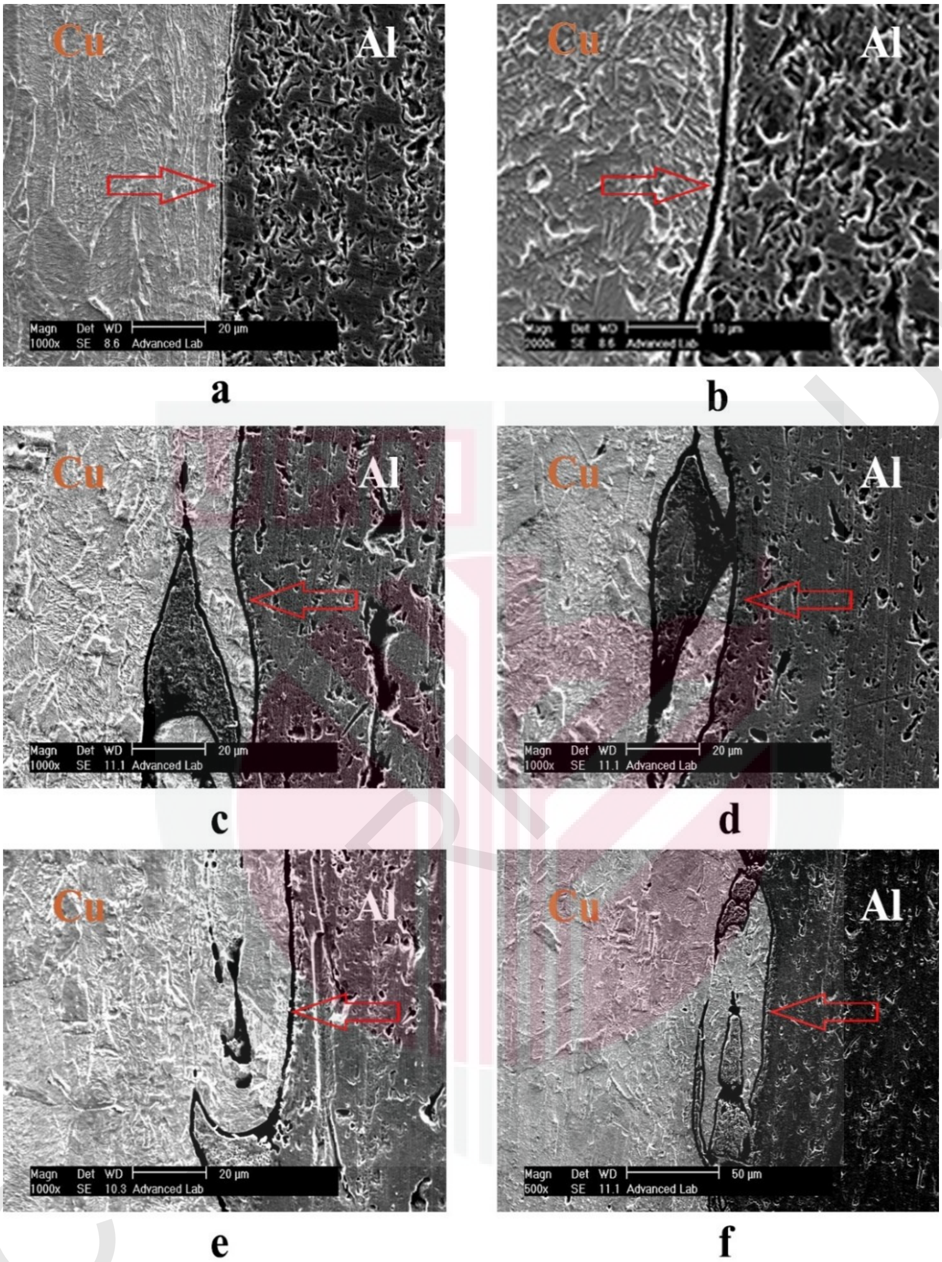

Figure 4.13 : Cross-section optical microscope image of the Al/Cu/Al interface (a) before annealing (b) after annealing (c) after two passes under route A (d) after two passes under route C (e) after five passes under route A (f) after five passes under route C

Typically, the molten nodes formed at the point of intersection solidify as a result of the substantial amount of metal present in the surrounding area, leading to the formation of cracks or freezing defects.

According to Figure 4.13, the control sample that underwent annealing exhibited cracks due to the heat treatment applied at its intersection. Furthermore, these cracks were further exacerbated by subjecting the specimens to additional passes. The kneading process has contributed to an increase in strength at the intersection of the specimens.

4.3.2 Analysis of the Grain Size

After the ECAR process, one aspect that is taken into consideration is the determination of grain size using scanning electron microscopy (SEM). Figure 4.14 illustrates the variations in grain size within a three-layer aluminium/copper/aluminium plate. In this figure, A) represents the aluminium layer, while B) represents the copper layer.

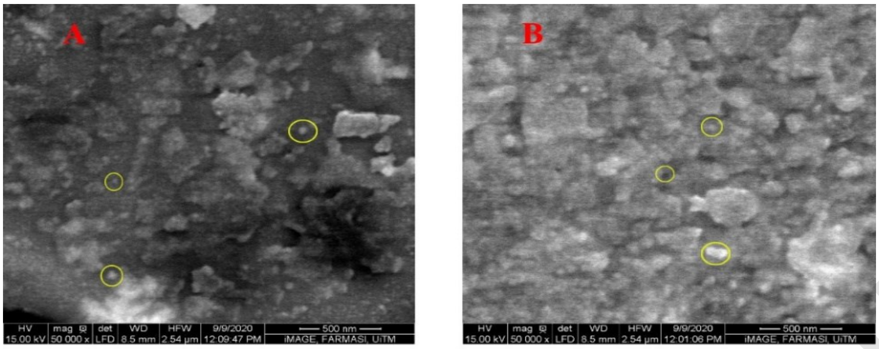

a

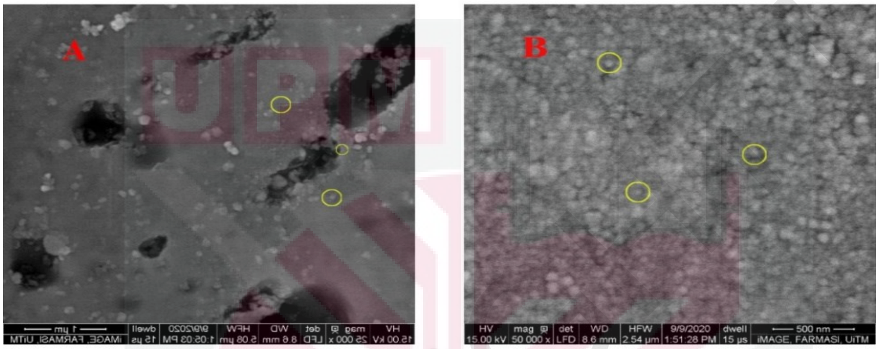

b

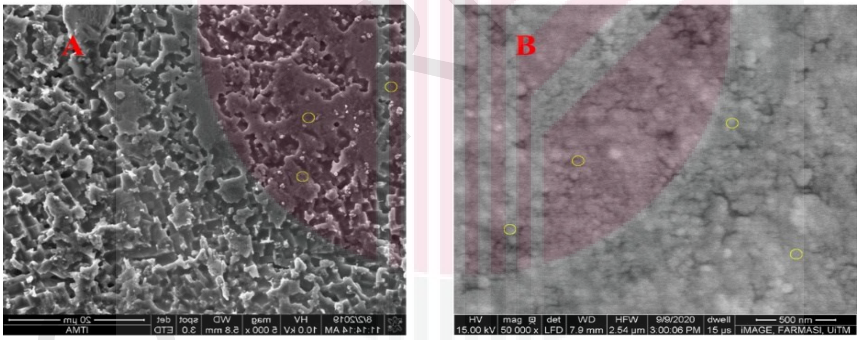

c

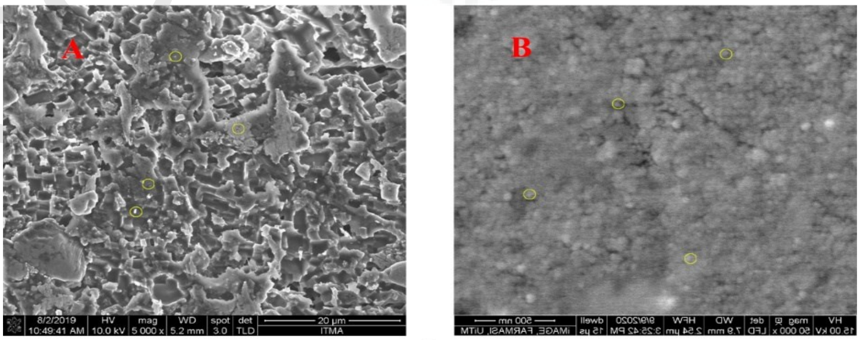

d

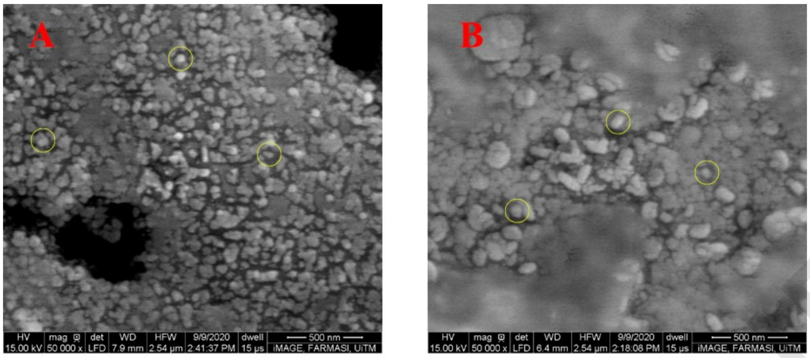

e

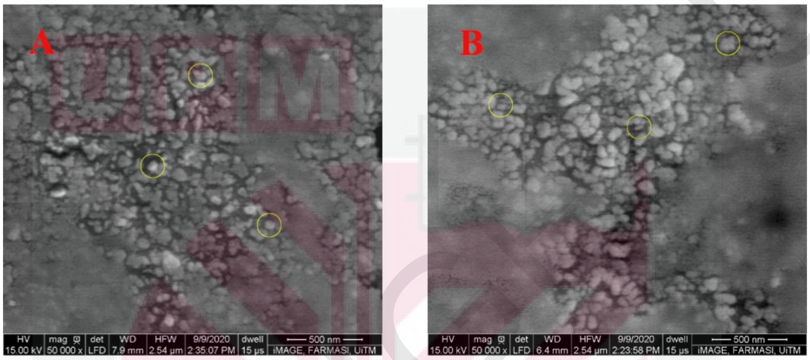

f

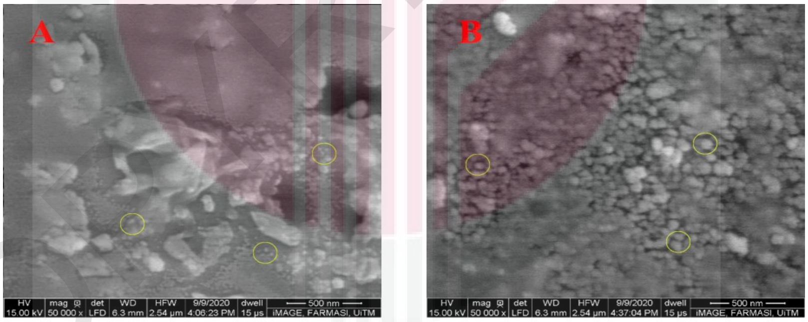

g

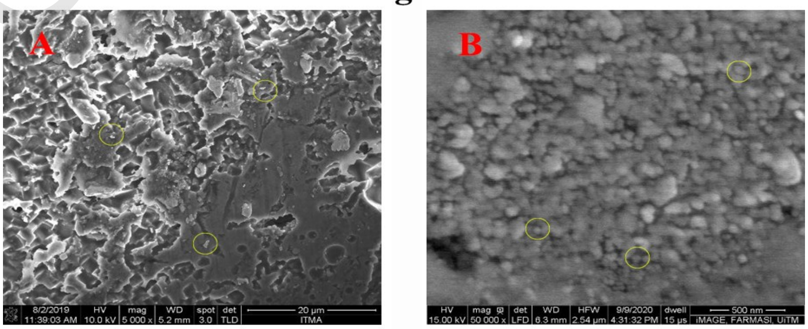

h

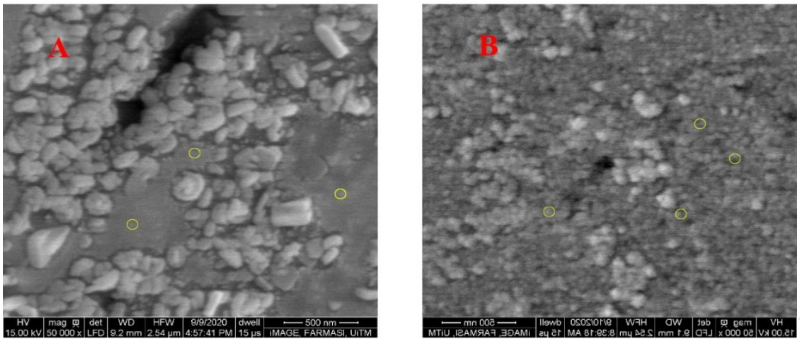

i

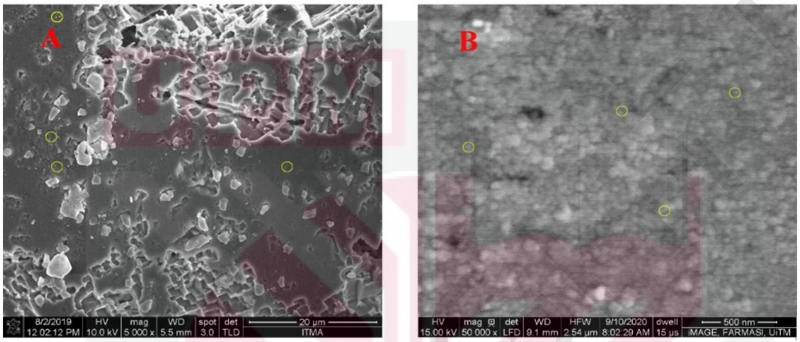

j

Figure 4.14 : SEM pics of Al/Cu/Al multilayer sheets (a) annealed (b) one pass (c) two passes under route A (d) two passes under route C (e) three passes under route A (f) three passes under route C (g) four passes under route A (h) four passes under route C (i) five passes under route A (j) five passes under route C

The grain size in the ECAR process is influenced by various parameters, including the number of rolling passes, the rolling path, the slip between the sheet and the channel, the structure of the mould, the preheating temperature, and its duration. As it is evident in Figure 4.15, the grain size of copper in the control sample is initially 5-6 micrometres, while the grain size of aluminium is 7.5-8.5 micrometres. However, after undergoing heat treatment, the grain size of copper increases to 10 micrometres, and the grain size of aluminium reaches 11.5-12 micrometres. This increase in grain size can be attributed to the formation of twins resulting from the application of heat treatment on the control sample. Table 4.1 illustrates the grain size before and after ECAR process on specimens in route A.

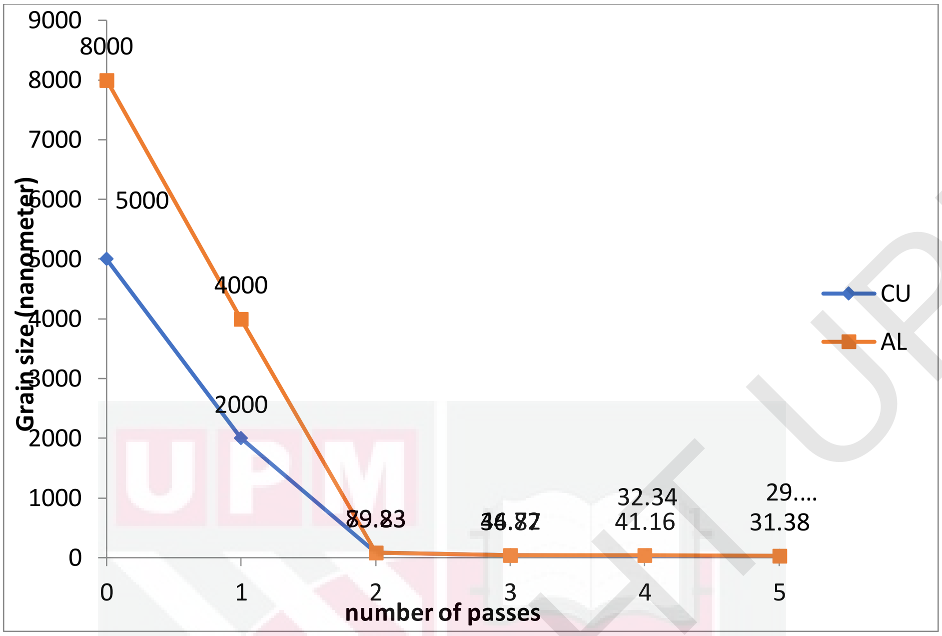

Figure 4.15 : Grain size after ECAR process in route A

Table 4.1 : Grain size before and after ECAR process on specimens in route A

Number of passes	Grain size (CU)	Grain size (Al)
Before annealing	5000-6000 nm	7500-8500 nm
Annealed	10000 nm	11500-12000 nm
1	2000 nm	4000 nm
2	79.83 nm	89.23 nm
3	36.87 nm	44.72 nm
4	32.34 nm	41.16 nm
5	29.02 nm	31.38 nm

Following the initial application of the ECAR process on the sample in route A, it is evident that the grain size of the copper in the middle layer has reduced to two micrometres, while the grain size of the aluminium on both sides has decreased to 4 µm.

This reduction in grain size is consistent with subsequent passes of the ECAR process that have been examined. In the second pass, the grain size of copper measures 78.83 nm, and the grain size of aluminium measures 89.23 nm. Similarly, in the third pass, the grain size of copper further decreases to 36.87 nm, while the grain size of aluminium reaches 44.72 nm.

In the fourth pass, the copper grain size attains a measurement of 32.34 nm, whereas the aluminium grain size reaches 41.16 nm. Conversely, in the subsequent pass, specifically the fifth pass, the copper grain size diminishes to 29.02 nm, while the aluminium grain size decreases to 31.38 nm.

In the subsequent steps, the research proceeded with thorough examination of identical procedure in route C. The thermal application sample was successfully executed, and upon the initial pass in routes A and C, the copper and aluminium grain size exhibited a similar pattern. Remarkably, the outcomes obtained align consistently with the findings of previous studies. Honarpisheh and Mansouri (2018) conducted research on a titanium alloy sample, which revealed that the ECAR process effectively diminishes the grain size from 10.5 micrometre to 3 micrometre after three passes.

In the second pass, the grain size of copper was observed to be 99.03 nm, as illustrated in Figure 4.16. On the other hand, the grain size of aluminium was measured to be one micrometre. It is noteworthy that the grain size was smaller than that of the heat treatment sample. However, when comparing it to route A, it was found that the grain size on route C is larger. This particular matter will be thoroughly investigated in the subsequent passes. Table 4.2 depicts the grain size before and after ECAR process on specimens in route C.

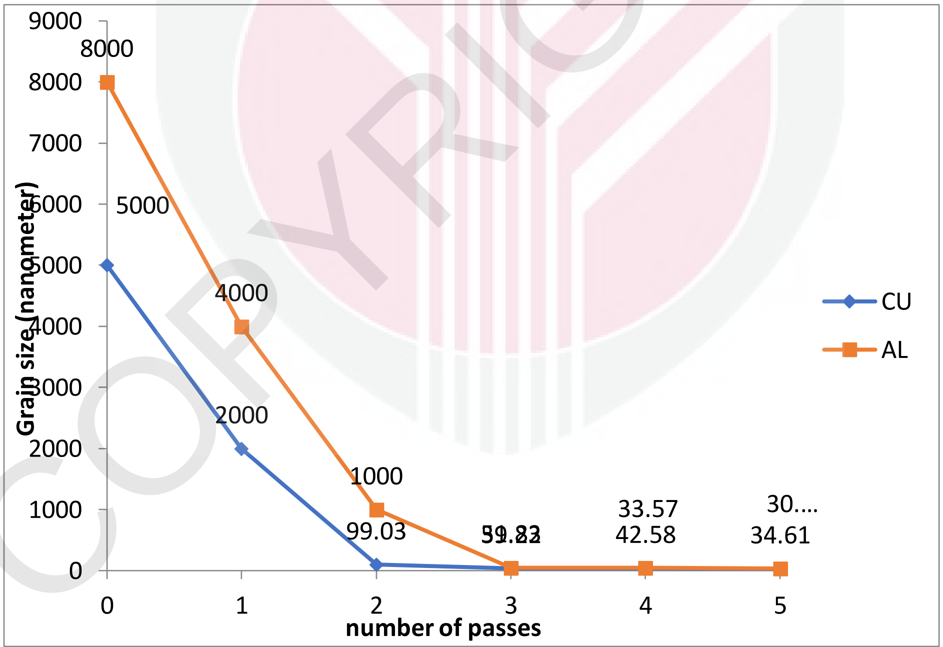

Figure 4.16 : Grain size after ECAR process in route C

Table 4.2 : Grain size before and after ECAR process on specimens in route C

Number of passes	Grain size (CU)	Grain size (Al)
Before annealing	5000-6000 nm	7500-8500 nm
Annealed	10000 nm	11500-12000 nm
1	2000 nm	4000 nm
2	99.03 nm	1000 nm
3	39.22 nm	51.83 nm
4	33.57 nm	42.58 nm
5	30.49 nm	34.61 nm

In the third pass, the copper grain size achieved a measurement of 39.22 nm, while the aluminium grain size reached 51.83 nm. Moving on to the fourth pass, the copper grain size decreased to 33.57 nm, while the aluminium grain size decreased to 42.58 nm. Finally, in the fifth pass, the copper grain size further reduced to 30.49 nm, while the aluminium grain size reached 34.61 nm.

With the aim of achieving a nanostructure, it is evident that both routes A and C exhibit Nano-sized grain sizes. However, a comparison between routes A and C, conducted over five passes, revealed that the ECAR process on route A was more effective in achieving the desired nanostructure for the three-layer AL/CU/AL sheet. This effectiveness is evident in the resulting nanostructure.

The aforementioned finding aligns with the research conducted by Honarpisheh et al. (2014), which demonstrated that conducting eight passes of the ECAR process on AL/CU double-layer sheets leads to a reduction in grain size by 2.5 micrometre in both routes A and C.

However, it is important to consider that during the ECAR process and the subsequent sample preparation stages for grain size analysis, certain issues such as surface smoothness and the presence of the ETCH solution may have hindered the visibility of the nanometre structure. To address these concerns, the samples in this project underwent daily sanding for three months to ensure surface smoothness, and the necessary chemicals were combined daily to prepare ETCH solutions for both alloys. Following the ETCH process, the grain size was thoroughly examined, resulting in improved quality and visibility for grain size analysis.

Upon analysing the findings, the samples revealed the presence of the nanostructure, which reached its minimum level after undergoing five passes. This particular aspect posed as one of the challenges in determining whether the ECAR process diminishes the grain size or not. Furthermore, it is crucial to ascertain the direction that exerts the most significant influence on the grain size. Similar to the enhancement of mechanical properties, it has been observed that route A has a more pronounced impact compared to route C. This observation holds true for the granulation structure as well.

4.4 Summary

The current chapter presented and discussed the results obtained from a series of conducted experiments. The main objectives of these experiments were to understand the mechanical properties and grain size of the ECAR process on a three-layer Al/Cu/Al sheet that was explosively welded.

The results of the tensile test examination revealed that the strength of the samples, consisting of three layers of explosively welded Al/Cu/Al, increased after performing the ECAR process. The strength reached its maximum after three passes on route A and one pass on route C.

Furthermore, the hardness test demonstrated that the ECAR process enhances the hardness of both aluminium and copper. By performing two passes on route A and three passes on route C, the hardness of copper reached its highest level. Similarly, after making one pass on both routes, the aluminium sheet reached its maximum hardness.

The examination of residual stress indicated that the ECAR process increases the residual stress in the sample. The maximum level of residual stress was observed after three passes in both routes. However, with further passes, the residual stress was released, resulting in a significant reduction in its magnitude.

Moreover, the analysis of grain size was conducted using SEM images of the samples. The findings revealed that the ECAR process reduces the grain size by causing failure in the grain boundaries. After five passes of the ECAR process on the specimens in routes A and C, a nanostructure was achieved in both copper and aluminium. Overall, the results demonstrate that the ECAR process improves the mechanical properties and reduces the grain size in the three-layer Al/Cu/Al samples. Additionally, it was observed that route A was more effective than route C in achieving these improvements.

CHAPTER 5

CONCLUSIONS AND RECOMMENDATION

5.1 Overview

The objective of this study was to focus on examining the mechanical and metallurgical properties of three-layer plates made of Al/Cu/Al after undergoing the ECAR process. Additionally, the effects of the ECAR process were analysed by varying the number of passes and routes (A, C), and the impact of heat treatment on the mechanical properties and grain size of the samples was also investigated. The aim was to gain a better understanding of the aluminium/copper/aluminium three-layer plates and their characteristics through thorough examination and analysis.

5.2 Conclusions

Various industries, such as aerospace, nuclear, medical technology, and industrial machinery, are currently considering the utilization of multilayer sheets. Equal channel angular rolling (ECAR) is a method of severe plastic deformation that aims to develop novel materials by enhancing the grain size structure and improving the mechanical properties of the samples through the plastic deformation of sheets. The objective of this research was to examine the impact of equal channel angular rolling, specifically feeding different routes (A and C), as well as the number of passes, on the mechanical properties and grain size of explosive-welded Al/Cu/Al multilayer sheets. In order to accomplish this goal, three layers of metal sheets (Al/Cu/Al) were fabricated using the explosive welding technique.

Among the objectives, one was to create novel materials comprising distinct layers and unique characteristics. The explosive welding technique offered a significant advantage by enabling the bonding of dissimilar metals that could not be joined via conventional welding methods due to the formation of fragile intermetallic compounds and a significant disparity in melting points. In this study, aluminium and copper sheets were utilized, with aluminium positioned at the top and bottom, and copper in the middle. The findings demonstrated that following the ECAR process on the explosive welded Al/Cu/Al 3-layer sheet, all properties underwent transformation, resulting in the development of a material possessing specific properties.

Another goal of the study was to enhance the mechanical properties of Al/Cu/Al 3-layer explosive welded samples via implementing ECAR Process. In order to assess the alterations in mechanical properties, various tests including micro-hardness, uniaxial tensile, and residual stress analyses were conducted. The findings indicate that the tensile strengths, micro-hardness, and residual stress exhibit an increase in both routes after undergoing the ECAR process. However, it is noteworthy that the ductility of the samples decreased as a result.

The reduction in grain size was one of the key aspects examined following the ECAR process on a three-layer sheet. This reduction was achieved through the utilization of scanning electron microscopy (SEM). Upon subjecting the sample to the ECAR process for the fifth time along route A, the grain size of copper in the middle layer measured 29.02 nm, while the grain size of aluminium measured 31.38 nm. Similarly, after the fifth pass, the grain size of copper measured 30.49 nm, whereas the size of aluminium measured 34.61 nm along route C. The analysis of the nanostructure revealed that the ECAR process was more effective in route A compared to route C for the three-layer AL/CU/AL sheet.

5.3 Recommendations for Future Research

Recommended to future research on this study could be proposed as follows:

1) It is recommended to extend the scope of this study by incorporating various layers in the research
2) In order to enhance the understanding of aluminium/copper/aluminium composites, it is suggested to incorporate additional layers and assess the properties of each intersection individually.
3) To gain insights into the fine grain size of the materials, it is advisable to utilize TEM images for examination.
4) In order to obtain comprehensive results, it is essential to conduct additional tests such as fatigue and cutting tests on the samples.
5) To ensure accurate analysis, it is recommended to subject the samples to heat treatment following each pass.
6) The measurement and examination of the microstructure should be conducted based on the plate thickness.

REFERENCES

Agarwal, K. M., Tyagi, R. K., Chaubey, V. K., & Dixit, A. (2019, November). Comparison of different methods of Severe Plastic Deformation for grain refinement. In IOP Conference Series: Materials Science and Engineering (Vol. 691, No. 1, p. 012074). IOP Publishing.

Arnett, K. (2019). Explosive Welding of Aluminium Plates: Experiments, Evaluation, and Modeling. University of California, San Diego.

ASTM E8 (2013). Standard test methods for tensile testing of metallic materials. ASTM International, Conshohocken, PA, USA.

ASTM E92 (1997). Standard method for HV hardness of metallic materials. ASTM International, Conshohocken, PA, USA.

Alateyah, A. I., Aljohani, T. A., Alawad, M. O., El-Hafez, H. A., Almutairi, A. N., Alharbi, E. S., ... & El-Garaihy, W. H. (2021). Improved Corrosion Behaviour of AZ31 Alloy through ECAP Processing. Metals, 11(2), 363.

Alizadeh, M., & Dashtestaninejad, M. K. (2018). Development of Cu-matrix, Al/Mn-reinforced, multi-layered composites by accumulative roll bonding (ARB). Journal of Alloys and Compounds, 732, 674-682.

ASM Handbook, Vol 6 (1998). Welding, Brazing and Soldering. Materials Park, Ohio, 9th edition.

AWS Handbook, Vol 2 (2004). "Welding processes", American welding society, FL, 9th edition.

Azimi, A., Tutunchilar, S., Faraji, G., & Givi, M. B. (2012). Mechanical properties and microstructural evolution during multi-pass ECAR of Al 1100–O alloy. Materials & Design, 42, 388-394.

Baig, M., Rehman, A. U., Mohammed, J. A., & Seikh, A. H. (2021). Effect of microstructure and mechanical properties of Al5083 alloy processed by ECAP at room temperature and high temperature. Crystals, 11(6), 683.

Balasubramanian, R., Nagumothu, R., Parfenov, E., & Valiev, R. (2021). Development of nanostructured titanium implants for biomedical implants–A short review. Materials Today: Proceedings, 46, 1195-1200.

Bisadi, H., & Meybodi, M. K. (2011). Experimental, numerical, and theoretical analyses of simultaneous forming–welding of inhomogeneous plates. Proceedings of the Institution of Mechanical Engineers, Part C: Journal of Mechanical Engineering Science, 225(11), 2552-2564.

Blazynski, T. Z. (2012). Explosive welding, forming and compaction. Springer Science & Business Media.

Bozcheloei, J. E., Sedighi, M., & Hashemi, R. (2019). The effect of temperature on the mechanical properties and forming limit diagram of Al 5083 produced by equal channel angular rolling. The International Journal of Advanced Manufacturing Technology, 105, 4389-4400.

Bryła, K., Morgiel, J., Faryna, M., Edalati, K., & Horita, Z. (2018). Effect of high-pressure torsion on grain refinement, strength enhancement and uniform ductility of EZ magnesium alloy. Materials Letters, 212, 323-326.

Carlone, P., & Palazzo, G. S. (2013). Longitudinal residual stress analysis in AA2024-T3 friction stir welding. The Open Mechanical Engineering Journal, 7(1).

Carvalho, G. H. S. F. L., Galvão, I., Mendes, R., Leal, R. M., & Loureiro, A. (2020). Explosive welding of aluminium to stainless steel using carbon steel and niobium interlayers. Journal of Materials Processing Technology, 283, 116707.

Chang, T. C., Wang, J. Y., Chia-Ming, O., & Lee, S. (2003). Grain refining of magnesium alloy AZ31 by rolling. Journal of Materials Processing Technology, 140(1-3), 588-591.

Cheng, Y. Q., Chen, Z. H., Xia, W. J., & Zhou, T. (2007a). Effect of channel clearance on crystal orientation development in AZ31 magnesium alloy sheet produced by equal channel angular rolling. Journal of materials processing technology, 184(1-3), 97-101.

Cheng, Y. Q., Chen, Z. H., & Xia, W. J. (2007b). Drawability of AZ31 magnesium alloy sheet produced by equal channel angular rolling at room temperature. Materials characterization, 58(7), 617-622

Chu, Q., Zhang, M., Li, J., & Yan, C. (2017). Experimental and numerical investigation of microstructure and mechanical behaviour of titanium/steel interfaces prepared by explosive welding. Materials Science and Engineering: A, 689, 323-331.

Cvijović-Alagić, I., Rakin, M., Laketić, S., & Zagorac, D. (2020). Microstructural study of Ti45Nb alloy before and after HPT processing using experimental and ab initio data mining approach. Materials Characterization, 169, 110635.

Davim, J. P. (Ed.). (2021). Welding technology. Springer.

de Oliveira, P. C., Montoro, L. A., Perez-Prado, M. T., Hohenwarter, A., Figueiredo, R. B., & Isaac, A. (2021). Development of segregations in a Mg–Mn–Nd alloy during HPT processing. Materials Science and Engineering: A, 802, 140423.

Ding, C., Xu, J., Li, X., Shan, D., Guo, B., & Langdon, T. G. (2020). Microstructural evolution and mechanical behaviour of Cu/Nb multilayer composites processed by accumulative roll bonding. Advanced Engineering Materials, 22(1), 1900702.

Dyakonov, G. S., Mironov, S., Semenova, I. P., Valiev, R. Z., & Semiatin, S. L. (2017). Microstructure evolution and strengthening mechanisms in commercial-purity titanium subjected to equal-channel angular pressing. Materials Science and Engineering: A, 701, 289-301.

Edalati, K., Emami, H., Hongo, T., Matsuda, J., Akiba, E., & Horita, Z. (2017). Significance of High-Pressure Torsion (HPT) on Solid-State Hydrogen Storage Properties. In New Energy and Sustainable Development: Proceedings of 2016 International Conference on New Energy and Sustainable Development (NESD 2016) (pp. 76-85).

Eisaabadi Bozcheloei, J., Sedighi, M. O. H. A. M. M. A. D., & Hashemi, R. (2020). Experimental study of the effect of temperature on mechanical properties of aluminum sheets produced by equal channel angular rolling process. Iranian Journal of Manufacturing Engineering, 6(9), 13-24.

El-Masry, M., & Abo-Elkhair, M. M. S. (2016, April). ULTRAFINE-GRAINED MATERIALS PRODUCED BY SEVERE PLASTIC DEFORMATION. In Proceedings of the 17th Int. AMME Conference (Vol. 19, p. 21).

Ensafi, M., Faraji, G., & Abdolvand, H. (2017). Cyclic extrusion compression angular pressing (CECAP) as a novel severe plastic deformation method for producing bulk ultrafine grained metals. Materials Letters, 197, 12-16.

Findik, F. (2011). Recent developments in explosive welding. Materials & Design, 32(3), 1081-1093.

Gadallah, R., Tsutsumi, S., Yonezawa, T., & Shimanuki, H. (2020). Residual stress measurement at the weld root of rib-to-deck welded joints in orthotropic steel bridge decks using the contour method. Engineering Structures, 219, 110946.

Gibbons, S. L., Abrahams, R. A., Vaughan, M. W., Barber, R. E., Harris, R. C., Arroyave, R., & Karaman, I. (2018). Microstructural refinement in an ultra-high strength martensitic steel via equal channel angular pressing. Materials Science and Engineering: A, 725, 57-64.

Ghaffari, Sina. (2014). Investigating the mechanical properties and microstructure of the 2-layer Al/Cu explosive-welded sheet after the ECAR process. Master project.

Habibi, A., Ketabchi, M., & Eskandarzadeh, M. (2017). Fatigue behaviour of nano-grained pure copper processed by equal channel angular rolling. Scientia Iranica, 24(2), 656-661.

Habibi, A., Ketabchi, M., & Eskandarzadeh, M. (2011). Nano-grained pure copper with high-strength and high-conductivity produced by equal channel angular rolling process. Journal of Materials Processing Technology, 211(6), 1085-1090.

Habibi, A., & Ketabchi, M. (2012). Enhanced properties of nano-grained pure copper by equal channel angular rolling and post-annealing. Materials & Design, 34, 483-487.

Honarpisheh, M., Entezami, S. S., & Akhavan, S. (2019). Effect of equal channel angular rolling process on the fracture mechanisms of Al-7057 and Al-5052 alloys. Metallography, Microstructure, and Analysis, 8(3), 336-348.

Honarpisheh, M., & Mansouri, H (2018). Investigation of Mechanical Properties of Titanium Alloy in the Equal Channel Angular Rolling Process. Conference paper, ICME.

Honarpisheh, M., Dehghani, M., & Ghaffari, S. (2014). Investigation of ECAR Routes on Mechanical Properties of Explosive-Welded Al-Cu Bimetal. Journal of Modern Processes in Manufacturing and Production, 3(4), 83-92.

Honarpisheh, M., Haghighat, E., & Kotobi, M. (2018). Investigation of residual stress and mechanical properties of equal channel angular rolled St12 strips. Proceedings of the Institution of Mechanical Engineers, Part L: Journal of Materials: Design and Applications, 232(10), 841-851.

Honarpisheh, M., Haddadi, A. A., & Mansouri, H. (2019). The Effect of Annealing Heat Treatment on the Bond of Explosive welded Copper/Steel after the ECAR Process. Journal of Modern Processes in Manufacturing and Production, 8(2), 29-38.

Honarpisheh, M., Asemabadi, M., & Sedighi, M. (2012). Investigation of annealing treatment on the interfacial properties of explosive-welded Al/Cu/Al multilayer. Materials & Design, 37, 122-127.

Hosford, W. F., & Caddell, R. M. (2011). Metal forming mechanics and metallurgy. Cambridge university press.

Hosseini, M., Pardis, N., Manesh, H. D., Abbasi, M., & Kim, D. I. (2017). Structural characteristics of Cu/Ti bimetal composite produced by accumulative roll-bonding (ARB). Materials & Design, 113, 128-136.

Jafarian, H. R., Mahdavian, M. M., Shams, S. A. A., & Eivani, A. R. (2021). Microstructure analysis and observation of peculiar mechanical properties of Al/Cu/Zn/Ni multi-layered composite produced by Accumulative-Roll-Bonding (ARB). Materials Science and Engineering: A, 805, 140556.

Kasaeian-Naeini, M., Sedighi, M., & Hashemi, R. (2022). Severe plastic deformation (SPD) of biodegradable magnesium alloys and composites: A review of developments and prospects. Journal of Magnesium and Alloys, 10(4), 938-955.

Kavyani, M., Ebrahimi, G. R., Ezatpour, H. R., & Jahazi, M. (2022). Microstructure refinement, mechanical and biocorrosion properties of Mg–Zn–Ca–Mn alloy improved by a new severe plastic deformation process. Journal of Magnesium and Alloys, 10(6), 1640-1662.

Khaled, M. H., Elkholy, A. N. M., & El-Abden, S. Z. (2022). Mechanical characteristics of AL-1050 and Al-6061 alloys deformed using equal channel angular rolling process. Zaštita materijala, 63(4), 484-492.

Kim, S. H., You, B. S., Yim, C. D., & Seo, Y. M. (2005). Texture and microstructure changes in asymmetrically hot rolled AZ31 magnesium alloy sheets. Materials letters, 59(29-30), 3876-3880.

Kim, W. J., Hong, S. I., Kim, Y. S., Min, S. H., Jeong, H. T., & Lee, J. D. (2003). Texture development and its effect on mechanical properties of an AZ61 Mg alloy fabricated by equal channel angular pressing. Acta materialia, 51(11), 3293-3307.

Kotobi, M., & Honarpisheh, M. (2017). Uncertainty analysis of residual stresses measured by slitting method in equal-channel angular rolled Al-1060 strips. The Journal of Strain Analysis for Engineering Design, 52(2), 83-92.

Kvačkaj, T., Kováčová, A., Kvačkaj, M., Kočiško, R., Lityńska-Dobrzyńska, L., Stoyka, V., & Miháliková, M. (2012). TEM studies of structure in OFHC copper processed by equal channel angular rolling. Micron, 43(6), 720-724.

Kvackaj, T., Kovacova, A., Kocisko, R., Bidulska, J., Lityńska–Dobrzyńska, L., Jenei, P., & Gubicza, J. (2017). Microstructure evolution and mechanical performance of copper processed by equal channel angular rolling. Materials Characterization, 134, 246-252.

Lee, J. C., Seok, H. K., Han, J. H., & Chung, Y. H. (2001). Controlling the textures of the metal strips via the continuous confined strip shearing (C2S2) process. Materials Research Bulletin, 36(5-6), 997-1004.

Lee, J. C., Chung, Y. H., Seok, H. K., Suh, J. Y., & Han, J. H. (2002). Structural evolution of a strip-cast al alloy sheet processed by continuous equal-channel angular pressing. Metallurgical and materials transactions A, 33(3), 665-673.

Mahmoodi, M., Sedighi, M., & Tanner, D. A. (2012). Investigation of through thickness residual stress distribution in equal channel angular rolled Al 5083 alloy by layer removal technique and X-ray diffraction. Materials & Design, 40, 516-520.

Mahmoodi, M., Naderi, A., & Dini, G. (2017). Correlation between structural parameters and mechanical properties of Al5083 sheets processed by ECAR. Journal of Materials Engineering and Performance, 26(12), 6022-6027.

Mahmoodi, M., & Naderi, A. (2019). Microstructure and its Relationship to Mechanical Properties in Equal Channel Angular Rolled Al6061 Alloy Sheets. Iranian Journal of Materials Forming, 6(1), 16-23.

Meuken, D., & Carton, E. P. (2004, July). Explosive welding and cladding. In AIP Conference Proceedings (Vol. 706, No. 1, pp. 1110-1113). American Institute of Physics.

Meselhy, A. F., & Reda, M. M. (2019). Investigation of mechanical properties of nanostructured Al-SiC composite manufactured by accumulative roll bonding. Journal of Composite Materials, 53(28-30), 3951-3961.

Milad M, Mohamad SH, Mustafa K. (2007). Investigate Mechanical Properties on St14 after ECAR process. 4th National Conference of Metals and Materials Forming.

Minárik, P., Zemková, M., Veselý, J., Bohlen, J., Knapek, M., & Král, R. (2021). The effect of Zr on dynamic recrystallization during ECAP processing of Mg-Y-RE alloys. Materials Characterization, 174, 111033.

Mohamad. Honarpisheh, Mahdi. Asem. Abadi & Mohamad. Sedighi. (2011). study of the effect of cold rolling process on the mechanical properties of Al / Cu / Al blast welding sheet. 5th conference on the formation of metals and materials in Iran.

Mousavi, S. A., & Sartangi, P. F. (2009). Experimental investigation of explosive welding of cp-titanium/AISI 304 stainless steel. Materials & Design, 30(3), 459-468.

Pérez-Prado, M. T., Del Valle, J. A., & Ruano, O. A. (2005). Achieving high strength in commercial Mg cast alloys through large strain rolling. Materials letters, 59(26), 3299-3303.

Prime, M. B. (2001). Cross-sectional mapping of residual stresses by measuring the surface contour after a cut. J. Eng. Mater. Technol., 123(2), 162-168.

Prime, M. B., Sebring, R. J., Edwards, J. M., Hughes, D. J., & Webster, P. J. (2004). Laser surface-contouring and spline data-smoothing for residual stress measurement. Experimental Mechanics, 44(2), 176-184.

Rahimi, H. R., Sedighi, M., & Hashemi, R. (2018). Forming limit diagrams of fine-grained Al 5083 produced by equal channel angular rolling process. Proceedings of the Institution of Mechanical Engineers, Part L: Journal of Materials: Design and Applications, 232(11), 922-930.

Rosochowski, A. (2005). Processing metals by severe plastic deformation. In Solid State Phenomena (Vol. 101, pp. 13-22). Trans Tech Publications Ltd.

Saito, Y., Utsunomiya, H., Suzuki, H., & Sakai, T. (2000). Improvement in the R-value of aluminium strip by a continuous shear deformation process. Scripta Materialia, 42(12), 1139-1144.

Safiri, M., Meratian, M., & Panjepour, M. (2019). Fabrication of Al-TiAl 3 Composite Via In-Situ Accumulative Roll Bonding (ARB) and Annealing. Metallurgical and Materials Transactions A, 50(1), 415-425.

Sedighi, M., Monshi, P., & Joudaki, J. (2017). Investigation of mechanical properties and fatigue life of ECARed AA5083 aluminium alloy. Fatigue & Fracture of Engineering Materials & Structures, 40(3), 412-422.

Segal, V. M. (1999). Equal channel angular extrusion: from micromechanics to structure formation. Materials Science and Engineering: A, 271(1-2), 322-333.

Sherpa, B. B., Kumar, P. D., Upadhyay, A., Kumar, S., Agarwal, A., & Tyagi, S. (2021). Effect of explosive welding parameters on Al/LCS interface cladded by low velocity of detonation explosive welding (LVEW) process. The International Journal of Advanced Manufacturing Technology, 113, 3303-3317.

Siahsarani, A., & Faraji, G. (2021). Processing and characterization of AZ91 magnesium alloys via a novel severe plastic deformation method: Hydrostatic cyclic extrusion compression (HCEC). Transactions of Nonferrous Metals Society of China, 31(5), 1303-1321.

Sułkowski, B., Janoska, M., Boczkal, G., Chulist, R., Mroczkowski, M., & Pałka, P. (2020). The effect of severe plastic deformation on the Mg properties after CEC deformation. Journal of Magnesium and Alloys, 8(3), 761-768.

Valiev, R. Z., & Langdon, T. G. (2006). Principles of equal-channel angular pressing as a processing tool for grain refinement. Progress in materials science, 51(7), 881-981.

Volokitina, I., Kolesnikov, A., Fediuk, R., Klyuev, S., Sabitov, L., Volokitin, A., ... & Kolesnikova, O. (2022). Study of the Properties of Antifriction Rings under Severe Plastic Deformation. Materials, 15(7), 2584.

Weman, K. (2011). Welding processes handbook. Elsevier.

Wojtas, D., Wierzbanowski, K., Chulist, R., Pachla, W., Bieda-Niemiec, M., Jarzębska, A., ... & Sztwiertnia, K. (2020). Microstructure-strength relationship of ultrafine-grained titanium manufactured by unconventional severe plastic deformation process. Journal of Alloys and Compounds, 837, 155576.

Woo, W., Choo, H., Prime, M. B., Feng, Z., & Clausen, B. (2008). Microstructure, texture, and residual stress in a friction-stir-processed AZ31B magnesium alloy. Acta materialia, 56(8), 1701-1711.

Yan, H., & Lenard, J. G. (2004). A study of warm and cold roll-bonding of an aluminium alloy. Materials Science and Engineering: A, 385(1-2), 419-428.

Yan, Z., Zhang, Z., Li, X., Xu, J., Wang, Q., Zhang, G., ... & Xue, Y. (2020). A novel severe plastic deformation method and its effect on microstructure, texture, and mechanical properties of Mg-Gd-Y-Zn-Zr alloy. Journal of Alloys and Compounds, 822, 153698.

Zeng, X. Y., Wang, Y. X., Li, X. Q., Li, X. J., & Zhao, T. J. (2019a). Effects of gaseous media on interfacial microstructure and mechanical properties of titanium/steel explosive welded composite plate. Fusion Engineering and Design, 148, 111292.

Zeng, X. Y., Li, X. Q., Li, X. J., Mo, F., & Yan, H. H. (2019b). Numerical study on the effect of thermal conduction on explosive welding interface. The International Journal of Advanced Manufacturing Technology, 104, 2607-2617.

Zhang, L., Wang, Q., Liu, G., Guo, W., Ye, B., Li, W., ... & Ding, W. (2018). Tribological behaviour of carbon nanotube reinforced AZ91D composites processed by cyclic extrusion and compression. Tribology Letters, 66(2), 1-11.

Zhang, Z. L., & Liu, M. B. (2019). Numerical studies on explosive welding with ANFO by using a density adaptive SPH method. Journal of Manufacturing Processes, 41, 208-220.

LIST OF PUBLICATIONS

Ghaffari, S., Tahir, S., Mohamed Ariff, A. H., & Ismail, M. I. S. (2022). Effects of ECAR process on the mechanical properties of explosively welded Al/Cu/Al. Australian Journal of Mechanical Engineering, 20(5), 1407-1412.

Ghaffari, S., Tahir, S., Mohamed Ariff, A. H., & Ismail, M. I. S. (2024). Effects of Feeding Routes of ECAR process on the residual stress and grain size of explosively welded Al/Cu/Al. Scientia Iranica. (Submitted)